

# On Two-User Gaussian Multiple Access Channels With Finite Input Constellations

J. Harshan and B. Sundar Rajan, *Senior Member, IEEE*

**Abstract**—Constellation Constrained (CC) capacity regions of two-user Single-Input Single-Output (SISO) Gaussian Multiple Access Channels (GMAC) are computed for several Non-Orthogonal Multiple Access schemes (NO-MA) and Orthogonal Multiple Access schemes (O-MA). For NO-MA schemes, a metric is proposed to compute the angle(s) of rotation between the input constellations such that the CC capacity regions are maximally enlarged. Further, code pairs based on Trellis Coded Modulation (TCM) are designed with PSK constellation pairs and PAM constellation pairs such that any rate pair within the CC capacity region can be approached. Such a NO-MA scheme which employs CC capacity approaching trellis codes is referred to as Trellis Coded Multiple Access (TCMA). Then, CC capacity regions of O-MA schemes such as Frequency Division Multiple Access (FDMA) and Time Division Multiple Access (TDMA) are also computed and it is shown that, unlike the Gaussian distributed continuous constellations case, the CC capacity regions with FDMA are strictly contained inside the CC capacity regions with TCMA. Hence, for finite constellations, a NO-MA scheme such as TCMA is better than FDMA and TDMA which makes NO-MA schemes worth pursuing in practice for two-user GMAC. Then, the idea of introducing rotations between the input constellations is used to construct Space-Time Block Code (STBC) pairs for two-user Multiple-Input Single-Output (MISO) fading MAC. The proposed STBCs are shown to have reduced Maximum Likelihood (ML) decoding complexity and information-losslessness property. Finally, STBC pairs with reduced sphere decoding complexity are proposed for two-user Multiple-Input Multiple-Output (MIMO) fading MAC.

**Index Terms**—Constellation constrained capacity, multiple access channels, MIMO, space-time block codes, trellis coded modulation, ungerboeck partitioning.

## I. INTRODUCTION AND PRELIMINARIES

CAPACITY regions of two-user Gaussian Multiple Access Channels (GMAC) (shown in Fig. 1) are well known wherein the capacity achieving input is *continuous* and *Gaussian distributed* [1]–[5]. Throughout the paper, Gaussian distributed continuous constellations are referred to as Gaussian constellations. Though, capacity regions of such channels provide insights into the achievable rate pairs in an information theoretic sense, they fail to provide information on the achievable rate pairs when

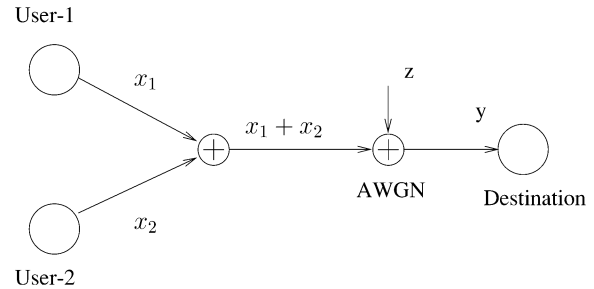


Fig. 1. Two-user Gaussian MAC model.

we consider finitary restrictions on the input constellations and analyze some real world practical signal constellations like QAM and PSK signal sets. Hence, there is a need to study GMAC with finite input constellations. Towards that direction, GMAC with finite complex input constellations was first studied in [6] along with the assumption of *random phase offsets* in the channel from every user to the destination. In the same work, constellation constrained (CC) sum-capacity values [7] have been computed for PSK and QAM constellations when all the users transmit simultaneously during the same time and in the same frequency band. Depending on how the users transmit to the destination, multiple access schemes can be broadly partitioned into two groups namely, Orthogonal Multiple Access Schemes (O-MA schemes) and Non-Orthogonal Multiple Access Schemes (NO-MA schemes), which are defined as follows:

**Definition 1:** A multiple access scheme is called an O-MA scheme if the users are separated either in the time (frequency) domain or in the code domain;<sup>1</sup> otherwise, it is called a NO-MA scheme.

In [8] and [9], trellis codes have been proposed for such NO-MA channels wherein the receiver performs joint decoding for the symbols of all the users. Since random phase offsets are assumed in the channel model in [6], [8], [9], the receiver can uniquely decode the symbols of all the users even when all the users employ identical input constellation. Subsequently, in [10], a NO-MA scheme based  $K$ -user GMAC model with *no random phase offsets* in the channel has been studied and codes based on trellis coded modulation (TCM) [11] have been proposed. In such a model, the unique decodability (UD) property (see Section II-A for the definition of the UD property) at the destination is achieved by employing distinct constellations for all the users. In particular, a constellation of size  $KM$  (example:  $KM$ -PSK or  $KM$ -QAM) is chosen and it is appropriately partitioned into  $K$  groups such that every user employs one of the  $K$  groups as its input constellation. Towards

Manuscript received January 06, 2009; revised March 27, 2010; accepted May 03, 2010. Date of current version February 18, 2011. B. Sundar Rajan was supported in part by grants from the DRDO-IISc program on Advanced Research in Mathematical Engineering and the INAE Chair Professorship. Different parts of the results presented in this paper are in the Proceedings of IEEE International Symposium on Information theory (ISIT) 2008, the IEEE ISIT 2009, the IEEE Global Telecommunication Conference (GLOBECOM) 2009, and the National Conference on Communications (NCC-09 and NCC-10).

The authors are with the Department of Electrical Communication Engineering, Indian Institute of Science, Bangalore-560012, India (e-mail: harshan@ece.iisc.ernet.in; bsrajan@ece.iisc.ernet.in).

Communicated by E. Viterbo, Associate Editor for Coding Techniques.

Digital Object Identifier 10.1109/TIT.2011.2104491

<sup>1</sup>TDMA, FDMA and CDMA are the examples for MA schemes with separation in time, frequency, and code domain respectively.

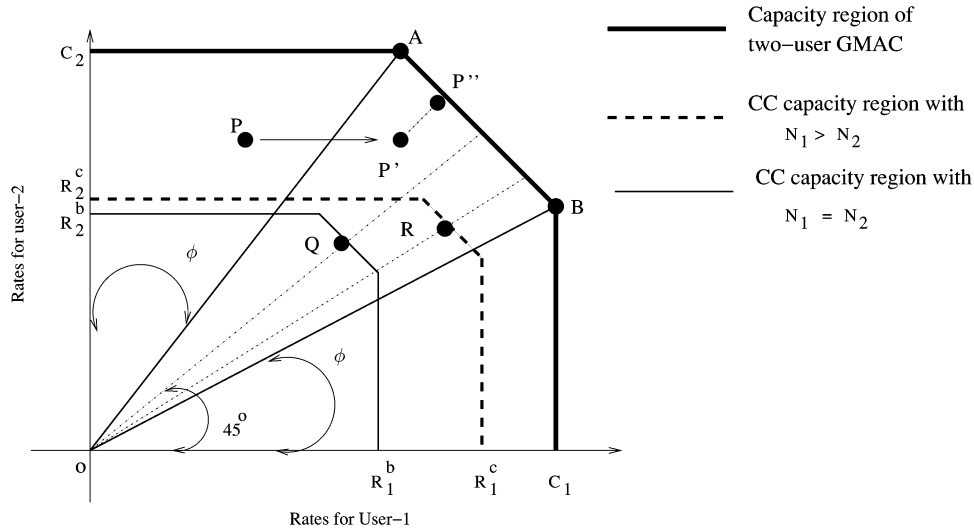


Fig. 2. Capacity regions of two-user GMAC (for a fixed equal average power constraint) with (i) finite constellations and (ii) Gaussian constellations.

designing trellis codes, the authors of [10] only propose steps to derive the labeling on the edges of the trellises of each user but do not derive explicit labeling rules on the individual trellises. Note that all the schemes proposed in [6], [8]–[10] belong to the class of NO-MA schemes.

In this paper, two-user GMAC with finite complex input constellations is studied *without* the assumption of random phase offsets in the channel (we show that random phase offsets in the channel lead to loss in the CC sum-capacity). Unlike the works of [6], [8]–[10], we compute the CC capacity regions of two-user GMAC when NO-MA schemes and O-MA schemes are employed. We show that NO-MA schemes offer larger CC capacity regions than the O-MA schemes such as Time-Division Multiple Access (TDMA) and Frequency Division Multiple Access (FDMA). For NO-MA schemes, we first investigate the impact of rotations between the constellations of the users on the CC capacity regions. Subsequently, we propose TCM based trellis codes to approach *any rate pair* (for example, the points R, Q shown in Fig. 2) within the CC capacity region. Throughout this paper, a NO-MA scheme which employs capacity approaching trellis codes is referred to as trellis coded multiple access (TCMA). We also use the terms *constellation* and *signal set* interchangeably.

Further, we extend the idea of introducing rotation between the constellations of the two users to construct Space-Time Block Code (STBC) pairs with low ML decoding complexity for two-user MIMO (Multiple-Input Multiple-Output) fading MAC. We focus on constructing STBC pairs that reduce the ML decoding complexity only. For a background on designing STBC pairs based on the dominant error region, we refer the readers to [12]. Algebraic STBCs for MIMO-MAC can be found in [13]. We are not aware of any prior work which explicitly address the design of STBC pairs with low ML decoding complexity for MIMO-MAC. Note that STBCs with minimum ML decoding complexity have been well studied in the literature for co-located MIMO channels [14]–[17] and distributed MIMO channels [18]. The contributions and the organization of this paper may be summarized as below:

- *Computing constellation constrained capacity regions:* For two-user GMAC, when the two users employ a NO-MA

scheme with identical input constellations, it has been pointed in [6] that an appropriate rotation between the input constellations can guarantee the UD property (see Definition 3) at the receiver. For such a setup, in this paper, we identify that the primary problem is to compute the angle(s) of rotation between the constellations such that the CC capacity region is maximally enlarged. A metric to compute the angle(s) of rotation is proposed which provides maximum enlargement of the CC capacity region (Theorem 1) at high signal to noise ratio (SNR) values. Through simulations, such angles of rotation are presented for some well known constellations such as  $M$ -PSK,  $M$ -QAM etc. for some values of  $M$  at some fixed SNR values (see Table I).

- *Designing CC capacity approaching trellis codes with PSK constellations:* For two-user GMAC, code pairs based on TCM are designed with PSK constellation pairs to approach any rate pair within the CC capacity region. In particular, for each  $i = 1$  and  $2$ , if User- $i$  employs a trellis  $T_i$  labeled with the symbols of the signal set  $\mathcal{S}_i$ , it is clear that the destination views the sum trellis,  $T_{\text{sum}}$  (see Definition 4) labeled with the symbols of the sum constellation,  $\mathcal{S}_{\text{sum}}$  (see Section II-A) in an equivalent SISO (Single-Input Single-Output) AWGN channel. For a SISO AWGN channel, it is well known that, Ungerboeck labeling on the trellis maximizes the guaranteed minimum squared Euclidean distance in the trellis, and hence, such a labeling scheme has become a systematic method of generating trellis codes to approach rates close to the CC capacity [11]. However, when TCM based trellis codes are designed for two-user GMAC, it is not clear if the two users can distributively achieve Ungerboeck labeling on the sum trellis through the trellises  $T_1$  and  $T_2$ . In other words, it is not known whether Ungerboeck labeling on  $T_1$  and  $T_2$  using  $\mathcal{S}_1$  and  $\mathcal{S}_2$  respectively induces an Ungerboeck labeling on  $T_{\text{sum}}$  using  $\mathcal{S}_{\text{sum}}$ . For the class of symmetric PSK signal sets, when the relative angle is  $\frac{\pi}{N_2}$  ( $N_1$  and  $N_2$  are the cardinalities of the signal sets of User-1 and User-2 respectively). Without loss of generality, we assume  $N_2 \geq N_1$ ), it is analytically proved that, Ungerboeck labeling on the trellis of each user induces an Ungerboeck labeling on  $T_{\text{sum}}$  which in-turn maximizes the guar-

TABLE I  
TWO-TUPLES  $(a, b)$  FOR  $M$ -PSK AND  $M$ -QAM CONSTELLATIONS FOR SOME  $M$ :  $a$ - $\theta^*$ ,  $b$ -MULTIPLICITY OF  $\theta^*$

SNR in dB	BPSK	QPSK	8-QAM	8-PSK	16-PSK
-2	(90, 1)	(45.0, 1)	(90, 1)	(22.5, 1)	(01.43, 1)
0	(90, 1)	(45.0, 1)	(90, 1)	(22.5, 1)	(09.12, 2)
2	(90, 1)	(45.0, 1)	(90, 1)	(22.5, 1)	(21.37, 1)
4	(90, 1)	(45.0, 1)	(90, 1)	(22.5, 1)	(11.25, 1)
6	(90, 1)	(45.0, 1)	(90, 1)	(22.5, 1)	(11.25, 1)
8	(90, 1)	(35.1, 2)	(110.12, 1)	(22.5, 1)	(11.25, 1)
10	(90, 118)	(58.1, 1)	(61.62, 1)	(18.5, 1)	(11.25, 1)
12	(90, 775)	(30.8, 1)	(119.25, 1)	(16.0, 1)	(09.50, 1)
14	(90, 1269)	(30.5, 1)	(118.75, 1)	(15.3, 1)	(10.56, 1)
16	(90, 1609)	(30.3, 2)	(118.0, 1)	(15.1, 1)	(08.31, 2)

anteed minimum squared Euclidean distance of  $T_{\text{sum}}$  (see Section IV.C). Hence, such a labeling scheme can be used as a systematic method of generating trellis code pairs for two-user GMAC to approach any rate pair within the CC capacity region (Section IV).

- *Designing CC capacity approaching trellis codes with PAM signal sets:* We design trellis code pairs with  $M$ -PAM signal set pairs also (see Section V). For such signal sets, it is shown that the relative angle of rotation that maximally enlarges the CC capacity region is  $\frac{\pi}{2}$  for all values of  $M$  and SNR. Note that the above structure on  $M$ -PAM constellation pairs keep the two users orthogonal to each other, and hence, the ML decoding complexity is significantly reduced when trellis codes with  $M$ -PAM signal sets are employed. Therefore, trellis codes designed for SISO AWGN channel with  $M$ -PAM constellations are applicable in this set-up. Through simulations, it is shown that, for any given SNR, the CC sum-capacity of 4-PAM signal sets (when used with a relative rotation of  $\frac{\pi}{2}$ ) and QPSK signal sets (with appropriate angles of rotation) are *almost* the same, and hence, unlike in a SISO AWGN channel, there is no loss in the CC sum-capacity by using 4-PAM constellations over QPSK signal sets in two-user GMAC (Section V).
- *Non-orthogonal multiple access versus orthogonal multiple access schemes for two-user GMAC:* We also compute the CC capacity regions of two-user GMAC when O-MA schemes such as TDMA and FDMA are employed for finite bandwidth. Unlike the behavior of Gaussian constellations (as shown in Fig. 15), it is shown that the CC capacity region with FDMA is strictly contained inside the CC capacity region with TCMA, essentially showing that TCMA is better than FDMA for finite constellations (see Figs. 16, 17 and 18). In particular, we show that the gap between the CC capacity regions with TCMA and FDMA is a function of the bandwidth  $W$  Hertz and the average power constraint  $P$  Watts. It is shown that, (i) for a fixed  $W$ , the gap between the CC capacity regions with FDMA and TCMA *increases* with the increase in  $P$  (see Figs. 16, 17 and 18 for a fixed  $W$  and varying  $P$ ), and (ii) for a fixed  $P$ , the gap between the CC capacity regions with FDMA and TCMA *decreases* with the increase in  $W$  (see Figs. 16 and 19 for a fixed  $P$  and varying  $W$ ) (Section VI).
- *Low ML decoding complexity codes for two-user MISO-MAC:* We extend the idea of introducing rotation between the PAM constellations in two-user GMAC to construct

STBC pairs for two-user MISO fading MAC (Section VII). In particular, we introduce the notion of information-losslessness (IL) property and propose a class of STBC pairs that has reduced ML decoding complexity and the IL property. To the best of our knowledge, this is the first work that (i) introduces the notion of IL property to MISO-MAC and (ii) propose STBC pairs with reduced ML decoding complexity as well as the IL property. We also compute the CC ergodic sum-capacity [19] of the proposed STBCs in a MISO fading MAC and compare them with the CC ergodic sum-capacity of VBLAST schemes for a fixed rate (in bits per channel use). It is shown that, in addition to the advantage of having reduced ML decoding complexity, the proposed STBC pairs have CC ergodic sum-capacity values comparable with VBLAST schemes.

- *Reduced sphere decoding complexity codes for two-user MIMO-MAC:* Finally, we propose STBC pairs for two-user MIMO fading MAC with  $N_t$  antennas at both the users and  $N_r$  antennas at the destination such that the sphere decoding [20], [21] complexity is reduced. When both the users employ identical STBCs from linear complex designs [22], a class of complex designs which results in a special class of lattice generators called row-column (RC) monomial lattice generators are identified (Definition 8 in Section VII-C). Employing Q-R decomposition on RC monomial lattice generators, we identify the positions of the zeros in the R matrix such that the worst-case sphere decoding complexity (WSDC) and/or the average sphere decoding complexity (ASDC) are reduced (Definition 9 and Definition 10). We explicitly construct STBCs which reduce the ASDC. The rate of the proposed STBCs in complex symbols per channel use per user is at most  $\frac{2}{N_t}$ . We also show that STBCs from the class of Complex Orthogonal designs (other than the Alamouti design) only reduce the WSDC (but not the ASDC). (Section VII-C4).

Section VIII constitutes conclusion and some directions for possible future work.

**Notations:** Throughout the paper, boldface letters and capital boldface letters are used to represent vectors and matrices, respectively. For a complex matrix  $\mathbf{X}$ , the matrices  $\mathbf{X}^*$ ,  $\mathbf{X}^T$ ,  $\mathbf{X}^H$ ,  $|\mathbf{X}|$ ,  $\text{Re}(\mathbf{X})$  and  $\text{Im}(\mathbf{X})$  denote, respectively, the conjugate, transpose, conjugate transpose, determinant, real part and imaginary part of  $\mathbf{X}$ . For any matrix  $\mathbf{X}$ , the symbol  $\mathbf{X}_c(j)$  denotes the  $j$ -th column of  $\mathbf{X}$  and  $[\mathbf{X}]_{i,j}$  denotes the element in the  $i$ -th row and the  $j$ -th column of  $\mathbf{X}$ . The tensor product of the matrix  $\mathbf{X}$  with itself  $r$  times is represented by  $\mathbf{X}^{\otimes r}$ . For a

random variable  $X$  which takes value from the set  $\mathcal{S}$ , we assume some ordering of its elements and use  $X(i)$  to represent the  $i$ -th element of  $\mathcal{S}$ , i.e.,  $X(i)$  represents a realization of the random variable  $X$ . The set of all integers, the real numbers, and the complex numbers are, respectively, denoted by  $\mathbb{Z}, \mathbb{R}$ , and  $\mathbb{C}$  and  $\mathbf{i}$  is used to represent  $\sqrt{-1}$ . For  $a, b \in \mathbb{C}$ , the Euclidean distance between  $a$  and  $b$  is denoted by  $d(a, b)$  whereas the line segment connecting  $a$  and  $b$  is denoted by  $l(a, b)$ . Cardinality of the set  $\mathcal{S}$  is denoted by  $|\mathcal{S}|$ . Absolute value of a complex number  $x$  is denoted by  $|x|$  and  $E[x]$  denotes the expectation of the random variable  $x$ . A circularly symmetric complex Gaussian random vector,  $\mathbf{x}$  with mean  $\boldsymbol{\mu}$  and covariance matrix  $\boldsymbol{\Gamma}$  is denoted by  $\mathbf{x} \sim \mathcal{CSCG}(\boldsymbol{\mu}, \boldsymbol{\Gamma})$ . The inner product of two vectors  $\mathbf{x}, \mathbf{y} \in \mathbb{R}^{T \times 1}$  is denoted by  $\langle \mathbf{x}, \mathbf{y} \rangle$ . The set of all real diagonal matrices is denoted by  $\mathcal{D}$ . For any complex vector  $\mathbf{x} \in \mathbb{C}^{k \times 1}$ ,  $\vec{\mathbf{x}}$  is given by  $\vec{\mathbf{x}} = [\text{Re}(\mathbf{x})^T \text{Im}(\mathbf{x})^T]^T \in \mathbb{R}^{2k \times 1}$ .

## II. TWO-USER GMAC: SIGNAL MODEL AND CONSTELLATION CONSTRAINED CAPACITY REGIONS

The model of two-user Gaussian MAC shown in Fig. 1 consists of two users that need to convey information to a single destination. It is assumed that User-1 and User-2 communicate to the destination at the same time and in the same frequency band (the two users employ a NO-MA scheme). Symbol level synchronization is assumed at the destination. The two users are equipped with constellations  $\mathcal{S}_1$  and  $\mathcal{S}_2$  of size  $N_1$  and  $N_2$  respectively such that for  $x_i \in \mathcal{S}_i$ , we have  $E[|x_i|^2] = 1$ . Let  $P$  be the average power constraint for each user. When User-1 and User-2 transmit symbols  $\sqrt{P}x_1$  and  $\sqrt{P}x_2$  simultaneously, the destination receives a symbol  $y$  given by

$$y = \sqrt{P}x_1 + \sqrt{P}x_2 + z \quad \text{where } z \sim \mathcal{CSCG}(0, \sigma^2) \quad (1)$$

such that  $\frac{\sigma^2}{2}$  is the variance of the AWGN in each dimension. Throughout the paper, unless specified otherwise, we assume equal average power constraint for the two users.

*Definition 2: (Constellation constrained capacity)* [7] The mutual information between the input and the output of a Gaussian channel is referred to as the Constellation Constrained (CC) capacity of the channel whenever (i) the input constellation is finite in size and (ii) the symbols from the input constellation are chosen with *uniform distribution*.

We compute the CC capacity values:  $I(\sqrt{P}x_2 : y)$  for User-2 and  $I(\sqrt{P}x_1 : y|\sqrt{P}x_2)$  for User-1<sup>2</sup> (assuming uniform distribution on the input constellations) [23]. By symmetry,  $I(\sqrt{P}x_1 : y)$  and  $I(\sqrt{P}x_2 : y|\sqrt{P}x_1)$  can similarly be computed. Towards computing  $I(\sqrt{P}x_2 : y)$ , we treat  $\sqrt{P}x_1 + z$  as the additive noise. From [1],  $I(\sqrt{P}x_2 : y)$  is given by

$$I(\sqrt{P}x_2 : y) = H(y) - H(y|x_2) \quad (2)$$

where  $H(y)$  and  $H(y|x_2)$  are respectively given by

$$H(y) = - \int p(y) \log_2(p(y)) dy \quad \text{and} \quad (3)$$

$$H(y|x_2) = \frac{1}{N_2} \sum_{i=0}^{N_2-1} H(y|x_2 = x_2(i)) \quad (4)$$

such that  $p(y)$  denotes the probability density function (p.d.f) of  $y$ , given by

$$p(y) = \frac{1}{N_1 N_2} \sum_{k=0}^{N_1-1} \sum_{i=0}^{N_2-1} p(y|x_1 = x_1(k), x_2 = x_2(i))$$

where  $p(y|x_1 = x_1(k), x_2 = x_2(i))$  is given in (5), shown at the bottom of the page. To compute  $H(y|x_2)$ , we need to compute  $H(y|x_2 = x_2(i))$  for each index  $i$ . The term  $H(y|x_2 = x_2(i))$  is as given in (6), shown at the bottom of the page, where

$$p(y|x_2 = x_2(i)) = \frac{1}{N_1} \sum_{k=0}^{N_1-1} p(y|x_1 = x_1(k), x_2 = x_2(i)).$$

<sup>2</sup>The term  $I(a : b)$  denotes the mutual information between the variables  $a$  and  $b$  whereas the term  $I(a : b|c)$  denotes the mutual information between the variables  $a$  and  $b$  conditioned on the knowledge of the variable  $c$ .

$$p(y|x_1 = x_1(k), x_2 = x_2(i)) = \frac{1}{\pi \sigma^2} \exp\left(-\frac{|y - x_1(k) - x_2(i)|^2}{\sigma^2}\right) \quad (5)$$

$$H(y|x_2 = x_2(i)) = - \int p(y|x_2 = x_2(i)) \log_2(p(y|x_2 = x_2(i))) dy \quad (6)$$

$$I(\sqrt{P}x_2 : y) = \log_2(N_2) - \frac{1}{N_1 N_2} \sum_{k_1=0}^{N_1-1} \sum_{k_2=0}^{N_2-1} E \left[ \log_2 \left[ \frac{\sum_{i_1=0}^{N_1-1} \sum_{i_2=0}^{N_2-1} \exp\left(-|\sqrt{P}x_1(k_1) + \sqrt{P}x_2(k_2) - \sqrt{P}x_1(i_1) - \sqrt{P}x_2(i_2) + z|^2/\sigma^2\right)}{\sum_{i_1=0}^{N_1-1} \exp\left(-|\sqrt{P}x_1(k_1) - \sqrt{P}x_1(i_1) + z|^2/\sigma^2\right)} \right] \right] \quad (7)$$

$$I(\sqrt{P}x_1 : y|\sqrt{P}x_2) = \log_2(N_1) - \frac{1}{N_1} \sum_{k_1=0}^{N_1-1} E \left[ \log_2 \left[ \frac{\sum_{i_1=0}^{N_1-1} \exp\left(-|\sqrt{P}x_1(k_1) - \sqrt{P}x_1(i_1) + z|^2/\sigma^2\right)}{\exp(-|z|^2/\sigma^2)} \right] \right] \quad (8)$$

Using (4) and (3) in (2), the CC capacity  $I(\sqrt{P}x_2 : y)$  is given in (7), shown at the bottom of the previous page, where the expectation is with respect to the distribution of  $z$ . Similarly, the CC capacity  $I(\sqrt{P}x_1 : y|\sqrt{P}x_2)$  can be computed to be in (8), shown at the bottom of the previous page.

Using (7) and (8), the CC sum-capacity is  $I(\sqrt{P}x_2 : y) + I(\sqrt{P}x_1 : y|\sqrt{P}x_2)$  which can be proved to satisfy the following equality:

$$I(\sqrt{P}x_2 : y) + I(\sqrt{P}x_1 : y|\sqrt{P}x_2) = I(\sqrt{P}x_1 + \sqrt{P}x_2 : y). \quad (9)$$

Hence, the CC sum-capacity is equal to the CC capacity of the virtual AWGN channel seen by the destination with the input variable  $\sqrt{P}x_1 + \sqrt{P}x_2$ . Therefore, the achievable sum rate is upper-bounded by  $I(\sqrt{P}x_1 + \sqrt{P}x_2 : y)$ . However, for each user, the rate of transmission is maximized when the destination has the knowledge of the symbols transmitted by the other users. As a result, the CC capacity region of two-user GMAC is, as given by [1]

$$\begin{aligned} R_1 &\leq I(\sqrt{P}x_1 : y|\sqrt{P}x_2) \\ R_2 &\leq I(\sqrt{P}x_2 : y|\sqrt{P}x_1) \quad \text{and} \\ R_1 + R_2 &\leq I(\sqrt{P}x_1 + \sqrt{P}x_2 : y). \end{aligned} \quad (10)$$

In the following subsection, we discuss the impact of choosing uniquely decodable constellation pairs on the CC capacity regions of two-user GMAC.

#### A. Uniquely Decodable Constellation Pairs for GMAC

In this subsection, we assume  $P = 1$  for simplicity. Given two constellations  $\mathcal{S}_1$  and  $\mathcal{S}_2$ , we denote the sum constellation of  $\mathcal{S}_1$  and  $\mathcal{S}_2$  by  $\mathcal{S}_{\text{sum}}$  defined as  $\mathcal{S}_{\text{sum}} = \{x_1 + x_2 | \forall x_1 \in \mathcal{S}_1, x_2 \in \mathcal{S}_2\}$ . The adder channel in the two-user GMAC (as shown in Fig. 1) can be viewed as a mapping  $\phi$  given by  $\phi : \mathcal{S}_1 \times \mathcal{S}_2 \rightarrow \mathcal{S}_{\text{sum}}$  where  $\phi((x_1, x_2)) = x_1 + x_2$ .

*Definition 3: (Uniquely decodable constellation pair)* A constellation pair  $(\mathcal{S}_1, \mathcal{S}_2)$  is said to be uniquely decodable if the mapping  $\phi$  is one-one.

Example for a UD constellation pair is  $\mathcal{S}_1 = \{1, -1\}$  and  $\mathcal{S}_2 = \{\mathbf{i}, -\mathbf{i}\}$ . An example for a non-UD constellation pair is given by  $\mathcal{S}_1 = \mathcal{S}_2 = \{1, -1\}$ . Note that if  $\mathcal{S}_1$  and  $\mathcal{S}_2$  have more than one element common, then the pair  $(\mathcal{S}_1, \mathcal{S}_2)$  is necessarily non-UD. However, not having more than one common signal point is not sufficient for a pair to be UD, as exemplified by the pair  $\mathcal{S}_1 = \{1, \omega, \omega^2\}$  and  $\mathcal{S}_2 = \{-1, 1 + \omega, 1 + \omega^2\}$  where  $\omega$  is a complex cube root of unity.

It is clear that uncoded NO-MA communication with non-UD constellation pair results in ambiguity while performing joint decoding for the symbols of both the users at the destination. In order to circumvent this ambiguity, the two users can jointly construct code pairs  $(\mathcal{C}_1, \mathcal{C}_2)$  (codes constructed by adding redundancy across time) over the non-UD constellation pair so that the codewords of both users can be uniquely decoded. However, there will be a loss in the rate of transmission (in other words, there will be an expansion in the bandwidth) by adopting such schemes. Therefore, for band-limited GMAC, coding across time is not desirable to achieve the UD property, and hence, the use of UD constellations is essential.

#### B. Capacity Maximizing Constellation Pairs From Rotations

For GMAC with  $\mathcal{S}_1 = \mathcal{S}_2$ , it is clear that if one of the users employ an appropriate rotated version of the constellation used by the other, then the UD property can be attained. Moving one step further, we consider the problem of finding the optimal angle(s) of rotation between the constellation pairs such that the CC capacity region is maximally enlarged for a given value of  $\frac{P}{\sigma^2}$ . Henceforth, we refer the ratio,  $\frac{P}{\sigma^2}$  as SNR.

For a given constellation  $\mathcal{S}_1$ , let  $\mathcal{S}_2$  denote the set of symbols obtained by rotating all the symbols of  $\mathcal{S}_1$  by  $\theta$  degrees. From (9) and (10), the CC capacity region is determined by the mutual information values  $I(\sqrt{P}x_1 : y|\sqrt{P}x_2)$ ,  $I(\sqrt{P}x_2 : y|\sqrt{P}x_1)$  and  $I(\sqrt{P}x_2 : y)$  (or  $I(\sqrt{P}x_1 : y)$ ). Note that, the terms

$$\theta^* = \arg \max_{\theta \in (0, 2\pi)} I(\sqrt{P}x_2' : y) \quad (11)$$

$$M(\theta) = \sum_{k_1=0}^{N_1-1} \sum_{k_2=0}^{N_2-1} \log_2 \left[ \sum_{i_1=0}^{N_1-1} \sum_{i_2=0}^{N_2-1} \exp \left( -|\sqrt{P}x_1(k_1) - \sqrt{P}x_1(i_1) + e^{i\theta}(\sqrt{P}x_2(k_2) - \sqrt{P}x_2(i_2))|^2 / 2\sigma^2 \right) \right] \quad (12)$$

$$I^{(1)}(\sqrt{P}x_2' : y) = \sum_{k_1=0}^{N_1-1} \sum_{k_2=0}^{N_2-1} E \left[ \log_2 \left[ \frac{\sum_{i_1=0}^{N_1-1} \sum_{i_2=0}^{N_2-1} \exp \left( -|\sqrt{P}x_1(k_1) + \sqrt{P}x_2'(k_2) - \sqrt{P}x_1(i_1) - \sqrt{P}x_2'(i_2) + z|^2 / \sigma^2 \right)}{\sum_{i_1=0}^{N_1-1} \exp \left( -|\sqrt{P}x_1(k_1) - \sqrt{P}x_1(i_1) + z|^2 / \sigma^2 \right)} \right] \right] \quad (13)$$

$$I^{(2)}(\sqrt{P}x_2' : y) = \sum_{k_1=0}^{N_1-1} \sum_{k_2=0}^{N_2-1} E \left[ \underbrace{\log_2 \left[ \sum_{i_1=0}^{N_1-1} \sum_{i_2=0}^{N_2-1} \exp \left( -|\sqrt{P}x_1(k_1) + \sqrt{P}x_2'(k_2) - \sqrt{P}x_1(i_1) - \sqrt{P}x_2'(i_2) + z|^2 / \sigma^2 \right)} \right]}_{\beta(k_1, k_2, z)} \right]_{\lambda(k_1, k_2)} \quad (14)$$

$I(\sqrt{P}x_1 : y|\sqrt{P}x_2)$  and  $I(\sqrt{P}x_2 : y|\sqrt{P}x_1)$  are functions of the distance distribution (DD) of  $\mathcal{S}_1$  and  $\mathcal{S}_2$  respectively. Since, we start with a known  $\mathcal{S}_1$ , and  $\mathcal{S}_2 = e^{i\theta}\mathcal{S}_1$ , the DD of  $\mathcal{S}_1$  and  $\mathcal{S}_2$  are the same. Hence,  $I(\sqrt{P}x_1 : y|\sqrt{P}x_2)$  and  $I(\sqrt{P}x_2 : y|\sqrt{P}x_1)$  are independent of  $\theta$ . However, from (7), the term  $I(\sqrt{P}x_2 : y)$  is a function of the DD of  $\mathcal{S}_{\text{sum}}$ . Note that the DD of  $\mathcal{S}_{\text{sum}}$  changes with  $\theta$ , and hence, the term  $I(\sqrt{P}x_2 : y)$  is a function of  $\theta$ .

For an arbitrary constellation pair  $(\mathcal{S}_1, \mathcal{S}_2)$ , let  $\mathcal{S}'_2 = e^{i\theta}\mathcal{S}_2$  for some  $\theta$ . Also, let  $\mathcal{S}_1$  and  $\mathcal{S}'_2$  be the constellations employed by User-1 and User-2, respectively, such that  $x_1$  and  $x'_2$  denote the corresponding input symbols, wherein  $x'_2 = x_2 e^{i\theta}$ . On the similar lines of the discussion in the preceding paragraph, the term  $I(\sqrt{P}x'_2 : y)$  is a function of  $\theta$ . As a result,  $I(\sqrt{P}x'_2 : y)$  is maximized by choosing the angle of rotation  $\theta^*$  as in (11), shown at the bottom of the previous page. Note that  $I(\sqrt{P}x'_2 : y)$  is an expectation of a nonlinear function of the random variable  $z$ , and hence, the closed form expression of  $I(\sqrt{P}x'_2 : y)$  is not available. Therefore, in general, computing  $\theta^*$  is not straightforward. However, for high SNR values, the following theorem provides a metric (which is independent of the variable  $z$ ) to choose  $\theta$  such that  $I(\sqrt{P}x'_2 : y)$  is maximized which in-turn maximally enlarges the CC capacity region.

**Theorem 1:** For a given constellation pair  $(\mathcal{S}_1, \mathcal{S}_2)$ , let  $\mathcal{S}'_2 = e^{i\theta}\mathcal{S}_2$  for a variable  $\theta$ . At high SNR values, the optimum angle

of rotation required to maximize  $I(\sqrt{P}x'_2 : y)$  is approximated closely by  $\theta^*$  where

$$\theta^* = \arg \min_{\theta \in (0, 2\pi)} M(\theta)$$

where  $M(\theta)$  is given by (12), shown at the bottom of the previous page.

*Proof:* Since  $N_1$  and  $N_2$  are fixed, we have the following equality:

$$\arg \max_{\theta \in (0, 2\pi)} I(\sqrt{P}x'_2 : y) = \arg \min_{\theta \in (0, 2\pi)} I^{(1)}(\sqrt{P}x'_2 : y)$$

where  $I^{(1)}(\sqrt{P}x'_2 : y)$  is given in (13), shown at the bottom of the previous page. Since the denominator term inside the logarithm of  $I^{(1)}(\sqrt{P}x'_2 : y)$  is independent of  $\theta$ , we have

$$\arg \min_{\theta \in (0, 2\pi)} I^{(1)}(\sqrt{P}x'_2 : y) = \arg \min_{\theta \in (0, 2\pi)} I^{(2)}(\sqrt{P}x'_2 : y)$$

where  $I^{(2)}(\sqrt{P}x'_2 : y)$  is given in (14), shown at the bottom of the previous page. Note that the individual terms  $\lambda(k_1, k_2)$  of  $I^{(2)}(\sqrt{P}x'_2 : y)$  are of the form  $E[\log_2(\beta(k_1, k_2, z))]$  for random variable  $\beta(k_1, k_2, z)$ . Applying Jensen's inequality:

$$E[\log_2(\beta(k_1, k_2, z))] \leq \log_2[E(\beta(k_1, k_2, z))]$$

on  $\lambda(k_1, k_2)$  and replacing each term of the form  $x'_2(\cdot)$  by  $e^{i\theta}x_2(\cdot)$ , we have

$$I^{(2)}(\sqrt{P}x'_2 : y) \leq M(\theta)$$

$$I^{(2)}(\sqrt{P}x'_2 : y) = \sum_{k_1=0}^{N_1-1} \sum_{k_2=0}^{N_2-1} E \left[ \log_2 \left[ \exp(-|z|^2/\sigma^2) + \underbrace{\sum_{\substack{i_1=0 \\ (i_1, i_2) \neq (k_1, k_2)}}^{N_1-1} \sum_{i_2=0}^{N_2-1} \exp(-|\mu(k_1, k_2, i_1, i_2) + z|^2/\sigma^2)}_{(i_1, i_2) \neq (k_1, k_2)} \right] \right] \quad (15)$$

$$= \sum_{k_1=0}^{N_1-1} \sum_{k_2=0}^{N_2-1} E \left[ \log_2 \left[ \exp(-|z|^2/\sigma^2) (1 + M(k_1, k_2)) + \underbrace{\sum_{\substack{i_1=0 \\ \mu(k_1, k_2, i_1, i_2) \neq 0}}^{N_1-1} \sum_{i_2=0}^{N_2-1} \exp(-|\mu(k_1, k_2, i_1, i_2) + z|^2/\sigma^2)}_{\mu(k_1, k_2, i_1, i_2) \neq 0} \right] \right] \quad (16)$$

$$I^{(3)}(\sqrt{P}x'_2 : y) = \sum_{k_1=0}^{N_1-1} \sum_{k_2=0}^{N_2-1} E \left[ \log_2 (1 + M(k_1, k_2)) + \log_2 \left[ 1 + \frac{1}{(1 + M(k_1, k_2))} \underbrace{\sum_{\substack{i_1=0 \\ \mu(k_1, k_2, i_1, i_2) \neq 0}}^{N_1-1} \sum_{i_2=0}^{N_2-1} \exp\left(\frac{-|\mu(k_1, k_2, i_1, i_2) + z|^2 + |z|^2}{\sigma^2}\right)}_{\mu(k_1, k_2, i_1, i_2) \neq 0} \right] \right] \quad (17)$$

$$I^{(4)}(\sqrt{P}x'_2 : y) = \sum_{k_1=0}^{N_1-1} \sum_{k_2=0}^{N_2-1} E \left[ \log_2 (1 + M(k_1, k_2)) + \log_2 \left[ 1 + \underbrace{\frac{1}{(1 + M(k_1, k_2))} \sum_{\substack{i_1=0 \\ \mu(k_1, k_2, i_1, i_2) \neq 0}}^{N_1-1} \sum_{i_2=0}^{N_2-1} \exp\left(\frac{-|\mu(k_1, k_2, i_1, i_2) + z|^2}{\sigma^2}\right)}_{\mu(k_1, k_2, i_1, i_2) \neq 0}}_{\gamma(k_1, k_2, z)} \right] \right] \quad (18)$$

where  $M(\theta)$  is given by (12). Note that unlike  $I^{(2)}(\sqrt{P}x'_2 : y)$ , the term  $M(\theta)$  is independent of the variable  $z$ . In the rest of the proof, we show that at high SNR values, the following approximation holds good:

$$\arg \min_{\theta \in (0, 2\pi)} M(\theta) \approx \arg \min_{\theta \in (0, 2\pi)} I^{(2)}(\sqrt{P}x'_2 : y).$$

Note that the term  $I^{(2)}(\sqrt{P}x'_2 : y)$  can be written as in (15) and (16), shown at the bottom of the previous page, where

$$\mu(k_1, k_2, i_1, i_2) = \sqrt{P}x_1(k_1) + \sqrt{P}x'_2(k_2) - \sqrt{P}x_1(i_1) - \sqrt{P}x'_2(i_2)$$

and  $M(k_1, k_2) = |\mathcal{M}(k_1, k_2)|$  such that  $\mathcal{M}(k_1, k_2)$  is given by

$$\mathcal{M}(k_1, k_2) = \{(i_1, i_2) \neq (k_1, k_2) | \mu(i_1, i_2, k_1, k_2) = 0\}.$$

Removing the terms independent of  $z$  in (16), we have

$$\arg \min_{\theta \in (0, 2\pi)} I^{(2)}(\sqrt{P}x'_2 : y) = \arg \min_{\theta \in (0, 2\pi)} I^{(3)}(\sqrt{P}x'_2 : y)$$

where  $I^{(3)}(\sqrt{P}x'_2 : y)$  is given in (17), shown at the bottom of the previous page. At high SNR values, we have the approximation

$$\arg \min_{\theta \in (0, 2\pi)} I^{(3)}(\sqrt{P}x'_2 : y) \approx \arg \min_{\theta \in (0, 2\pi)} I^{(4)}(\sqrt{P}x'_2 : y)$$

where  $I^{(4)}(\sqrt{P}x'_2 : y)$  is given by (18), shown at the bottom of the previous page. At high SNR values, each term  $\gamma(k_1, k_2, z)$  in (18) is small, and hence, we use the approximation  $\log_2(1 + \gamma(k_1, k_2, z)) \approx \log_2(e)(\gamma(k_1, k_2, z))$  to obtain (20), shown at the bottom of the page. Solving expectation in (20), we get (21), shown at the bottom of the page. Once again, applying the approximation  $\log_2(1 + \delta(k_1, k_2)) \approx \log_2(e)(\delta(k_1, k_2))$  in (21), we get (22), shown at the bottom of the page, which is denoted by  $I^{(5)}(\sqrt{P}x'_2 : y)$ .

Now, we consider the term  $I^{(6)}(\sqrt{P}x'_2 : y)$ , given in (23), shown at the bottom of the page, and prove the following equality:

$$\arg \min_{\theta \in (0, 2\pi)} I^{(6)}(\sqrt{P}x'_2 : y) = \arg \min_{\theta \in (0, 2\pi)} I^{(5)}(\sqrt{P}x'_2 : y). \quad (19)$$

Once the above equality is proved, the statement of this theorem also gets proved since  $I^{(6)}(\sqrt{P}x'_2 : y)$  is a scaled version of  $M(\theta)$  [as shown in (24), at the bottom of the page]. Towards proving the equality in (19), note that at high SNR values,  $\delta(k_1, k_2)$  is small for all values of  $\theta$ . For those values of  $\theta$  which provide the UD property, we have  $\log_2(1 + M(k_1, k_2)) =$

$$I^{(4)}(\sqrt{P}x'_2 : y) \approx \sum_{k_1=0}^{N_1-1} \sum_{k_2=0}^{N_2-1} \left[ \log_2(1 + M(k_1, k_2)) + E \left[ \frac{\log_2(e)}{(1 + M(k_1, k_2))} \sum_{\substack{i_1=0 \\ \mu(k_1, k_2, i_1, i_2) \neq 0}}^{N_1-1} \sum_{i_2=0}^{N_2-1} \exp \left( \frac{-|\mu(k_1, k_2, i_1, i_2) + z|^2}{\sigma^2} \right) \right] \right] \quad (20)$$

$$= \sum_{k_1=0}^{N_1-1} \sum_{k_2=0}^{N_2-1} \left[ \log_2(1 + M(k_1, k_2)) + \left[ \frac{\log_2(e)}{2} \right] \underbrace{\left[ \frac{1}{(1 + M(k_1, k_2))} \sum_{\substack{i_1=0 \\ \mu(k_1, k_2, i_1, i_2) \neq 0}}^{N_1-1} \sum_{i_2=0}^{N_2-1} \exp \left( \frac{-|\mu(k_1, k_2, i_1, i_2)|^2}{2\sigma^2} \right) \right]}_{\delta(k_1, k_2)} \right] \quad (21)$$

$$I^{(5)}(\sqrt{P}x'_2 : y) = \sum_{k_1=0}^{N_1-1} \sum_{k_2=0}^{N_2-1} \left[ \log_2(1 + M(k_1, k_2)) + \left[ \frac{1}{2} \right] \log_2 \left[ 1 + \frac{1}{(1 + M(k_1, k_2))} \sum_{\substack{i_1=0 \\ \mu(k_1, k_2, i_1, i_2) \neq 0}}^{N_1-1} \sum_{i_2=0}^{N_2-1} \exp \left( \frac{-|\mu(k_1, k_2, i_1, i_2)|^2}{2\sigma^2} \right) \right] \right] \quad (22)$$

$$I^{(6)}(\sqrt{P}x'_2 : y) = \sum_{k_1=0}^{N_1-1} \sum_{k_2=0}^{N_2-1} \left[ \frac{1}{2} \right] \left[ \log_2(1 + M(k_1, k_2)) + \log_2 \left[ 1 + \frac{1}{(1 + M(k_1, k_2))} \sum_{\substack{i_1=0 \\ \mu(k_1, k_2, i_1, i_2) \neq 0}}^{N_1-1} \sum_{i_2=0}^{N_2-1} \exp \left( \frac{-|\mu(k_1, k_2, i_1, i_2)|^2}{2\sigma^2} \right) \right] \right] \quad (23)$$

$$= \left[ \frac{1}{2} \right] \sum_{k_1=0}^{N_1-1} \sum_{k_2=0}^{N_2-1} \log_2 \left[ \sum_{i_1=0}^{N_1-1} \sum_{i_2=0}^{N_2-1} \exp \left( -|\sqrt{P}x_1(k_1) - \sqrt{P}x_1(i_1) + e^{i\theta}(\sqrt{P}x_2(k_2) - \sqrt{P}x_2(i_2))|^2 / 2\sigma^2 \right) \right] = \frac{1}{2} M(\theta) \quad (24)$$

$0 \forall k_1, k_2$ . However, for those values of  $\theta$  which do not provide the UD property, we have

$$\log_2(1 + M(k_1, k_2)) \geq 1$$

for some  $k_1, k_2$ . And, at high SNR, for all  $\theta$ ,  $\log_2(1 + \delta(k_1, k_2)) \ll 1, \forall k_1, k_2$ . Due to these reasons, the values of  $\theta$  which do not provide the UD property do not minimize  $I^{(6)}(\sqrt{P}x_2' : y)$  as well as  $I^{(5)}(\sqrt{P}x_2' : y)$ . As a result, the optimal value of  $\theta$  must belong to the set of angles which provide the UD property. For such values of  $\theta$ , we have

$$I^{(6)}(\sqrt{P}x_2' : y) = I^{(5)}(\sqrt{P}x_2' : y)$$

and hence, the equality in (19) holds. Therefore, for high SNR values, instead of finding  $\theta^*$  which minimizes  $I^{(2)}(\sqrt{P}x_2' : y)$ , we propose to find  $\theta^*$  which minimizes  $M(\theta)$ , a tight upper bound on  $I^{(2)}(\sqrt{P}x_2' : y)$ . ■

From Theorem 1, it is clear that solving (12) is easier than solving (11) since  $M(\theta)$  is independent of the term  $z$ . However, note that for moderate and smaller values of SNR, the values of  $\theta^*$  obtained by solving (12) need not maximize  $I(\sqrt{P}x_2' : y)$  since the bound in (Section II-B) is not tight.

### C. Optimal Rotations for Some Known Constellations

In this subsection, we find angle(s) of rotation,  $\theta^*$  (in degrees) that minimizes  $M(\theta)$  for a given constellation  $\mathcal{S}_1$  and for a given SNR value such that  $\mathcal{S}_2 = e^{i\theta} \mathcal{S}_1$ . For the simulation results, we assume  $\sigma^2 = 2$ . The values of  $\theta^*$  are obtained by varying the relative angle of rotation from 0 to 180 in steps of 0.0625 degrees. In Table I, the values of  $\theta^*$  are presented for some well known constellations such as  $M$ -QAM,  $M$ -PSK for  $M = 4, 8$  and 16. Against every signal set, a two-tuple  $(a, b)$  is presented where the variable  $a$  denotes  $\theta^*$  and the variable  $b$  represents the multiplicity of  $\theta^*$  since, for some SNR values, there could be more than one value of  $\theta^*$  that minimizes  $M(\theta)$  (Example : QPSK at SNR = 8 dB, 16-PSK at SNR = 16 dB). In general, if  $\theta^*$  is calculated by varying the angle of rotation with different intervals, then the value of  $\theta^*$  and the multiplicity of  $\theta^*$  may change. When there are multiple values of  $\theta^*$  for a signal set, only one of them is provided in the table. Among the several angles available at high SNR values, the ones presented for BPSK reduces the complexity at the transmitters compared to the rest of the angles. This is because, for angles other than 90 degrees, each user should use more than one dimension which results in higher complexity. However, for complex signal sets, we present the one with the least value (Example: for QPSK at SNR = 8 dB and 16 dB).

1) *CC Capacity Regions of GMAC With  $\mathcal{S}_1 = \text{BPSK}$* : In Fig. 3, the CC capacity regions using BPSK constellation pair with optimal rotation and without rotation are given at SNR = -2 dB and 2 dB. Capacity regions of GMAC are also given in Fig. 3 at -2 dB and 2 dB. The plot shows that, for a given SNR value, CC capacity region of the BPSK constellation pair is contained inside the capacity region. Note that, with rotation, both users can transmit at rates equal to SISO AWGN channel capacity with BPSK constellation simultaneously. This is because  $\theta^* = 90$  degrees (at all SNR values) makes  $\mathcal{S}_1$  and  $\mathcal{S}_2$  orthogonal. Hence, both users can achieve the rates close to

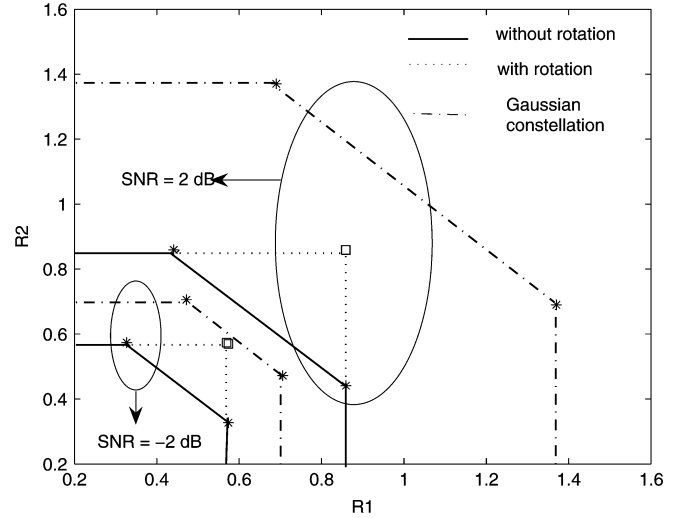


Fig. 3. CC capacity regions of BPSK constellation pair with optimal rotation and without rotation at SNR = -2 and 2 dB.

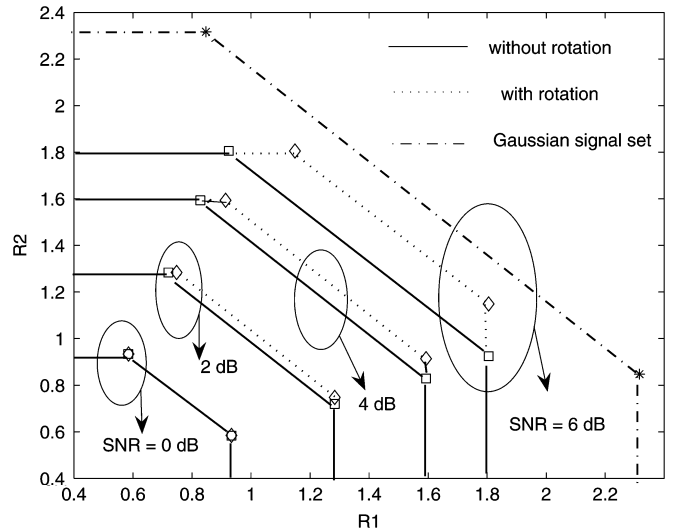


Fig. 4. CC capacity regions of QPSK constellation pair with optimal rotation and without rotation at SNR = 0, 2, 4 and 6 dB.

$I(\sqrt{P}x_1 : y|\sqrt{P}x_2)$  and  $I(\sqrt{P}x_2 : y|\sqrt{P}x_1)$  respectively at all SNR values. From Table I, note that there are several angles apart from 90 degrees which minimizes  $M(\theta)$  albeit they do not provide orthogonality to the users. The reason being that for BPSK constellation, the SNR values of 10 dB and higher are enough to make the additive noise at the destination negligible, and hence, a nonzero angle of rotation (not necessarily 90 degrees) is sufficient for both the users to communicate 1 bit each. In general, multiple optimal angles exist for any constellation at values of SNR beyond which the CC sum-capacity saturates.

2) *CC Capacity Regions of GMAC With  $\mathcal{S}_1 = \text{QPSK}$* : CC capacity regions for QPSK constellation pair is shown with optimal rotation and without rotation at different SNR values in Fig. 4. It is to be observed that rotation provides enlarged CC capacity region from the SNR value of 2 dB onwards. However, at SNR = 0 dB, CC capacity regions with optimal rotation and without rotation coincide. The percentage increase in  $I(\sqrt{P}x_2 : y)$  ranges from 4.3 percent at 2 dB to 100 percent for large SNR values. At SNR = 6 dB, capacity region of

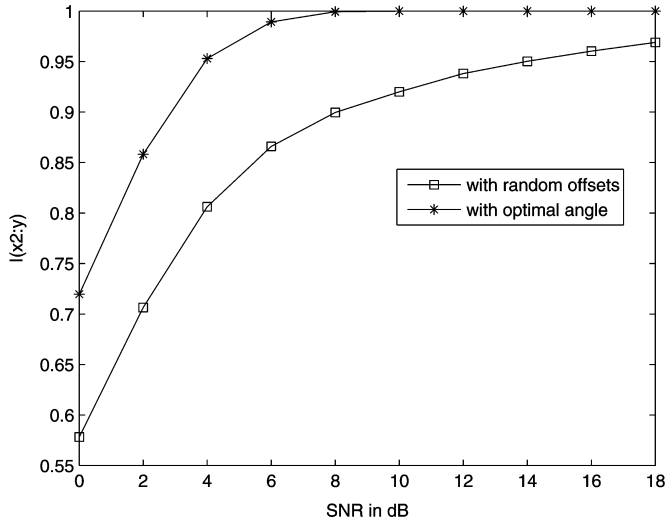


Fig. 5.  $I(x_2 : y)$  for BPSK constellation pair with (i) random offsets and (ii) without random offsets.

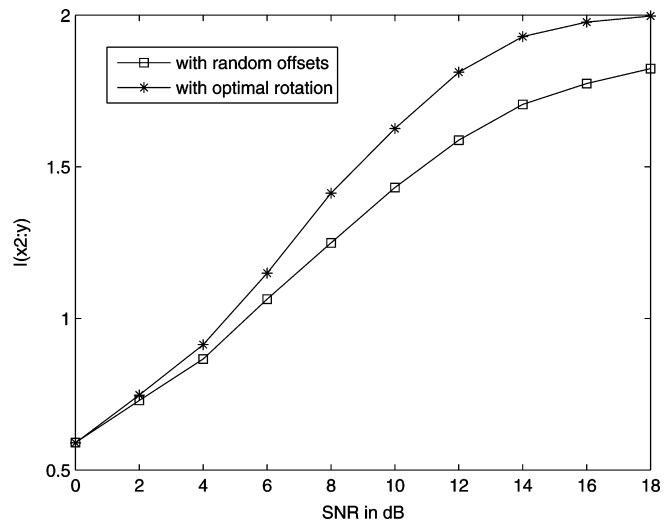


Fig. 6.  $I(x_2 : y)$  for QPSK constellation pair with (i) random offsets and (ii) without random offsets.

GMAC is also provided and it can be observed that the capacity region contains the CC capacity region of GMAC with QPSK constellation.

#### D. CC Capacity Region With Random Phase-Offsets

In this subsection, CC capacity regions of GMAC which are computed using the channel model in (1) are compared with those of GMAC when random phase offsets are introduced in the channel. The GMAC model with random offsets has been considered in [6], wherein the CC capacity of the resulting sum constellation has been computed in an AWGN channel. For such a setup, it is clear that the problem of designing UD constellation pairs is completely avoided. However, there will be a loss in the CC sum-capacity since the relative angle between the constellations is a random variable which can also take values other than  $\theta^*$ . Since  $I(\sqrt{P}x_2 : y)$  is the only term which is variant to rotations, we have plotted  $I(\sqrt{P}x_2 : y)$  at different SNR values with and without random offsets for BPSK and QPSK constellation pairs in Figs. 5 and 6 respectively. For the case with no

random offsets, values of  $\theta^*$  presented in Table I are used to plot  $I(\sqrt{P}x_2 : y)$ .

### III. TRELLIS CODED MODULATION (TCM) FOR TWO-USER GMAC: SIGNAL MODEL AND PROBLEM STATEMENT

In this section, we design code pairs based on TCM to achieve sum rates close to the CC sum-capacity (given in (10)) of GMAC.

For each  $i = 1, 2$ , let User- $i$  be equipped with a convolutional encoder  $C_i$  with  $m_i$  input bits and  $m_i + 1$  output bits. Throughout the section, we consider convolutional codes which add only 1-bit redundancy. Let the  $m_i + 1$  output bits of  $C_i$  take values from a complex signal set  $\mathcal{S}_i$  such that  $|\mathcal{S}_i| = 2^{m_i+1}$ . Henceforth, the set of codewords generated from  $C_1$  and  $C_2$  are represented by trellises  $T_1$  and  $T_2$  respectively. The sum trellis,  $T_{\text{sum}}$  for the trellis pair  $(T_1, T_2)$  is given in the following definition:

*Definition 4: (Sum trellis)* Let  $T_1$  and  $T_2$  represent two trellises with  $n + 1$  stages having the state complexity profiles  $\{q_{1,0}, q_{1,1}, \dots, q_{1,n}\}$  and  $\{q_{2,0}, q_{2,1}, \dots, q_{2,n}\}$  respectively. Let  $E_{1,i}^a$  and  $E_{2,i}^b$  respectively denote the edge sets originating from the state  $(a)$  of  $T_1$  and the state  $(b)$  of  $T_2$  in the  $i$ -th stage where  $1 \leq a \leq q_{1,i}$  and  $1 \leq b \leq q_{2,i}$ . Let the edge sets  $E_{1,i}^a$  and  $E_{2,i}^b$  be labeled with the symbols of the sets  $\mathcal{X}_i^a$  and  $\mathcal{Y}_i^b$  respectively. For the above trellis pair, the sum trellis,  $T_{\text{sum}}$  is a  $n + 1$  stage trellis such that

- The state complexity profile is

$$\{q_{1,0}q_{2,0}, q_{1,1}q_{2,1}, \dots, q_{1,n}q_{2,n}\}$$

where a particular state in the  $i$ -th stage is denoted by  $(a, b)$  such that  $1 \leq a \leq q_{1,i}$  and  $1 \leq b \leq q_{2,i}$ .

- The edge set originating from the state  $(a, b)$  in the  $i$ -th stage is given by  $E_i^{(a,b)} = E_{1,i}^a \times E_{2,i}^b$ . In particular, if  $2^{m_1}$  and  $2^{m_2}$  edges originate from state  $(a)$  and state  $(b)$  of  $T_1$  and  $T_2$  in the  $i$ -th stage respectively, then  $2^{m_1+m_2}$  edges originate from the state  $(a, b)$  in the  $i$ -th stage.
- The edges of the set  $E_i^{(a,b)}$  are labeled with the symbols of the set  $\mathcal{X}_i^a + \mathcal{Y}_i^b$ .

*Example 1:* For the trellis pair (shown in Fig. 9) labeled with elements of  $\mathcal{S}_1$  and  $\mathcal{S}_2$  (shown in Fig. 7), the sum trellis  $T_{\text{sum}}$  is as shown in Fig. 10 which is labeled with the elements of  $\mathcal{S}_{\text{sum}}$  (shown in Fig. 8).

We assume that the destination performs joint decoding of the symbols of User-1 and User-2 by decoding for a sequence over  $\mathcal{S}_{\text{sum}}$  on the sum trellis,  $T_{\text{sum}}$ . For the trellis pair  $(T_1, T_2)$  and the constellation pair  $(\mathcal{S}_1, \mathcal{S}_2)$ , the destination views an equivalent SISO AWGN channel with a virtual source equipped with the trellis,  $T_{\text{sum}}$  labeled with the elements of  $\mathcal{S}_{\text{sum}}$ . For a SISO AWGN channel, if the source is equipped with a trellis,  $T$  and a constellation  $\mathcal{S}$ , the following Ungerboeck design rules [11] are well known:

- All the symbols of  $\mathcal{S}$  should occur with equal frequency and with some amount of regularity.
- Transitions originating from the same state (or joining the same state) must be labeled with subsets of  $\mathcal{S}$  whose minimum Euclidean distance is maximized.

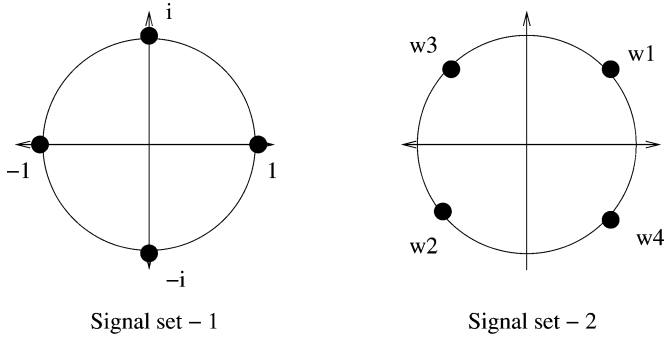
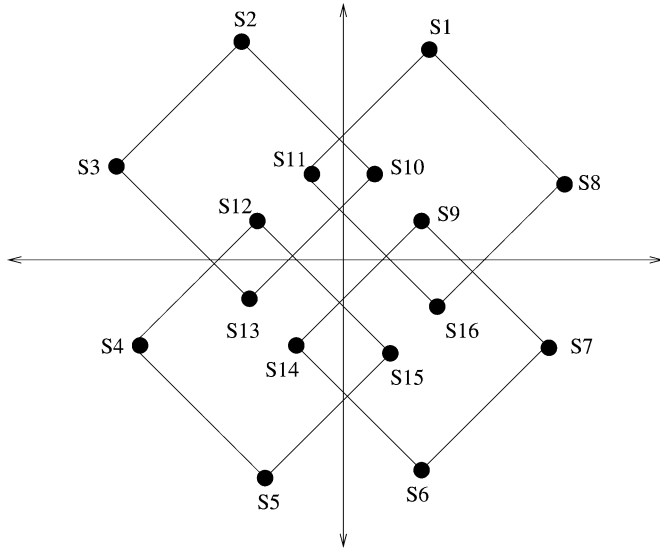
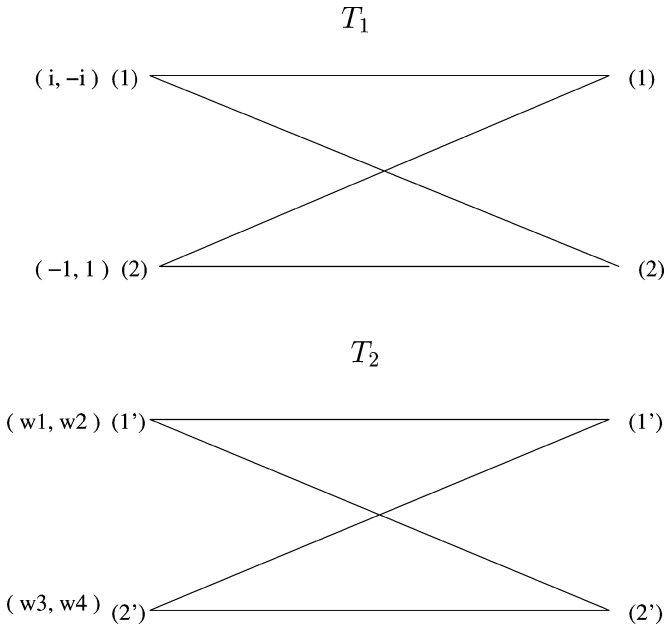
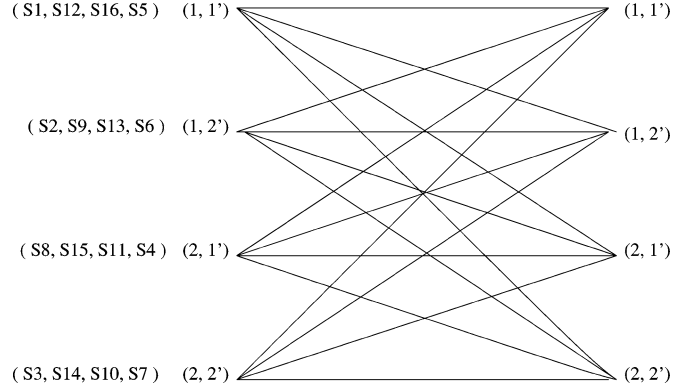


Fig. 7. Constellations used by User-1 and User-2.

Fig. 8. Sum constellation,  $\mathcal{S}_{\text{sum}}$  for the signal sets presented in Fig. 7.Fig. 9. Two state trellises of User-1 ( $T_1$ ) and User-2 ( $T_2$ ).

Due to the existence of an equivalent AWGN channel in the GMAC set-up, the sum trellis,  $T_{\text{sum}}$  has to be labeled with the

Fig. 10. Sum trellis,  $T_{\text{sum}}$  of trellises  $T_1$  and  $T_2$  presented in Fig. 9.

elements of  $\mathcal{S}_{\text{sum}}$  satisfying the above design rules. However, such a labeling rule can be obtained on  $T_{\text{sum}}$  only through the pairs  $(T_1, T_2)$  and  $(\mathcal{S}_1, \mathcal{S}_2)$ . Hence, we propose labeling rules on  $T_1$  and  $T_2$  using  $\mathcal{S}_1$  and  $\mathcal{S}_2$  respectively such that  $T_{\text{sum}}$  is labeled with the elements of  $\mathcal{S}_{\text{sum}}$  as per Ungerboeck rules. The problem statement has been explained below.

Since the number of input bits to  $C_i$  is  $m_i$ , there are  $2^{m_i}$  edges diverging from (or converging to; henceforth, we only refer to diverging edges) each state of  $T_i$ . Also, as there is only one bit redundancy added by the encoder, and as  $|\mathcal{S}_i| = 2^{m_i+1}$ , the edges diverging from each state have to be labeled with the elements of a subset of  $\mathcal{S}_i$  of size  $2^{m_i}$ . Therefore, for each  $i$ ,  $\mathcal{S}_i$  has to be partitioned into two sets  $\mathcal{S}_i^1$  and  $\mathcal{S}_i^2$  and the diverging edges from each state of  $T_i$  have to be labeled with the elements of either  $\mathcal{S}_i^1$  or  $\mathcal{S}_i^2$ . From the definition of sum trellis, there are  $2^{m_1+m_2}$  edges diverging from each state of  $T_{\text{sum}}$  and these edges get labeled with the elements of one of the following sets:

$$\mathcal{A} = \{\mathcal{S}_1^i + \mathcal{S}_2^j | i, j \in \{1, 2\}\}.$$

To satisfy Ungerboeck design rules, the transitions originating from the same state of  $T_{\text{sum}}$  must be assigned symbols that are separated by largest minimum distance.

**Problem Statement:** Therefore, the problem addressed is to find a partitioning of  $\mathcal{S}_i$  into two sets  $\mathcal{S}_i^1$  and  $\mathcal{S}_i^2$  of equal cardinality such that the minimum Euclidean distance,  $d_{\min}$  of each one of the sets in  $\mathcal{A}$  is maximized. However, since  $d_{\min}$  values of the sets in  $\mathcal{A}$  can potentially be different, we find a partitioning such that the minimum of the  $d_{\min}$  values of the sets in  $\mathcal{A}$  is maximized.

#### IV. DESIGNING TCM SCHEMES WITH PSK CONSTELLATIONS

The *set partitioning problem* described above is applicable to arbitrary constellations  $\mathcal{S}_1$  and  $\mathcal{S}_2$ . Also, from Subsection II-B, a relative angle of rotation,  $\theta$  has to be introduced to obtain the UD property. As a result, the solution to the *set partitioning problem* also depends on  $\theta$ . In this section, we present the solution to the above problem for the class of PSK signal sets with arbitrary values of  $N_1$  and  $N_2$  but, for the specific value of  $\theta = \frac{\pi}{N_2}$  [24]. In other words, we propose labeling rules on the trellis codes to approach *any rate pair* (for example, the points R, Q shown in Fig. 2) within the CC capacity region of PSK signal

sets with equal power constraint for the two users. In particular, we propose a solution to the problem of designing labeling rules when  $\mathcal{S}_1$  and  $\mathcal{S}_2$  are symmetric PSK signal sets of cardinality  $N_1$  and  $N_2$  respectively where  $N_1 = 2^{u_1}$  and  $N_2 = 2^{u_2}$  for some  $u_1, u_2 \geq 1$ . Without loss of generality, we assume  $P = 1$  and  $N_2 \geq N_1$ . Let  $k$  denote the ratio  $\frac{N_2}{N_1}$  (note that  $\frac{N_2}{N_1} \geq 1$ ). To obtain the UD property at the receiver and to enlarge the CC capacity region, we employ a  $\frac{\pi}{N_2}$  rotated version of  $\mathcal{S}_2$ .

#### A. Structure of the Sum Constellation of Two PSK Constellations

Let  $\mathcal{S}_1$  and  $\mathcal{S}_2$  represent two symmetric PSK signal sets of cardinality  $N_1$  and  $N_2$  respectively such that the signal set  $\mathcal{S}_2$  is rotated by an angle  $\frac{\pi}{N_2}$ . Let  $x(n_1)$  and  $x'(n_2)$  denote the points  $e^{\frac{i2\pi n_1}{N_1}}$  and  $e^{\frac{i2\pi n_2}{N_2}} e^{\frac{i\pi}{N_2}}$  of  $\mathcal{S}_1$  and  $\mathcal{S}_2$  respectively for  $0 \leq n_1 \leq N_1 - 1$  and  $0 \leq n_2 \leq N_2 - 1$ . The sum constellation  $\mathcal{S}_{\text{sum}}$  of  $\mathcal{S}_1$  and  $\mathcal{S}_2$  can be written as given in (25), shown at the bottom of the page, where

$$x(n_1) + x'(kn_1 + m) = e^{\frac{i2\pi n_1}{N_1}} + e^{i\left\{\frac{2\pi n_1}{N_1} + \frac{\pi(2m+1)}{N_2}\right\}}$$

and

$$x(n_1) + x'(kn_1 - m - 1) = e^{\frac{i2\pi n_1}{N_1}} + e^{i\left\{\frac{2\pi n_1}{N_1} - \frac{\pi(2m+1)}{N_2}\right\}}$$

such that  $x'(-p) = x'(N_2 - p)$  for any  $0 \leq p \leq N_2 - 1$ . The phase components of the points  $x(n_1) + x'(kn_1 + m)$  and  $x(n_1) + x'(kn_1 - m - 1)$  are given by  $\frac{2\pi n_1}{N_1} + \frac{\pi(2m+1)}{2N_2}$  and  $\frac{2\pi n_1}{N_1} - \frac{\pi(2m+1)}{2N_2}$  respectively. For a fixed  $m$ , the set of points of the form  $x(n_1) + x'(kn_1 + m)$  and  $x(n_1) + x'(kn_1 - m - 1)$  lie on a circle of radius  $2\cos\left(\frac{\pi(2m+1)}{2N_2}\right)$  and let that circle be denoted by  $C^m$ . Therefore,  $\mathcal{S}_{\text{sum}}$  takes the structure of  $\frac{N_2}{2}$  concentric *asymmetric* PSK signal sets. As a special case,  $\mathcal{S}_{\text{sum}}$  takes the structure of  $\frac{N_2}{2}$  concentric *symmetric* PSK signal sets when  $N_1 = N_2$  [25]. As an example, see Fig. 12 which shows  $\mathcal{S}_{\text{sum}}$  when  $\mathcal{S}_1$  is a QPSK signal set and  $\mathcal{S}_2$  is a 8-PSK signal set. The set containing the radii of the  $\frac{N_2}{2}$  circles is given by

$$\mathcal{R} = \left\{ 2\cos\left(\frac{\pi(2m+1)}{2N_2}\right) \mid 0 \leq m \leq \frac{N_2}{2} - 1 \right\}.$$

Henceforth, throughout the section,  $r(C^m)$  denotes the radius of the circle  $C^m$ . Since the radius of each circle is a cosine function, the elements of  $\mathcal{R}$  satisfies the following relation:

$$r(C^{M/2-1}) \leq r(C^{M/2-2}) \leq \dots \leq r(C^0).$$

For the elements of  $\mathcal{R}$ , we have the following proposition.

**Proposition 1:** The sequence  $\{r(C^q) - r(C^{q+1})\}$  from  $q = 0$  to  $\frac{N_2}{2} - 2$  is an increasing sequence.

*Proof:* Using standard trigonometric identities, the term  $r(C^q) - r(C^{q+1})$  is given by  $4\sin\left(\frac{\pi}{N_2}\right)\sin\left(\frac{\pi(q+1)}{2N_2}\right)$ . Since  $\frac{\pi(\frac{N_2}{2}-1)}{2N_2} \leq \frac{\pi}{2}$ , the sequence  $\{\sin\left(\frac{\pi(q+1)}{2N_2}\right)\}$  is an increasing sequence as  $q$  increases from 0 to  $\frac{N_2}{2} - 2$ . ■

Using the phase information of each point in  $\mathcal{S}_{\text{sum}}$ , the following observations can be made:

- 1) For a fixed  $m$ , the angular separation between the two points  $x(n_1) + x'(kn_1 + m)$  and  $x(n'_1) + x'(kn'_1 + m)$  on  $C^m$  is  $\frac{2\pi(n_1 - n'_1)}{N_1}$  for all  $m = 0$  to  $\frac{N_2}{2} - 1$ . Similarly, for a fixed  $m$ , the angular separation between the two points  $x(n_1) + x'(kn_1 - m - 1)$  and  $x(n'_1) + x'(kn'_1 - m - 1)$  on  $C^m$  is  $\frac{2\pi(n_1 - n'_1)}{N_1}$  for all  $m = 0$  to  $\frac{N_2}{2} - 1$ .
- 2) For a fixed  $m$ , the angular separation between the point,  $x(n_1) + x'(kn_1 + m)$  on  $C^m$  and the point  $x(n'_1) + x'(kn'_1 - m - 1)$  on  $C^m$  is  $\frac{2\pi(n_1 - n'_1)}{N_1} + \frac{\pi(2m+1)}{N_2}$  for all  $m = 0$  to  $\frac{N_2}{2} - 1$ .
- 3) For a fixed  $m$ , the angular separation between the point  $x(n_1) + x'(kn_1 + m)$  on  $C^m$  and the point  $x(n'_1) + x'(kn'_1 - (m - 1) - 1)$  on  $C^{m-1}$  is  $\frac{2\pi(n_1 - n'_1)}{N_1} + \frac{\pi(2m)}{N_2}$  for all  $m = 1$  to  $\frac{N_2}{2} - 1$ .
- 4) For a fixed  $m$ , the angular separation between the point  $x(n_1) + x'(kn_1 - m - 1)$  on  $C^m$  and the point  $x(n'_1) + x'(kn'_1 + (m - 1))$  on  $C^{m-1}$  is  $\frac{2\pi(n_1 - n'_1)}{N_1} - \frac{\pi(2m)}{N_2}$  for all  $m = 1$  to  $\frac{N_2}{2} - 1$ .

#### B. Structure of the Sets in $\mathcal{A}$ Induced by Ungerboeck Partitioning on $\mathcal{S}_1$ and $\mathcal{S}_2$

In this subsection, first, we partition both  $\mathcal{S}_1$  and  $\mathcal{S}_2$  into two groups (due to one bit redundancy added by the two encoders) using Ungerboeck rules and then, exploiting the structure of  $\mathcal{S}_{\text{sum}}$ , we compute the minimum Euclidean distance,  $d_{\min}$  of each one of the sets in  $\mathcal{A}$ . For each  $i = 1, 2$ , let  $\mathcal{S}_i$  be partitioned into two sets of equal size using Ungerboeck rules which results in two sets denoted by  $\mathcal{S}_i^e$  and  $\mathcal{S}_i^o$  such that  $d_{\min}$  of  $\mathcal{S}_i^e$  and  $\mathcal{S}_i^o$  is maximized. Since the number of sets resulting from the partition is two, the minimum angular separation,  $\phi_{\min}$  between the points in each set is  $\frac{4\pi}{N_i}$ . The two groups of  $\mathcal{S}_1$  are of the form

$$\mathcal{S}_1^e = \left\{ x(n_1) \mid n_1 = 2q \text{ for } 0 \leq q \leq \frac{N_1}{2} - 1 \right\} \quad \text{and} \\ \mathcal{S}_1^o = \left\{ x(n_1) \mid n_1 = 2q + 1 \text{ for } 0 \leq q \leq \frac{N_1}{2} - 1 \right\}.$$

Similarly, the two groups of  $\mathcal{S}_2$  are of the form

$$\mathcal{S}_2^e = \left\{ x'(n_2) \mid n_2 = 2l \text{ for } 0 \leq l \leq \frac{N_2}{2} - 1 \right\} \quad \text{and} \\ \mathcal{S}_2^o = \left\{ x'(n_2) \mid n_2 = 2l + 1 \text{ for } 0 \leq l \leq \frac{N_2}{2} - 1 \right\}.$$

It is clear that the four sets  $\mathcal{S}_1^e + \mathcal{S}_2^e, \mathcal{S}_1^e + \mathcal{S}_2^o, \mathcal{S}_1^o + \mathcal{S}_2^e$  and  $\mathcal{S}_1^o + \mathcal{S}_2^o$  form a partition of  $\mathcal{S}_{\text{sum}}$ . The partition induced on  $\mathcal{S}_{\text{sum}}$  due to the partition of  $\mathcal{S}_1$  and  $\mathcal{S}_2$  has been depicted in Fig. 11. Henceforth, the set  $\mathcal{S}_1^e + \mathcal{S}_2^e$  and its minimum Euclidean distance are denoted by  $\mathcal{S}_{\text{sum}}^{\alpha\beta}$  and  $d_{\min}^{\alpha\beta}$  respectively  $\forall \alpha, \beta = e$  and  $o$ . In the next subsection, the structure of  $\mathcal{S}_{\text{sum}}^{eo}$  is studied and  $d_{\min}^{eo}$  value is calculated. The  $d_{\min}$  values of the rest of the sets in  $\mathcal{A}$  can be calculated on the similar lines.

$$\mathcal{S}_{\text{sum}} = \left\{ x(n_1) + x'(kn_1 + m), x(n_1) + x'(kn_1 - m - 1) \mid 0 \leq n_1 \leq N_1 - 1 \text{ and } 0 \leq m \leq \frac{N_2}{2} - 1 \right\} \quad (25)$$

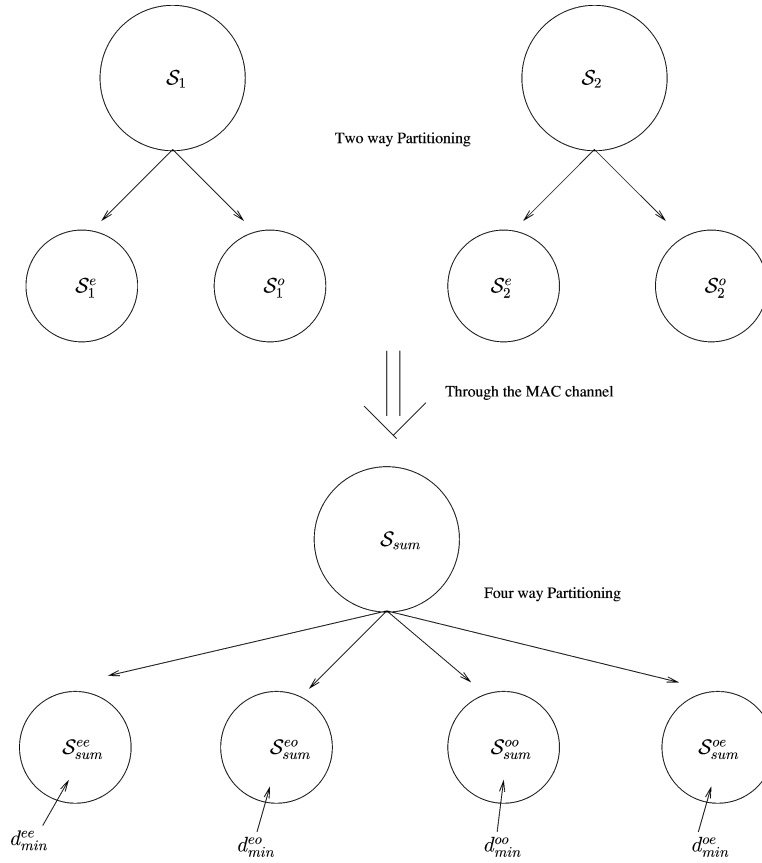


Fig. 11. Set partitioning of  $S_{sum}$  induced by the set partitioning of  $S_1$  and  $S_2$ .

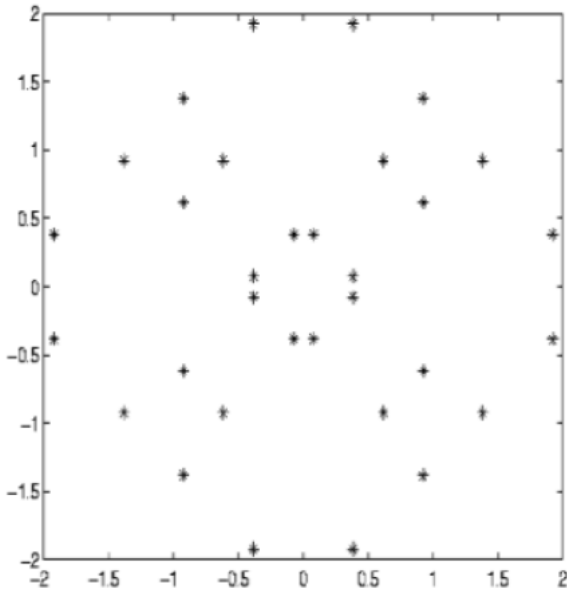


Fig. 12. The structure of  $S_{sum}$  when  $S_1 = \text{QPSK}$  and  $S_2 = 8\text{-PSK}$  when  $\theta = \frac{\pi}{8}$ .

1) Calculation of  $d_{\min}$  of  $S_1^e + S_2^o$ : The elements of  $S_1^e + S_2^o$  [as given in (26), shown at the bottom of the page] are of the form  $x(n_1) + x'(kn_1 + m)$  and  $x(n_1) + x'(kn_1 - m - 1)$  where  $n_1$  takes even value while  $kn_1 + m$  and  $kn_1 - m - 1$  take odd values. When  $m$  is odd, note that  $kn_1 + m$  is odd and  $kn_1 - m - 1$  is even, and hence,  $S_{sum}^{eo}$  will have  $\frac{N_1}{2}$  points of the form  $x(n_1) + x'(kn_1 + m)$  and no points of the form  $x(n_1) + x'(kn_1 - m - 1)$  on  $C^m$ . Similarly, when  $m$  is even,  $S_{sum}^{eo}$  will have  $\frac{N_1}{2}$  points of the form  $x(n_1) + x'(kn_1 - m - 1)$  and no points of the form  $x(n_1) + x'(kn_1 + m)$  on  $C^m$ .

Since  $n_1$  takes only even values, using *observation 1*) in the previous subsection,  $\phi_{\min}$  between the points of  $S_{sum}^{eo}$  on any circle is  $\frac{4\pi}{N_1}$ . Hence, the points of  $S_{sum}^{eo}$  are maximally separated on every circle. The following two propositions help in finding the  $d_{\min}$  value of  $S_{sum}^{eo}$ .

*Proposition 2:* For all  $q = 1$  to  $\frac{N_2}{2} - 1$ ,  $r(C^{q-1})$  and  $r(C^q)$  satisfy the inequality

$$d\left(r(C^{q-1}), r(C^q)e^{i\frac{2\pi}{N_2}}\right) \geq d\left(r(C^q), r(C^q)e^{i\frac{2\pi}{N_2}}\right).$$

*Proof:* For  $a, b \in \mathbb{C}$ , let  $l(a, b)$  denote the line segment joining  $a$  and  $b$ . Note that the three complex points  $0, r(C^{q-1})$

$$S_1^e + S_2^o = \left\{ x(n_1) + x'(n_2) | n_1 = 2q \text{ and } n_2 = 2l + 1 \text{ for } q = 0 \text{ to } \frac{N_1}{2} - 1 \text{ and } l = 0 \text{ to } \frac{N_2}{2} - 1 \right\} \quad (26)$$

and  $r(C^{q-1})e^{i\frac{2\pi}{N_2}}$  form the three vertices of an isosceles triangle in  $\mathbb{R}^2$ . Since  $r(C^q) \leq r(C^{q-1})$ , we have

$$d\left(0, r(C^q)e^{i\frac{2\pi}{N_2}}\right) \leq d\left(0, r(C^{q-1})e^{i\frac{2\pi}{N_2}}\right).$$

Therefore, the four points  $r(C^q), r(C^q)e^{i\frac{2\pi}{N_2}}, r(C^{q-1})$  and  $r(C^{q-1})e^{i\frac{2\pi}{N_2}}$  form the vertices of an isosceles trapezoid  $\Upsilon$  such that  $l(r(C^q), r(C^q)e^{i\frac{2\pi}{N_2}})$  is parallel to  $l(r(C^{q-1}), r(C^{q-1})e^{i\frac{2\pi}{N_2}})$ . Also, note that  $d(r(C^{q-1}), r(C^q)e^{i\frac{2\pi}{N_2}})$  is the length of the diagonal of the trapezoid  $\Upsilon$ . Since the angle between the line segments  $l(r(C^q), r(C^q)e^{i\frac{2\pi}{N_2}})$  and  $l(r(C^q), r(C^{q-1}))$  is obtuse, we have  $d(r(C^{q-1}), r(C^q)e^{i\frac{2\pi}{N_2}}) \geq d(r(C^q), r(C^q)e^{i\frac{2\pi}{N_2}})$ . ■

*Proposition 3:* For  $N_1 \geq 8$ ,  $r(C^{2k-1})$  satisfy the inequality

$$d\left(r(C^{2k-1}), r(C^{2k-1})e^{i\frac{2\pi}{N_2}}\right) \geq 4\sin\left(\frac{\pi}{N_2}\right)\sin\left(\frac{2\pi}{N_1}\right).$$

*Proof:* We prove the inequality

$$2r\left(C^{\frac{N_2}{2}-1}\right)\sin\left(\frac{2\pi}{N_1}\right) \leq d\left(r(C^{2k-1}), r(C^{2k-1})e^{i\frac{2\pi}{N_2}}\right).$$

The two terms across the inequality can be written as a ratio as

$$\frac{2r\left(C^{\frac{N_2}{2}-1}\right)\sin\left(\frac{2\pi}{N_1}\right)}{d\left(r(C^{2k-1}), r(C^{2k-1})e^{i\frac{2\pi}{N_2}}\right)} = \frac{\sin\left(\frac{\pi}{2N_2}\right)\sin\left(\frac{4k\pi}{2N_2}\right)}{\cos\left(\frac{\pi(4k-1)}{2N_2}\right)\sin\left(\frac{\pi}{N_2}\right)}. \quad (27)$$

Since  $\sin\left(\frac{\pi}{2N_2}\right) < \sin\left(\frac{\pi}{N_2}\right)$ , we have to prove that  $\sin\left(\frac{4k\pi}{2N_2}\right) < \cos\left(\frac{\pi(4k-1)}{2N_2}\right)$ . Note that

$$\frac{\sin\left(\frac{4k\pi}{2N_2}\right)}{\cos\left(\frac{\pi(4k-1)}{2N_2}\right)} \leq \frac{\sin\left(\frac{4k\pi}{2N_2}\right)}{\cos\left(\frac{\pi 4k}{2N_2}\right)} = \tan\left(\frac{\pi 4k}{2N_2}\right)$$

and  $\tan\left(\frac{\pi 4k}{2N_2}\right) \leq 1$  whenever  $\frac{4k}{2N_2} \leq \frac{1}{4}$ . The inequality  $\frac{4k}{2N_2} \leq \frac{1}{4}$  holds when  $N_1 \geq 8$ . This completes the proof. ■

Using the above two propositions, the  $d_{\min}$  value of the set  $\mathcal{S}_{\text{sum}}^{eo}$  is presented in the following lemma:

*Lemma 1:* The minimum Euclidean distance of  $\mathcal{S}_{\text{sum}}^{eo}$  is

$$d_{\min}^{eo} = 4\sin\left(\frac{\pi}{2N_2}\right)\sin\left(\frac{2\pi}{N_1}\right). \quad (28)$$

*Proof:* Since the points of  $\mathcal{S}_{\text{sum}}^{eo}$  are maximally separated on every circle (with  $\phi_{\min} = \frac{4\pi}{N_1}$ ) and  $C^{\frac{N_2}{2}-1}$  is the innermost circle,  $d(r(C^{\frac{N_2}{2}-1}), r(C^{\frac{N_2}{2}-1})e^{i\frac{4\pi}{N_1}}) = 4\sin\left(\frac{\pi}{2N_2}\right)\sin\left(\frac{2\pi}{N_1}\right) = d_1$  is a contender for  $d_{\min}^{eo}$ . For this to be true, all other intradisances in the set must be larger than or equal to  $d_1$ . In particular, we have to show that the distances between the points on any two consecutive circles must be larger than  $d_1$ . In that direction, the first observation is the equality,  $r(C^{2k-1}) - r(C^{2k}) = d_1$ . From Proposition 1,  $r(C^q) - r(C^{q+1}) \geq d_1$  for all  $q \geq 2k-1$ . Hence,

the points on  $C^q$  and  $C^{q-1}$  (irrespective of their angular separation) are separated by a distance larger than  $d_1$  for all  $q = 2k$  to  $\frac{N_2}{2} - 1$ . Further, we must prove that a point on  $C^q$  and a point on  $C^{q-1}$  are separated by a distance larger than  $d_1$  for all  $q = 1$  to  $2k-1$ . In that direction, it can be shown that  $\phi_{\min}$  between a point on  $C^q$  and a point on  $C^{q-1}$  is one of the values from the set,  $\Omega = \{\pm\frac{2\pi}{N_2}, \pm\frac{4\pi}{N_2}, \dots, \pm\frac{2(k-1)\pi}{N_2}\}$  depending on the value of  $q$  for all  $q = 1$  to  $2k-1$ . Using Proposition 2, we have

$$d\left(r(C^{2k-2}), r(C^{2k-1})e^{i\frac{2\pi}{N_2}}\right) \geq d\left(r(C^{2k-1}), r(C^{2k-1})e^{i\frac{2\pi}{N_2}}\right).$$

Furthermore, using the above inequality with the inequality in Proposition 3, we have

$$d\left(r(C^{2k-2}), r(C^{2k-1})e^{i\frac{2\pi}{N_2}}\right) \geq d_1. \quad (29)$$

Note that the above inequality holds only when  $N_1 \geq 8$ . However, when  $N_1 = 4$ , we have  $2k-1 = \frac{N_2}{2} - 1$ . Therefore,  $r(C^{2k-1}) = r(C^{\frac{N_2}{2}-1})$  will be the radius of the innermost circle wherein the minimum angular separation is  $\frac{4\pi}{N_1}$ . Hence, Proposition 3 is not applicable when  $N_1 = 4$ . Since  $r(C^{q-1}) > r(C^q)$ , the inequality in (29) can be extended to

$$d\left(r(C^{q-1}), r(C^q)e^{i\frac{2\pi}{N_2}}\right) \geq d_1 \quad \text{for all } q = 1 \text{ to } 2k-1.$$

Hence,  $d(r(C^{q-1}), r(C^q)e^{i\theta'}) \geq d_1$  for all  $\theta' \in \Omega$ . With this, we have proved that a point on  $C^q$  and a point on  $C^{q-1}$  are separated by a distance larger than  $d_1$  for all  $q = 1$  to  $2k-1$ . This completes the proof. ■

The  $d_{\min}$  values of the rest of the sets in  $\mathcal{A}$  can be calculated on the similar lines. The following lemma provides the  $d_{\min}$  values of  $\mathcal{S}_{\text{sum}}^{oo}, \mathcal{S}_{\text{sum}}^{ee}$  and  $\mathcal{S}_{\text{sum}}^{oe}$ .

*Lemma 2:* The minimum Euclidean distances of  $\mathcal{S}_{\text{sum}}^{oo}, \mathcal{S}_{\text{sum}}^{ee}$  and  $\mathcal{S}_{\text{sum}}^{oe}$  are given by

$$d_{\min}^{ee} = d_{\min}^{oe} = d_{\min}^{oo} = 4\sin\left(\frac{\pi}{2N_2}\right)\sin\left(\frac{2\pi}{N_1}\right). \quad (30)$$

*Proof:* The proof is on the similar lines of the proof for Lemma 1. ■

### C. Optimality of Ungerboeck Partitioning for PSK Constellations

In the preceding subsection,  $d_{\min}$  values of each one of the sets of  $\mathcal{A}$  induced by Ungerboeck partition on  $\mathcal{S}_1$  and  $\mathcal{S}_2$  have been computed (from (28) and (30), since all the  $d_{\min}$  values are the same, we refer to them as  $d_{\min}^U$ ). In this subsection, we show that a non-Ungerboeck partition on either  $\mathcal{S}_1$  or  $\mathcal{S}_2$  results in a set  $\mathcal{A}$  such that the  $d_{\min}$  of at least one of the sets in  $\mathcal{A}$  is lesser than  $d_{\min}^U$ .

*Theorem 2:* For  $\theta = \frac{\pi}{N_2}$ , Ungerboeck partitioning on  $\mathcal{S}_1$  and  $\mathcal{S}_2$  into two sets is optimal in maximizing the minimum of the  $d_{\min}$  values of the sets in  $\mathcal{A}$ .

*Proof:* Let  $\mathcal{S}_i^1$  and  $\mathcal{S}_i^2$  be the two sets (of equal cardinality) resulting from a partition of  $\mathcal{S}_i$  for  $i = 1, 2$ . If either  $\mathcal{S}_1$  or  $\mathcal{S}_2$  is not Ungerboeck partitioned, then it is to be shown that,  $d_{\min}$  of

at least one of the sets in the set  $\mathcal{A} = \{\mathcal{S}_1^i + \mathcal{S}_2^j | \forall i, j = 1, 2\}$  is lesser than  $d_{\min}^U$ . Here, we prove the above result when  $\mathcal{S}_2$  is not Ungerboeck partitioned. On the similar lines, the above result can be proved when  $\mathcal{S}_1$  is not Ungerboeck partitioned as well. We show that  $\phi_{\min}$  between any two points in one of sets in  $\mathcal{A}$  is smaller than  $\frac{4\pi}{N_1}$  on the circle  $C^{\frac{N_2}{2}-1}$ . It is assumed that there are exactly  $\frac{N_1}{2}$  points on  $C^{\frac{N_2}{2}-1}$  in each set of  $\mathcal{A}$ . Otherwise, at least one set contains more than  $\frac{N_1}{2}$  points on  $C^{\frac{N_2}{2}-1}$ , and hence,  $\phi_{\min}$  between a pair of points in that set will be lesser than  $\frac{4\pi}{N_1}$ . Therefore, the sub-optimality of the partition can be proved. Without loss of generality, we assume that  $x'(a), x'(a+1) \in \mathcal{S}_2^1$  for some  $a$  such that  $0 \leq a \leq N_2 - 2$ . Note that the elements of  $\mathcal{S}_2$  are of the form  $x'(kn_1+m)$  or  $x'(kn_1-m-1)$ . Since  $m = \frac{N_2}{2} - 1$  is odd and  $(a, a+1)$  is an (even, odd) pair,  $x'(a)$  can be of the form  $x'(kn_1+m)$  and  $x'(a+1)$  can be of the form  $x'(kn_1-m-1)$  or vice-versa. Without loss of generality, we assume that  $x'(a)$  is of the form  $x'(kn_1 + \frac{N_2}{2} - 1)$  and  $x'(a+1)$  is of the form  $x'(kn_1' - \frac{N_2}{2})$  for some  $n_1, n_1'$ . Note that, the points  $x(n_1) + x'(kn_1 + \frac{N_2}{2} - 1)$  and  $x(n_1') + x'(kn_1' - \frac{N_2}{2})$  belong to one of the sets in  $\mathcal{A}$  and have an angular separation of  $\frac{2\pi(n_1-n_1')}{N_1} + \frac{(N_2-1)\pi}{N_2}$ . This implies that there exists a pair of points on  $C^{\frac{N_2}{2}-1}$  such that  $\phi_{\min}$  between them is lesser than  $\frac{4\pi}{N_1}$ . This completes the proof. ■

For PSK signal sets, when  $\theta \neq \frac{\pi}{N_2}$ , the optimal partitioning on  $\mathcal{S}_1$  and  $\mathcal{S}_2$  is not known. However, we present an example (see Example 2) wherein for a particular value of  $\theta$ , a non-Ungerboeck partition on  $\mathcal{S}_1$  and  $\mathcal{S}_2$  results in a set  $\mathcal{A}$  such that the minimum of the  $d_{\min}$  of all the sets in  $\mathcal{A}$  is larger than that induced by Ungerboeck partition.

*Example 2:* Consider  $\mathcal{S}_1$ , a uniform 8-PSK signal set and  $\mathcal{S}_2 = \mathcal{S}_1 e^{i\theta}$  with  $\theta = \frac{\pi}{25}$ . With the partition of  $\mathcal{S}_1$  and  $\mathcal{S}_2$  as

$$\begin{aligned} \mathcal{S}_1^1 &= \left\{ e^{\frac{i2\pi}{8}}, e^{\frac{i4\pi}{8}}, e^{\frac{i8\pi}{8}}, e^{\frac{i12\pi}{8}} \right\} \\ \mathcal{S}_1^2 &= \left\{ e^{\frac{i6\pi}{8}}, e^{\frac{i10\pi}{8}}, e^{\frac{i14\pi}{8}}, e^{\frac{i16\pi}{8}} \right\} \\ \mathcal{S}_2^2 &= \left\{ e^{\frac{i4\pi}{8}+i\theta}, e^{\frac{i6\pi}{8}+i\theta}, e^{\frac{i12\pi}{8}+i\theta}, e^{\frac{i14\pi}{8}+i\theta} \right\} \quad \text{and} \\ \mathcal{S}_2^1 &= \left\{ e^{\frac{i2\pi}{8}+i\theta}, e^{\frac{i8\pi}{8}+i\theta}, e^{\frac{i10\pi}{8}+i\theta}, e^{\frac{i16\pi}{8}+i\theta} \right\} \end{aligned}$$

it can be checked that the minimum of the  $d_{\min}$  values of all the sets in  $\mathcal{A}$  is 0.2319. However, with Ungerboeck partition, the corresponding value is 0.1774.

#### D. On the Choice of the Cardinality of PSK Constellations

Using the results presented in the preceding subsection, we illustrate how to choose the cardinality of PSK signal sets to achieve any rate pair  $(r_1, r_2)$  (assuming  $r_2 \geq r_1$ ) within the sector O-A-B shown in Fig. 2. We do not consider achieving rate pairs outside the sector O-A-B since such points can be moved either horizontally or vertically (or both) into the sector O-A-B which in-turn either increases the rate for both users or increases the rate for one of the users by keeping the rate for the other intact. For a given equal power constraint, to approach a rate pair  $(r_1, r_2)$  (note that the rate pair  $(r_1, r_2)$  should be within the CC capacity region of PSK signal sets for some  $N_1 < \infty$

and  $N_2 < \infty$ ), we choose sufficiently large values of  $N_1$  and  $N_2$  such that:

- 1)  $N_1$  and  $N_2$  satisfies the following approximation:

$$\frac{\log_2(N_2)}{\log_2(N_1)} \simeq \frac{r_2}{r_1} \quad \text{and}$$

- 2) the CC capacity region with  $N_1$ -PSK and  $N_2$ -PSK signal sets encloses the point  $(r_1, r_2)$ .

For the above choice of  $(N_1, N_2)$ , if the number of input bits for user- $i$  is  $\log_2(N_i) - 1$ , and Ungerboeck labeling is employed on the trellis (with larger number of states) of each user, then the rate pair  $(r_1, r_2)$  can be approached. Therefore, with sufficiently large values of  $N_1$  and  $N_2$  satisfying the conditions 1) and 2), any pair,  $(r_1, r_2)$  within the CC capacity region can be approached.

#### V. DESIGNING TCM SCHEMES WITH PAM CONSTELLATIONS

In the previous section, a systematic method of labeling the trellis pair  $(T_1, T_2)$  has been obtained when PSK signal sets are employed by the two users. In this section, we present TCM schemes when  $M$ -PAM signal sets are used by the two users. For this set-up, using the metric presented in Theorem 1, it can be verified that the optimal angle of rotation  $\theta^*$  is  $\frac{\pi}{2}$  for all  $M$  and for all SNR values. Recall that, when  $M$ -PSK signal sets are employed,  $\mathcal{S}_{\text{sum}}$  takes the structure of concentric PSK signal sets. However, when  $M$ -PAM signal sets are used,  $\mathcal{S}_{\text{sum}}$  is a regular  $M^2$ -QAM (since  $\theta^* = \frac{\pi}{2}$ ). In this set-up, for a chosen trellis pair, the destination sees the corresponding sum trellis  $T_{\text{sum}}$  labeled with symbols from a  $M^2$ -QAM signal set. Since the two users transmit along the in-phase and the quadrature components respectively, decoding for the symbols of one user is independent of the other. Hence, the destination can decode for a sequence over  $M$ -PAM constellation on the individual trellises  $T_1$  and  $T_2$  instead of decoding for a sequence over  $M^2$  QAM constellation on  $T_{\text{sum}}$ . Therefore, all TCM based trellis codes with  $M$ -PAM constellations existing for SISO AWGN channel are applicable in the two-user GMAC setup. With this, the decoding complexity at the destination is significantly reduced as the state complexity profile of the trellis over which the decoder works is  $\{q_{i,0}, q_{i,1}, \dots, q_{i,n}\}$  (when decoding for User- $i$ ) instead of  $\{q_{1,0}q_{2,0}, q_{1,1}q_{2,1}, \dots, q_{1,n}q_{2,n}\}$ . In general, when a complex signal set is used by either one of the users, the destination has to necessarily decode for a sequence over  $\mathcal{S}_{\text{sum}}$  on  $T_{\text{sum}}$  which has high decoding complexity.

1) *On the CC Sum-Capacity With PAM Signal Sets:* From the above discussion, it is clear that for two-user GMAC, single-dimensional signal sets can be preferred over complex signal sets for reducing the ML decoding complexity. However, it is not clear if there is any loss in the CC sum-capacity by using single-dimensional signal sets. In Fig. 13, we plot the CC sum-capacity as a function of SNR for two scenarios; (i) when QPSK signal sets are used with angles of rotation as given in Table I and (ii) when 4-PAM signal sets are used with  $\theta^* = \frac{\pi}{2}$ . For both the scenarios, average power per symbol per user is made the same. As shown in the plot, there is a marginal difference in the CC sum-capacity between the two schemes and in particular, at high SNR the sum-capacity of the former scheme is higher

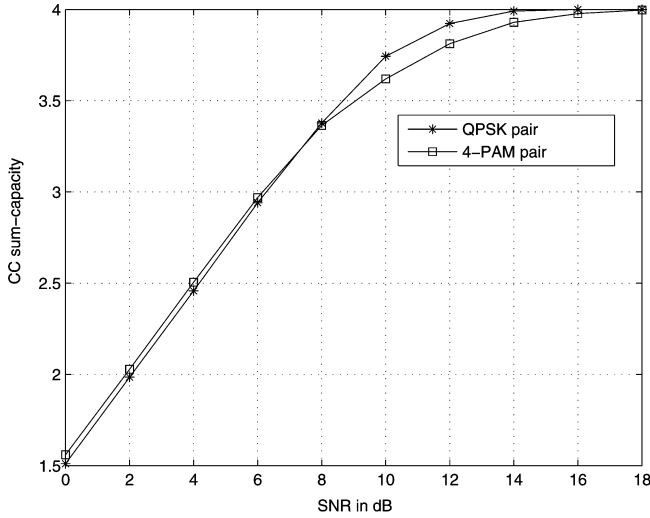


Fig. 13. CC sum-capacity of QPSK signal set pair and 4-PAM signal set pair with optimal rotations.

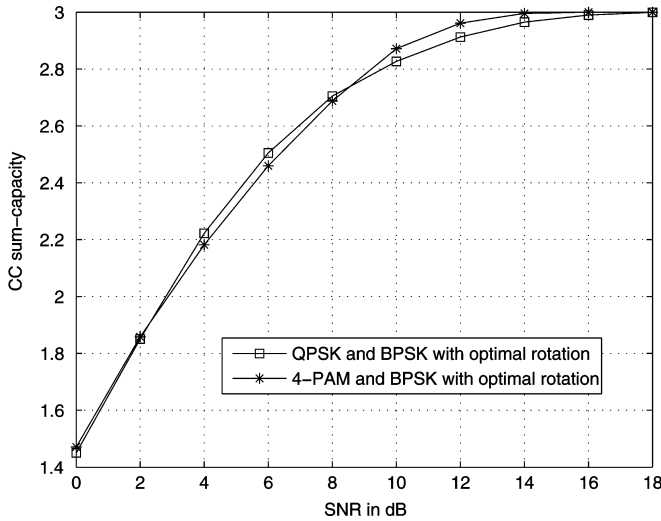


Fig. 14. CC sum-capacity of the QPSK/BPSK signal set pair and the 4-PAM/BPSK signal set pair with optimal rotation.

than the later. Therefore, 4-PAM signal sets provide reduced decoding complexity with *almost* the same CC sum-capacity as that of QPSK signal sets. Similar plots have been obtained in Fig. 14 for the following scenario: (i) when User-1 and User-2 uses QPSK and BPSK signal set respectively (with appropriate angle of rotation) and (ii) when User-1 uses 4-PAM signal set, User-2 uses BPSK with  $\theta^* = \frac{\pi}{2}$ .

In a SISO AWGN channel, it is well known that, single-dimensional signal sets incur some loss in the CC capacity when compared to *well packed* complex signal sets having the same average power and equal number of points. However, for GMAC, the CC capacity of individual signal sets,  $\mathcal{S}_1$  and  $\mathcal{S}_2$  are of little importance, since for an input constellation pair  $(\mathcal{S}_1, \mathcal{S}_2)$ , the destination sees an equivalent AWGN channel with the corresponding  $\mathcal{S}_{\text{sum}}$  as its input (neither  $\mathcal{S}_1$  nor  $\mathcal{S}_2$ ). Hence, in order to maximize the CC sum-capacity, the constellation pair  $(\mathcal{S}_1, \mathcal{S}_2)$  has to be chosen such that CC capacity of  $\mathcal{S}_{\text{sum}}$  is maximized. Since we have shown that, for a given

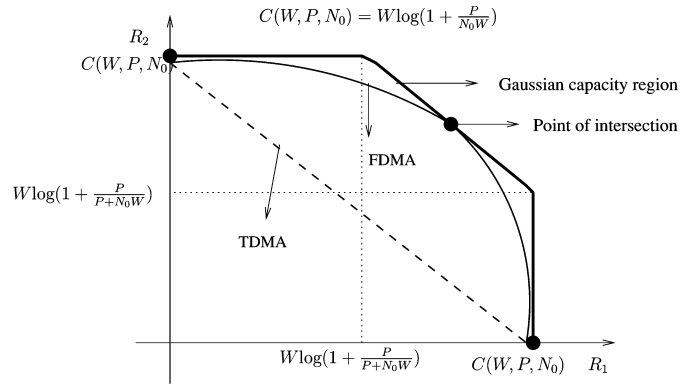


Fig. 15. Achievable rate pairs (in bits per second) for TDMA and FDMA for a total bandwidth of  $W$  Hertz.

SNR, the sum-capacity of 4-PAM constellation pair is close to that of a QPSK constellation pair, we conjecture that for any  $M, M$ -PAM constellation pairs (with  $\theta^* = \frac{\pi}{2}$ ) do not incur significant loss in the sum-capacity when compared to  $M$ -PSK and  $M$ -QAM constellation pairs.

### VI. COMPARING THE CC CAPACITY REGIONS OF O-MA AND NO-MA SCHEMES

In the preceding sections, code pairs based on TCM [11] are proposed such that *any rate pair* within the CC capacity region can be approached. Such a NO-MA scheme which employs capacity approaching trellis codes is referred to as trellis coded multiple access (TCMA). *Henceforth, throughout this section, CC capacity regions obtained in Section II are referred to as CC capacity regions with TCMA since TCMA can approach any rate pair within the CC capacity region.*

For two-user GMAC with Gaussian distributed continuous input constellations, it is well known that successive interference cancellation decoder can achieve any point on the capacity region, provided the codebooks contain infinite length code-words [1], [26]. It is also known that TDMA and FDMA, two of the widely known O-MA techniques do not achieve all the points on the capacity region. In particular, if FDMA is used such that the bandwidth allocated to each user is proportional to its transmit power, then one of the points on the maximum sum rate line of the capacity region can be achieved [1]. The set of achievable rate pairs using TDMA and FDMA are provided in Fig. 15 along with the capacity region wherein the total bandwidth (for both the users) is  $W$  Hertz, the power constraint for each user is  $P$  Watts and the power spectral density of the AWGN is  $N_0$ .

In this section, we compute the CC capacity regions of two-user GMAC when O-MA schemes such as TDMA and FDMA are employed for finite bandwidth. Since FDMA (with Gaussian constellations) achieves one of the sum-capacity points with single-user decoding complexity, it is stated in [1] that “*the improvement in the capacity due to multiple access ideas such as the one achieved by the successive interference decoder (a NO-MA scheme) may not be sufficient to warrant the increased complexity*” (see line 11–14, page 548, Section 15.3.6 of Chapter 15 in [1]). In this section, we point out that

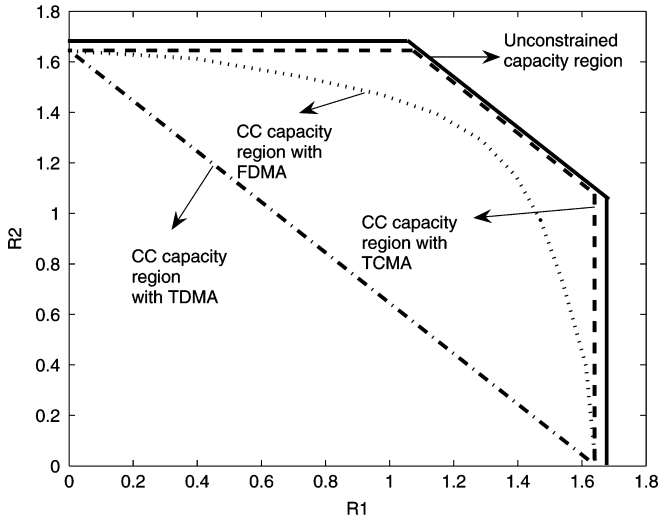


Fig. 16. CC Capacity regions (in bits/sec) for various multiple access schemes with QPSK signal sets when  $P = 2$  dB,  $N_0 = 1$ , and  $W = 2$  Hertz.

the above comment in [1] does not hold good for GMAC with finite constellations which is the case in practical scenarios. In particular, unlike the behavior of Gaussian constellations (as shown in Fig. 15), it is shown that the CC capacity region with FDMA is strictly contained inside the CC capacity region with TCMA, essentially showing that TCMA is better than FDMA for finite constellations (see Figs. 16, 17, and 18). Note that this result is not apparent unless CC capacity regions with FDMA and TCMA are plotted.

The result presented in this section is another example to illustrate the differences in the capacity behavior when the input constellations are constrained to have finite cardinality. An earlier example is in Section II, wherein a relative angle of rotation between the input constellations is shown to enlarge the CC capacity region with TCMA.<sup>3</sup> Note that such a capacity enlargement is not applicable for Gaussian constellations.

#### A. Signal Model

The model of the two-user GMAC considered in this section is similar to the one presented in Section II. Hence, we point out only the changes in the signal model with respect to the one in Section II. For the NO-MA scheme, it is assumed that User-1 and User-2 communicate to the destination at the same time and in the same frequency band of  $W$  Hertz. To take bandwidth into consideration, the variance of the additive noise is given by  $\sigma^2 = WN_0$ . When User-1 and User-2 transmit symbols  $\sqrt{P}x_1$  and  $\sqrt{P}x_2$  simultaneously, the destination receives the symbol  $y$  given by

$$y = \sqrt{P}x_1 + \sqrt{P}x_2 + z \quad \text{where } z \sim \mathcal{CSCG}(0, WN_0) \quad (33)$$

where  $\frac{N_0}{2}$  is the power spectral density of the AWGN in each dimension. We assume equal average power constraint for the two users.

<sup>3</sup>Note that the CC capacity region for two-user GMAC is referred to as the CC capacity region with TCMA since TCMA can approach any rate pair on the CC capacity region.

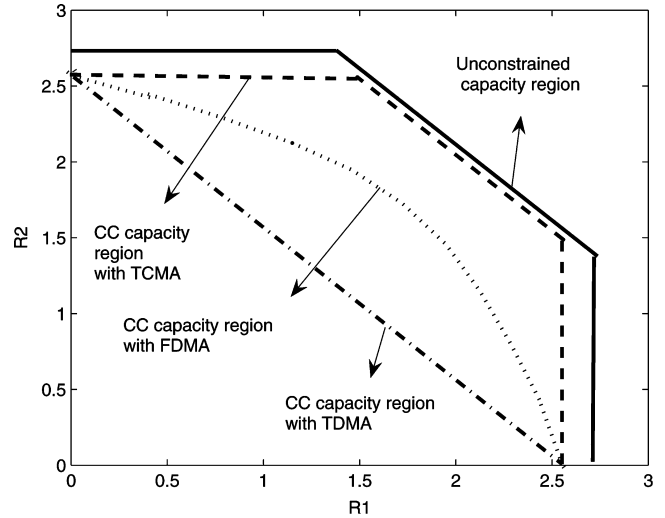


Fig. 17. CC Capacity regions (in bits/sec) for various multiple access schemes with QPSK signal sets when  $P = 5$  dB,  $N_0 = 1$ , and  $W = 2$  Hertz.

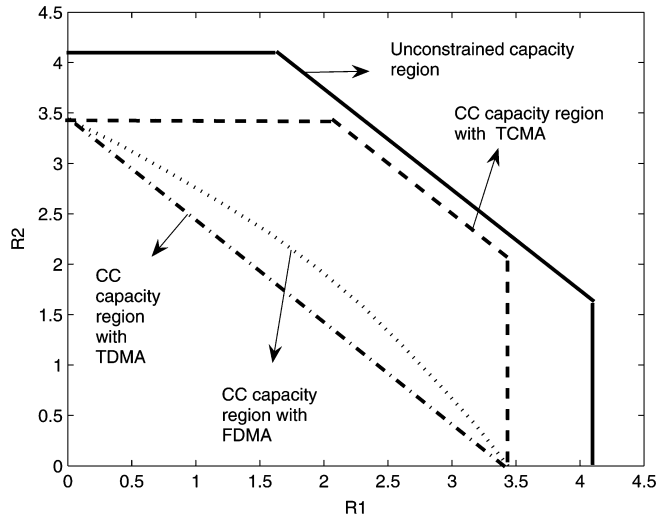


Fig. 18. CC Capacity regions (in bits/sec) for various multiple access schemes with QPSK signal sets when  $P = 8$  dB,  $N_0 = 1$ , and  $W = 2$  Hertz.

Applying the CC capacity regions obtained in Section II to the channel model in (33), the set of CC capacity values (in bits per channel use) that define the boundary of the CC capacity region are

$$\begin{aligned} R_1 &\leq I(\sqrt{P}x_1 : y | \sqrt{P}x_2) \\ R_2 &\leq I(\sqrt{P}x_2 : y | \sqrt{P}x_1) \quad \text{and} \\ R_1 + R_2 &\leq I(\sqrt{P}x_1 + \sqrt{P}x_2 : y) \end{aligned} \quad (34)$$

where the expressions for  $I(\sqrt{P}x_2 : y)$ ,  $I(\sqrt{P}x_1 : y | \sqrt{P}x_2)$  are given in (31) and (32), respectively, shown at the bottom of the next page. The term  $I(\sqrt{P}x_1 + \sqrt{P}x_2 : y)$  can be calculated as  $I(\sqrt{P}x_2 : y) + I(\sqrt{P}x_1 : y | \sqrt{P}x_2)$ . Since the terms  $I(\sqrt{P}x_2 : y)$  and  $I(\sqrt{P}x_1 : y | \sqrt{P}x_2)$  are functions of the bandwidth  $W$ ; henceforth, we denote them as  $I_W(\sqrt{P}x_2 : y)$  and  $I_W(\sqrt{P}x_1 : y | \sqrt{P}x_2)$  respectively. Also, since every

channel use consumes  $\frac{1}{W}$  seconds, the rate pairs (in bits per second) that define the CC capacity region are given by

$$\begin{aligned} R_1 &\leq WI_W(\sqrt{P}x_1 : y|\sqrt{P}x_2) \\ R_2 &\leq WI_W(\sqrt{P}x_2 : y|\sqrt{P}x_1) \quad \text{and} \\ R_1 + R_2 &\leq WI_W(\sqrt{P}x_1 + \sqrt{P}x_2 : y). \end{aligned} \quad (35)$$

### B. Unconstrained Capacity Regions of Two-User GMAC

In this subsection, we revisit the capacity region of two-user Gaussian MAC (henceforth, referred as unconstrained capacity region). In the channel model described in Subsection VI.A, the input constellations are finite in size and the symbols take values with uniform distribution. However, if the input constellations are continuous and distributed as  $x_1, x_2 \sim \mathcal{CSCG}(0, P)$ , then the unconstrained capacity region in bits per second is given by

$$\begin{aligned} R_1 &\leq W \log_2 \left( 1 + \frac{P}{WN_0} \right) = C(W, P, N_0) \\ R_2 &\leq W \log_2 \left( 1 + \frac{P}{WN_0} \right) = C(W, P, N_0) \quad \text{and} \\ R_1 + R_2 &\leq W \log_2 \left( 1 + \frac{2P}{WN_0} \right). \end{aligned} \quad (36)$$

Now, we recall the set of achievable rate pairs when the two users employ FDMA and TDMA. When the two users employ FDMA, let  $W_1 = \alpha W$  and  $W_2 = (1 - \alpha)W$  be the nonoverlapping bandwidth occupied by User-1 and User-2 respectively where  $0 < \alpha < 1$ . For such a scheme, the maximum achievable rates (in bits per second) for the two users are given by

$$\begin{aligned} R_1 &\leq W_1 \log_2 \left( 1 + \frac{P}{N_0 W_1} \right) \quad \text{and} \\ R_2 &\leq W_2 \log_2 \left( 1 + \frac{P}{N_0 W_2} \right). \end{aligned} \quad (37)$$

Therefore, the maximum achievable sum rate when  $\alpha = 0.5$  is given by

$$(R_1 + R_2)_{\text{FDMA}, \alpha=0.5} \leq W \log_2 \left( 1 + \frac{2P}{N_0 W} \right) \quad (38)$$

which is equal to the sum-capacity of the two-user GMAC given in (36). Hence, for Gaussian constellations, FDMA can achieve

one of the points on the maximum sum rate line of the unconstrained capacity region.

In TDMA, the two users use the same bandwidth of  $W$  Hertz but transmit over different time durations. If User-1 uses the channel for  $\alpha$  seconds and User-2 uses the channel for  $(1 - \alpha)$  seconds for some  $0 < \alpha < 1$ , then the maximum achievable rates (in bits per second) for two users are given by  $R_1 \leq \alpha W \log_2(1 + \frac{P}{N_0 W})$  and  $R_2 \leq (1 - \alpha)W \log_2(1 + \frac{P}{N_0 W})$ . Therefore, the maximum achievable sum rate is

$$(R_1 + R_2)_{\text{TDMA}} \leq W \log_2 \left( 1 + \frac{P}{N_0 W} \right).$$

In Fig. 15, the set of achievable rate pairs for FDMA and TDMA are provided along with the capacity region for a bandwidth of  $W$  Hertz. On the similar lines of the discussion in this subsection, in the following subsection, we discuss the CC capacity region with FDMA and TDMA.

### C. CC Capacity Regions With FDMA and TDMA

Let  $W_1 = \alpha W$  and  $W_2 = (1 - \alpha)W$  be the disjoint band of frequencies occupied by User-1 and User-2 respectively where  $0 < \alpha < 1$ . Hence, for each  $i = 1, 2$ , User- $i$  views a SISO AWGN channel to the destination with the input constellation  $\mathcal{S}_i$  and bandwidth  $W_i$ . Therefore, the CC capacity values (in bits per second) for the two users are given by

$$\begin{aligned} R_1 &\leq W_1 I_{W_1}(\sqrt{P}x_1 : y|\sqrt{P}x_2) \quad \text{and} \\ R_2 &\leq W_2 I_{W_2}(\sqrt{P}x_2 : y|\sqrt{P}x_1). \end{aligned}$$

Note that with  $\alpha = 0.5$ , the CC sum-capacity with FDMA is given by

$$\begin{aligned} R_1 + R_2 &\leq \frac{W}{2} I_{\frac{W}{2}}(\sqrt{P}x_1 : y|\sqrt{P}x_2) \\ &\quad + \frac{W}{2} I_{\frac{W}{2}}(\sqrt{P}x_2 : y|\sqrt{P}x_1). \end{aligned}$$

If we assume identical signal sets for the two users, then the CC sum-capacity (denoted by  $(R_1 + R_2)_{\text{FDMA}, \alpha=0.5}$ ) is given by

$$(R_1 + R_2)_{\text{FDMA}, \alpha=0.5} \leq WI_{\frac{W}{2}}(\sqrt{P}x_1 : y|\sqrt{P}x_2) \quad (39)$$

$$\begin{aligned} &I(\sqrt{P}x_2 : y) \\ &= \log_2(N_2) \\ &\quad - \frac{1}{N_1 N_2} \sum_{k_1=0}^{N_1-1} \sum_{k_2=0}^{N_2-1} E \left[ \log_2 \left[ \frac{\sum_{i_1=0}^{N_1-1} \sum_{i_2=0}^{N_2-1} \exp \left( -|\sqrt{P}(x_1(k_1) + x_2(k_2) - x_1(i_1) - x_2(i_2)) + z|^2 / WN_0 \right)}{\sum_{i_1=0}^{N_1-1} \exp \left( -|\sqrt{P}x_1(k_1) - \sqrt{P}x_1(i_1) + z|^2 / WN_0 \right)} \right] \right] \end{aligned} \quad (31)$$

$$\begin{aligned} &I(\sqrt{P}x_1 : y|\sqrt{P}x_2) \\ &= \log_2(N_1) - \frac{1}{N_1} \sum_{k_1=0}^{N_1-1} E \left[ \log_2 \left[ \frac{\sum_{i_1=0}^{N_1-1} \exp \left( -|\sqrt{P}x_1(k_1) - \sqrt{P}x_1(i_1) + z|^2 / WN_0 \right)}{\exp \left( -|z|^2 / WN_0 \right)} \right] \right] \end{aligned} \quad (32)$$

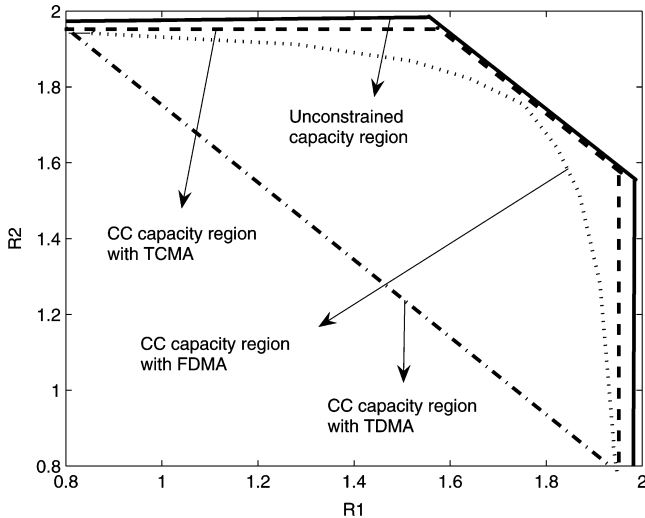


Fig. 19. CC Capacity regions (in bits/sec) for various multiple access schemes with QPSK signal sets when  $P = 2$  dB,  $N_0 = 1$ , and  $W = 5$  Hertz.

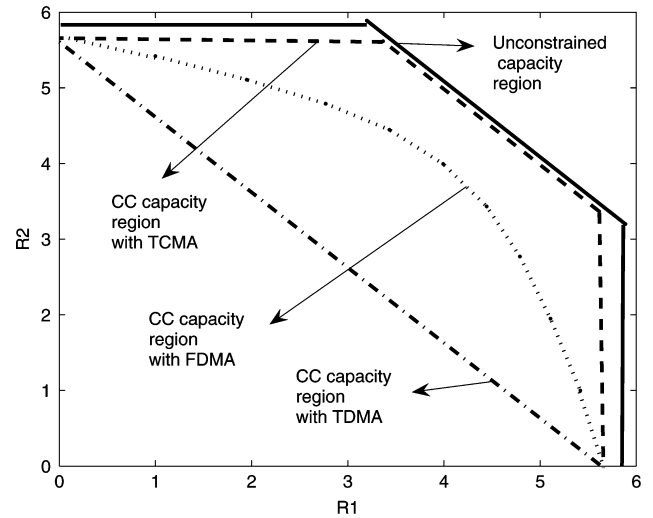


Fig. 21. CC Capacity regions (in bits/sec) for various multiple access schemes with QPSK signal sets when  $P = 8$  dB,  $N_0 = 1$ , and  $W = 5$  Hertz.

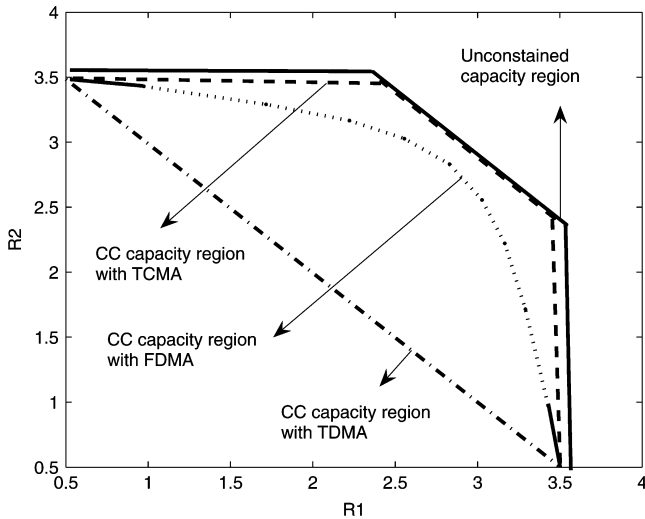


Fig. 20. CC Capacity regions (in bits/sec) for various multiple access schemes with QPSK signal sets when  $P = 5$  dB,  $N_0 = 1$ , and  $W = 5$  Hertz.

wherein without loss of generality, we have used the variable  $x_1$  for both the users. Let the CC sum-capacity with TCMA given in (10) be denoted by

$$(R_1 + R_2)_{\text{TCMA}} \leq W I_W(\sqrt{P}x_1 + \sqrt{P}x_2 : y). \quad (40)$$

Comparing (39) and (40), it is not straightforward to comment whether, the CC sum-capacity offered by FDMA is equal to or different from the CC sum-capacity with TCMA. In Figs. 16, 17 and 18, CC capacity regions with TCMA, and FDMA are presented for QPSK signal sets when bandwidth  $W = 2$  Hertz. Similarly, in Figs. 19, 20 and 21, CC capacity regions with TCMA, and FDMA are presented for QPSK signal sets when bandwidth  $W = 5$  Hertz. From the above figures, it is clear that the gap between the CC capacity regions with TCMA and FDMA is a function of the bandwidth  $W$  Hertz and the average power constraint  $P$  Watts. In particular, (i) for a fixed  $W$ , the gap between the CC capacity regions with FDMA and TCMA *increases* with the increase in  $P$  (see Figs. 16, 17 and 18 for a fixed

$W$  and varying  $P$ ), and (ii) for a fixed  $P$ , the gap between the CC capacity regions with FDMA and TCMA *decreases* with the increase in  $W$  (see Figs. 16 and 19 for a fixed  $P$  and varying  $W$ ).

For calculating the CC capacity region with TCMA, a relative angle of rotation chosen from Table I is used between the signal sets. The plots show that the CC capacity region with FDMA is strictly enclosed within the CC capacity region with TCMA. Note that, for a given value of  $W$ , the difference between the regions with FDMA and TCMA becomes significant for larger values of  $P$ . In particular, the plots show the following inequality,

$$(R_1 + R_2)_{\text{FDMA}, \alpha=0.5} < (R_1 + R_2)_{\text{TCMA}}.$$

Note that the difference between  $(R_1 + R_2)_{\text{FDMA}, \alpha=0.5}$  and  $(R_1 + R_2)_{\text{TCMA}}$  depends on  $W$  for a given value of  $P$  and  $\sigma^2$ . We calculate the percentage increase in the CC sum-capacity from  $(R_1 + R_2)_{\text{FDMA}, \alpha=0.5}$  to  $(R_1 + R_2)_{\text{TCMA}}$  (denoted as  $\mu$ ) given by

$$\begin{aligned} \mu &= \frac{W I_W(\sqrt{P}x_1 + \sqrt{P}x_2 : y) - W I_{\frac{W}{2}}(\sqrt{P}x_1 : y | \sqrt{P}x_2)}{W I_{\frac{W}{2}}(\sqrt{P}x_1 : y | \sqrt{P}x_2)} \\ &= \frac{I_W(\sqrt{P}x_1 + \sqrt{P}x_2 : y) - I_{\frac{W}{2}}(\sqrt{P}x_1 : y | \sqrt{P}x_2)}{I_{\frac{W}{2}}(\sqrt{P}x_1 : y | \sqrt{P}x_2)}. \end{aligned}$$

In Table II, we provide the values of  $\mu$  for different values of  $P$  when (i)  $N_0 = 1$ , (ii)  $W = 1$ , and (iii) the input constellations are QPSK signal sets. For calculating the values of  $I_W(\sqrt{P}x_1 + \sqrt{P}x_2 : y)$ , relative angles of rotation presented in Table I are used between the signal sets. The values of  $I_W(\sqrt{P}x_1 + \sqrt{P}x_2 : y)$  and  $I_{\frac{W}{2}}(\sqrt{P}x_1 : y | \sqrt{P}x_2)$  have also been plotted as a function of  $P$  in Fig. 22.

From Table II, it is clear that  $\mu$  increases as  $P$  increase. An intuitive reasoning for such a behavior is as follows: The term  $I_W(\sqrt{P}x_1 + \sqrt{P}x_2 : y)$  is the CC capacity of a 16 point constellation (sum constellation of two appropriately rotated QPSK signal sets) with an average power of  $2P$

TABLE II  
PERCENTAGE INCREASE IN THE SUM-CAPACITY FROM FDMA TO TCMA FOR QPSK SIGNAL SETS

$P$ in dB	-2	0	2	4	6	8	10	12
$\mu$ in %	5.46	9.31	17.79	32.48	50.55	68.33	82.70	92.78

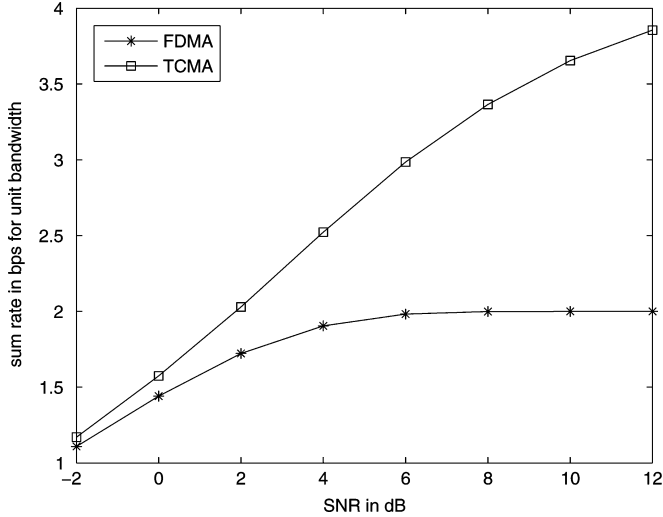


Fig. 22. CC sum-capacity in bits per second per Hertz where  $\text{SNR} = P$

whereas  $I_{\frac{W}{2}}(\sqrt{P}x_1 : y|\sqrt{P}x_2)$  is the CC capacity of a 4 point constellation (QPSK signal set) with the same average power of  $2P$ . Note that, asymptotically (for large values of  $P$ ),  $I_{\frac{W}{2}}(\sqrt{P}x_1 : y|\sqrt{P}x_2)$  and  $I_W(\sqrt{P}x_1 + \sqrt{P}x_2 : y)$  saturate to 2 bits and 4 bits, respectively. Therefore, at moderate values of  $P$ , as  $P$  increases, the term  $I_{\frac{W}{2}}(\sqrt{P}x_1 : y|\sqrt{P}x_2)$  increases at a slower rate to saturate to 2 bits. However,  $I_W(\sqrt{P}x_1 + \sqrt{P}x_2 : y)$  increases at a faster rate as its saturation is at 4 bits. A similar reasoning holds good for constellations with arbitrary size. However, the difference in the CC sum-capacity may differ depending on the constellations size.

In the rest of this subsection, we obtain the CC capacity pairs when the two users employ TDMA. If User-1 uses the channel for  $\alpha$  seconds and User-2 uses the channel for  $(1 - \alpha)$  seconds for some  $0 < \alpha < 1$ , then the CC capacity values (in bits per second) for the two users are given by

$$R_1 \leq \alpha W I_W(\sqrt{P}x_1 : y|\sqrt{P}x_2) \quad \text{and}$$

$$R_2 \leq (1 - \alpha) W I_W(\sqrt{P}x_2 : y|\sqrt{P}x_1).$$

Assuming identical constellations for the two users, the CC sum-capacity with TDMA is given by

$$R_1 + R_2 \leq W I_W(\sqrt{P}x_1 : y|\sqrt{P}x_2).$$

The set of CC capacity pairs when the two users employ TDMA are shown in Figs. 16, 17 and 18 which shows that TCMA is better than TDMA for finite constellations as well. We highlight that, along with the substantial improvement in the CC capacity, low complexity trellis codes proposed for TCMA in Section V makes TCMA worth pursuing in practice for two-user GMAC.

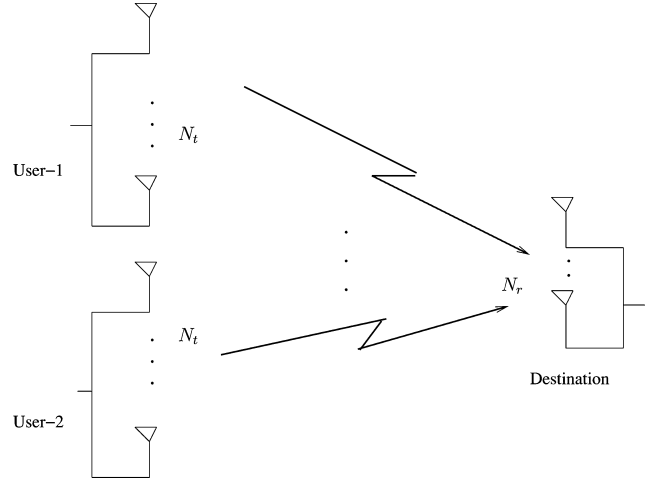


Fig. 23. Two-user MIMO-MAC model.

## VII. SPACE-TIME BLOCK CODES (STBCs) WITH LOW-ML DECODING COMPLEXITY FOR TWO-USER MIMO-MAC

In Section V, it is shown that when PAM signal sets are employed in two-user GMAC with  $\theta = \frac{\pi}{2}$ , then the ML decoding complexity is reduced with marginal loss in the CC sum-capacity when compared to other 2-D signal sets. In this section, we extend the idea of introducing rotation between the PAM constellations to two-user MISO (Multiple-Input Single-Output) flat fading, quasi-static MAC. In particular, we propose STBC pairs having the information-losslessness (IL) property and minimum ML decoding complexity [27]. Note that the IL property is defined assuming the input constellations to be continuous and Gaussian distributed. Hence, we first study the IL property and subsequently study the CC ergodic sum-capacity of the proposed STBCs. In the later part of this section, we also propose STBC pairs with reduced sphere decoding complexity for MIMO-MAC. In the following subsection, we first describe the MIMO-MAC model and then consider the MISO-MAC model as its special case.

### A. Channel Model of Two-User MIMO-MAC

The two-user MIMO-MAC as shown in Fig. 23 consists of two users each equipped with  $N_t$  antennas and a destination equipped with  $N_r$  antennas. The MIMO channels from User-1 to the destination and from User-2 to the destination are respectively denoted by  $\mathbf{H}^{(1)} \in \mathbb{C}^{N_r \times N_t}$  and  $\mathbf{H}^{(2)} \in \mathbb{C}^{N_r \times N_t}$ , where  $[\mathbf{H}^{(1)}]_{i,j}, [\mathbf{H}^{(2)}]_{i,j} \sim \text{CSCG}(0, 1) \forall i = 1$  to  $N_r$  and  $j = 1$  to  $N_t$ . The two MIMO channels are assumed to be flat fading and quasi-static with a coherence time of at least  $T$  channel uses. We assume that each user communicates its information to the destination using an STBC. Let  $\mathcal{C}_1$  and  $\mathcal{C}_2$  represent STBCs of dimension  $T \times N_t$  employed by User-1 and User-2 respectively. If  $\mathbf{X}_1 \in \mathcal{C}_1$  and  $\mathbf{X}_2 \in \mathcal{C}_2$  are the codeword matrices chosen for

transmission from User-1 and User-2 simultaneously, then the received matrix  $\mathbf{Y} \in \mathbb{C}^{T \times N_r}$  at the destination is of the form

$$\mathbf{Y} = \sqrt{\frac{\rho}{2N_t}} \mathbf{X}_1 \mathbf{H}^{(1)} + \sqrt{\frac{\rho}{2N_t}} \mathbf{X}_2 \mathbf{H}^{(2)} + \mathbf{N} \quad (41)$$

where  $\mathbf{N} \in \mathbb{C}^{T \times N_r}$  is the additive noise at the destination such that each component of  $\mathbf{N}$  is distributed as  $\mathcal{CSCG}(0, 1)$ . In this model, we assume equal average power constraint for both the users. Assuming  $E[[\mathbf{X}_1]_{t,i} [\mathbf{X}_1]_{t,i}^*] = E[[\mathbf{X}_2]_{t,i} [\mathbf{X}_2]_{t,i}^*] = 1$  for all  $t = 1$  to  $T$  and  $i = 1$  to  $N_t$ , the average receive signal to noise ratio (SNR) at the destination is  $\rho$ . We assume the perfect knowledge of both  $\mathbf{H}^{(1)}$  and  $\mathbf{H}^{(2)}$  at the destination for every codeword use.

1) *Two-User MISO-MAC Model*: In this subsection, we consider a MIMO-MAC model with  $N_r = 1$ , i.e., a MISO-MAC model. For such a channel, if  $\mathbf{X}_j \in \mathbb{C}^{1 \times N_t}$  is the vector transmitted by User- $j$ , then the received complex symbol at the destination for every channel use is given by (41) where  $\mathbf{N} \in \mathbb{C}^{1 \times 1}$  is the additive noise at the destination distributed as  $\mathcal{CSCG}(0, 1)$  and  $\mathbf{H}^{(j)} \in \mathbb{C}^{N_t \times 1}$  for each  $j$ . Such a two-user MISO-MAC model is referred to as  $(N_t, N_t, 1)$ -MIMO-MAC.

For the MISO-MAC model, we assume the perfect knowledge of the phase components of  $\mathbf{H}^{(j)}$  at the  $j$ -th user which we refer to as CSIT-P. The  $(N_t, N_t, 1)$ -MIMO-MAC with the assumption of CSIT-P is referred to as the  $(N_t, N_t, 1, p)$ -MIMO-MAC where  $p$  highlights the assumption of CSIT-P in the channel model. Note that, we do not assume the complete knowledge of  $\mathbf{H}^{(j)}$  at the transmitters, in which case, optimal power allocation techniques can be applied to improve the system performance. Since CSIT-P is known, each transmit antenna can compensate for the rotation introduced by the channel, and hence, the channel equation in (41) becomes

$$\mathbf{Y} = \sqrt{\frac{\rho}{2N_t}} \mathbf{X}_1 \tilde{\mathbf{H}}^{(1)} + \sqrt{\frac{\rho}{2N_t}} \mathbf{X}_2 \tilde{\mathbf{H}}^{(2)} + \mathbf{N} \quad (42)$$

where  $\tilde{\mathbf{H}}^{(j)} = [|[[\mathbf{H}^j]_{1,1}|], |[[\mathbf{H}^j]_{2,1}|], \dots, |[[\mathbf{H}^j]_{N_t,1}|]|]^T \in \mathbb{R}^{N_t \times 1}$ .

Henceforth, for simplicity,  $(N_t, N_t, 1, p)$ -MIMO-MAC is denoted as  $N_t$ -MISO-MAC. With equal average power constraint for the two users, it is well known that the sum-capacity of a  $(N_t, N_t, 1)$ -MIMO-MAC is equal to the capacity of a  $2N_t \times 1$  point to point co-located MISO channel (with CSIR) which is given in (43) (see Section 6 in [28] for the result)

$$C(N_t, N_t, 1) = E \left[ \log_2 \left( 1 + \frac{\rho}{2N_t} \times \left( \mathbf{H}^{(1)} \mathbf{H}^{(1)H} + \mathbf{H}^{(2)} \mathbf{H}^{(2)H} \right) \right) \right]. \quad (43)$$

where the expectation is over the random variables  $|[[\mathbf{H}^{(j)}]_{i,1}|]^2 \forall i, j$ .

*Lemma 3*: If  $C(N_t, N_t, 1, p)$  denotes the sum-capacity of  $N_t$ -MISO-MAC with CSIR, then

$$C(N_t, N_t, 1, p) = C(N_t, N_t, 1).$$

*Proof*: The above result can be proved on the similar lines of the proof for Theorem 1 in Section 4.1 in [28]. With the assumption of CSIT-P, the vector transmitted by User- $j$  for every

channel use is  $\mathbf{X}'_j = \mathbf{X}_j \mathbf{D}(\mathbf{H}^{(j)})$ , where  $\mathbf{D}(\mathbf{H}^{(j)})$  is the  $N_t \times N_t$  diagonal unitary matrix (a function of  $\mathbf{H}^{(j)}$ ) which compensates for the phase introduced by the channel. From Theorem 1 in Section 4.1 in [28],  $\mathbf{X}'_j$  must be a circularly symmetric complex Gaussian vector to maximize the mutual information. Since the diagonal elements of  $\mathbf{D}(\mathbf{H}^{(j)})$  are unit norm elements and their phase components are uniformly distributed, it follows that, if  $\mathbf{X}_j$  is a circularly symmetric complex Gaussian vector, then  $\mathbf{X}'_j$  is also a circularly symmetric complex Gaussian vector. Therefore,  $C(N_t, N_t, 1, p) = C(N_t, N_t, 1)$ . ■

The sum-capacity of  $N_t$ -MISO-MAC (which is given by  $C(N_t, N_t, 1, p)$ ) is computed by assuming that independent vectors are transmitted every channel use from both the users. However, when an STBC pair  $(\mathcal{C}_1, \mathcal{C}_2)$  is employed ( $\mathcal{C}_1$  is used by User-1 and  $\mathcal{C}_2$  is used by User-2), the vectors transmitted at every channel use need not be independent. Let the dimensions of the STBC used by the two users be  $T \times N_t$  (where  $T$  denotes the number of complex channel uses). We assume that STBCs for both the users have the same dimensions. If the  $T \times N_t$  matrices transmitted by User-1 and User-2 are  $\mathbf{X}_1$  and  $\mathbf{X}_2$  respectively, then the received vector  $\mathbf{Y} \in \mathbb{C}^{T \times 1}$  is of the form as given by (42) where  $\mathbf{N} \sim \mathcal{CSCG}(\mathbf{0}_{T \times 1}, \mathbf{I}_T)$  denotes the complex  $T \times 1$  additive noise vector. If the STBCs used are of rate  $R$  complex symbols per channel use, then there are  $TR$  independent complex variables for each user describing the corresponding matrix. Let the vector containing  $TR$  variables of  $\mathbf{X}_1$  and  $\mathbf{X}_2$  be denoted by  $\mathbf{x}_1 \in \mathbb{C}^{TR \times 1}$  and  $\mathbf{x}_2 \in \mathbb{C}^{TR \times 1}$  respectively. Totally, there are  $2TR$  independent variables denoted by  $\mathbf{z} \in \mathbb{C}^{2TR \times 1}$ , where  $\mathbf{z} = [\mathbf{x}_1^T \mathbf{x}_2^T]^T$ . If  $\mathbf{X}_1$  and  $\mathbf{X}_2$  are such that (42) can be written as

$$\mathbf{Y} = \sqrt{\frac{\rho}{2N_t}} \tilde{\mathbf{H}} \mathbf{z} + \mathbf{N} \quad (44)$$

where  $\tilde{\mathbf{H}} \in \mathbb{C}^{T \times 2TR}$ , then the average mutual information of the channel  $\tilde{\mathbf{H}}$  is given by [28]

$$E \left[ \log_2 \left( \det \left( \mathbf{I}_T + \frac{\rho}{2N_t} \tilde{\mathbf{H}} \mathbf{Q} \tilde{\mathbf{H}}^H \right) \right) \right]$$

where  $\mathbf{Q}$  is the covariance matrix of  $\mathbf{z}$ . Therefore, after introducing the STBC pair  $(\mathcal{C}_1, \mathcal{C}_2)$ , the average mutual information,  $E[I(\mathbf{z} : \mathbf{y} | \tilde{\mathbf{H}})]$  between the vectors  $\mathbf{z}$  and  $\mathbf{y}$  for every channel use is

$$E[I(\mathbf{z} : \mathbf{y} | \tilde{\mathbf{H}})] = \frac{1}{T} E \left[ \log_2 \left( \det \left( \mathbf{I}_T + \frac{\rho}{2N_t} \tilde{\mathbf{H}} \mathbf{Q} \tilde{\mathbf{H}}^H \right) \right) \right]$$

where the factor  $\frac{1}{T}$  takes care of the rate loss due to coding across time. It is clear that the above value cannot be more than  $C(N_t, N_t, 1, p)$ . Similar to the definition of information-lossless STBCs for co-located MIMO channels [29], information-lossless STBC pairs are defined below for  $N_t$ -MISO-MAC.

*Definition 5: (Information lossless STBC pair)* For an STBC pair  $(\mathcal{C}_1, \mathcal{C}_2)$  used for  $N_t$ -MISO-MAC, if the maximum average mutual information (maximized over all covariance matrices,  $\mathbf{Q}$  with the average power constraint),  $\max_{\mathbf{Q}} E[I(\mathbf{z} : \mathbf{y} | \tilde{\mathbf{H}})]$  is equal to the sum-capacity of  $N_t$ -MISO-MAC, then the pair  $(\mathcal{C}_1, \mathcal{C}_2)$  is called an information-lossless STBC pair.

In this paper, we propose a class of STBC pairs derived from Real Orthogonal Designs (RODs) for  $N_t$ -MISO-MAC. For deriving certain properties of the codes that are to be proposed, the following definition on *single-dimensional real MISO channels* is important.

*Definition 6: (Single-dimensional real MISO channels)* Let the channel equation of a co-located MISO fading channel with  $N_t$  transmit antennas be represented as  $\mathbf{y} = \sqrt{\frac{\rho}{N_t}} \mathbf{x} \mathbf{h} + \mathbf{n}$ , where  $\mathbf{y}$  is the received symbol at the destination,  $\mathbf{h}$  is the additive white Gaussian noise,  $\mathbf{h}$  is the  $N_t \times 1$  channel vector,  $\rho$  is the average receive SNR and  $\mathbf{x}$  is the  $1 \times N_t$  input vector. The above MISO channel is referred as a single-dimensional real MISO channel whenever  $\mathbf{x}, \mathbf{h} \in \mathbb{R}^{N_t}$  and  $\mathbf{n} \in \mathbb{R}$ .

*Theorem 3:* STBCs from the rate-1 ROD (which also includes rate-1 rectangular ROD) are information-lossless for a single-dimensional MISO channel for all values of  $N_t$ .

*Proof:* With the assumption of CSIT-P, each transmit antenna compensates for the rotation introduced by the channel. Let  $\mathbf{X}$  represent the  $T \times N_t$  ROD for  $N_t$  antennas in the real variables  $x_1, x_2, \dots, x_T$ . Note that the number of channel uses is equal to the number of real variables since  $\mathbf{X}$  is a rate-1 ROD. Also,  $\mathbf{X}$  has the following column vector representation

$$\mathbf{X} = [\mathbf{A}_1 \mathbf{x} \mathbf{A}_2 \mathbf{x} \cdots \mathbf{A}_{N_t} \mathbf{x}]$$

where  $\{\mathbf{A}_i | i = 1 \text{ to } N_t\}$  is the set of column vector representation matrices of  $\mathbf{X}$  and  $\mathbf{x}^T = [x_1, x_2, \dots, x_T]$ . The MISO channel equation with the above design is,  $\mathbf{y} = \sqrt{\frac{\rho}{N_t}} \mathbf{X} \tilde{\mathbf{h}} + \mathbf{n}$  where  $\rho$  is the average receive SNR and  $\mathbf{n} \sim \mathcal{N}(\mathbf{0}_{T \times 1}, \mathbf{I}_T)$ . It is assumed that the average power per real symbol of the design is unity. The above channel equation can also be written as

$$\mathbf{y} = \sqrt{\frac{\rho}{N_t}} \hat{\mathbf{H}} \mathbf{x} + \mathbf{n}$$

where  $\hat{\mathbf{H}} = \sum_{i=1}^{N_t} |h_i| \mathbf{A}_i$  with  $h_i$  denoting the channel from the  $i$ -th antenna to the destination. If  $\mathbf{x} \sim \mathcal{N}(\mathbf{0}_{T \times 1}, \mathbf{I}_T)$ , the average mutual information of the above channel is

$$\frac{1}{2} E \left[ \log_2 \left( \det \left( \mathbf{I}_T + \frac{\rho}{N_t} \hat{\mathbf{H}} \hat{\mathbf{H}}^H \right) \right) \right].$$

Since  $\mathbf{A}_i$ 's are unitary and  $\mathbf{A}_i \mathbf{A}_j^T + \mathbf{A}_j \mathbf{A}_i^T = \mathbf{0}_{T \times T} \forall i, j$  such that  $i \neq j$ , we have  $\hat{\mathbf{H}} \hat{\mathbf{H}}^H = (\sum_{i=1}^{N_t} h_i^2) \mathbf{I}_T$ , and hence, the average mutual information of a single-dimensional MISO channel with the ROD,  $\mathbf{X}$  is

$$\frac{1}{2} E \left[ \log_2 \left( 1 + \frac{\rho}{N_t} \left( \sum_{i=1}^{N_t} h_i^2 \right) \right) \right]$$

which is equal to the capacity of a single-dimensional MISO channel. Hence, STBCs from the rate-1 ROD are information-lossless. ■

In the following subsection, we propose STBC pairs  $(\mathcal{C}_1, \mathcal{C}_2)$  for  $N_t$ -MISO-MAC such that the ML-decoding complexity at the destination is minimum. The STBC pair  $(\mathcal{C}_1, \mathcal{C}_2)$  is specified by presenting a complex design pair  $(\mathbf{X}_1, \mathbf{X}_2)$  and a complex signal set pair  $(\mathcal{S}_1, \mathcal{S}_2)$  such that  $\mathcal{C}_1$  and  $\mathcal{C}_2$  are generated by making the complex variables of  $\mathbf{X}_1$  and  $\mathbf{X}_2$  take values from  $\mathcal{S}_1$

and  $\mathcal{S}_2$  respectively. In particular, we employ identical complex designs for both the users.

### B. STBC Pairs From Real Orthogonal Designs for $N_t$ -MISO-MAC

In this subsection, we propose a new class of STBC pairs from RODs wherein each user is interference free from the other. In the proposed scheme, User-1 employs a rate-1 ROD  $\mathbf{X}_1$  for  $N_t$  antennas and User-2 employs an identical ROD  $\mathbf{X}_2$ . The variables of  $\mathbf{X}_1$  take values from a  $M$ -PAM signal set whereas the variables of  $\mathbf{X}_2$  take values from a signal set which is 90 degrees rotated version of signal set used for  $\mathbf{X}_1$ . In general, both users can use PAM signal sets with different cardinalities. Since rate-1 RODs exist for all values of  $N_t$  [15], the proposed scheme is applicable for a  $N_t$ -MISO-MAC for any  $N_t$ .

*Example 3:* For a 4-MISO-MAC, the designs,  $\mathbf{X}_1$  and  $\mathbf{X}_2$  are as given in (45) and (46) where the variables  $x_{11}, x_{12}, \dots, x_{14}$  can take values from  $\mathcal{S}_1 = \{-3, -1, 1, 3\}$  and the variables  $x_{21}, x_{22}, \dots, x_{24}$  can take values from  $\mathcal{S}_2 = \{-3i, -1i, 1i, 3i\}$ .

$$\mathbf{X}_1 = \begin{bmatrix} x_{11} & x_{12} & x_{13} & x_{14} \\ -x_{12} & x_{11} & -x_{14} & x_{13} \\ -x_{13} & x_{14} & x_{11} & -x_{12} \\ -x_{14} & -x_{13} & x_{12} & -x_{11} \end{bmatrix} \quad \text{and} \quad (45)$$

$$\mathbf{X}_2 = \begin{bmatrix} x_{21} & x_{22} & x_{23} & x_{24} \\ -x_{22} & x_{21} & -x_{24} & x_{23} \\ -x_{23} & x_{24} & x_{21} & -x_{22} \\ -x_{24} & -x_{23} & x_{22} & -x_{21} \end{bmatrix}. \quad (46)$$

In the proposed scheme, since  $\tilde{\mathbf{H}}^{(j)}$ 's are real vectors and the two designs take values from orthogonal signal sets, the two users are interference free from each other. With this, the  $N_t$ -MISO-MAC channel splits into two parallel single-user MISO channels (one for each user) such that the MISO channel from (i) User-1 to the destination is given by

$$\mathbf{Y}_I = \sqrt{\frac{\rho}{2N_t}} \mathbf{X}_1 \tilde{\mathbf{H}}^{(1)} + \mathbf{N}_I \quad (47)$$

and (ii) the channel from User-2 to the destination is given by

$$\mathbf{iY}_Q = \sqrt{\frac{\rho}{2N_t}} \mathbf{X}_2 \tilde{\mathbf{H}}^{(2)} + \mathbf{iN}_Q. \quad (48)$$

Now, we proceed to study the capacity of the proposed scheme for different values of  $N_t$ .

1) *Capacity of a  $N_t$ -MISO-MAC With RODs:* Note that the channels in (47) and (48) are single-dimensional real MISO channels with  $\mathbf{N}_I, \mathbf{N}_Q \sim \mathcal{N}(\mathbf{0}_{T \times 1}, \frac{1}{2} \mathbf{I}_T)$ . Hence, the average receive SNR in each dimension is  $\rho$ . Since the rate-1 ROD for  $N_t$  antennas is information-lossless for a single-dimensional real MISO channel (Theorem 3), the capacity for User- $j$  is

$$\frac{1}{2} E \left[ \log_2 \left( 1 + \frac{\rho}{N_t} \tilde{\mathbf{H}}^{(j)} \tilde{\mathbf{H}}^{(j)H} \right) \right].$$

Therefore, the sum-capacity of the proposed scheme is given by

$$E \left[ \log_2 \left( 1 + \frac{\rho}{N_t} \tilde{\mathbf{H}}^{(2)} \tilde{\mathbf{H}}^{(2)H} \right) \right] \quad (49)$$

which is equal to the capacity of a  $N_t \times 1$  MIMO channel for an average SNR value of  $\rho$ . Without loss of generality, we have

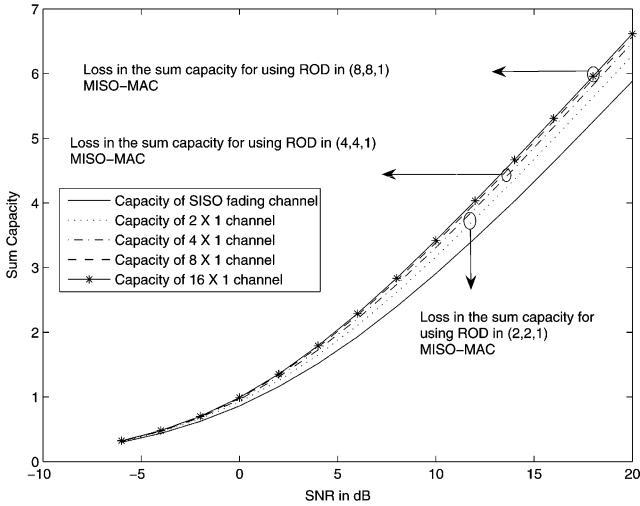


Fig. 24. Ergodic sum-capacity of  $N_t$ -MISO-MAC with RODs in comparison with  $C(N_t, N_t, 1)$  for  $N_t = 2, 4$  and  $8$ .

used  $\tilde{\mathbf{H}}^{(2)}$  as the channel vector. However, the sum-capacity of  $N_t$ -MISO-MAC is given in (43) which is equal to the capacity of a  $2N_t \times 1$  MIMO channel for an average SNR value of  $\rho$ . By comparing (49) with  $C(N_t, N_t, 1, p)$ , it is clear that the proposed scheme is not information-lossless for a  $N_t$ -MISO-MAC. Through simulations, in Fig. 24, the sum-capacity of the proposed scheme is compared with  $C(N_t, N_t, 1, p)$  for  $N_t = 2, 4$  and  $8$  respectively at different SNR values. Note that when  $N_t = 2$  and  $4$ , the proposed scheme is information-lossy by a small margin and the difference in the capacity keeps diminishing as  $N_t$  increases (see Fig. 24 for  $N_t = 8$ ). In particular, using strong law of large numbers, for large values of  $N_t$ , we have

$$\lim_{N_t \rightarrow \infty} E \left[ \log_2 \left( 1 + \frac{\rho}{N_t} \tilde{\mathbf{H}}^{(2)} \tilde{\mathbf{H}}^{(2)H} \right) \right] = C(N_t, N_t, 1, p)$$

and hence, the proposed designs are information-lossless for large values of  $N_t$ . The above discussion can be summarized in the following theorem:

**Theorem 4:** For large values of  $N_t$ , STBC pairs from rate-1 RODs are information-lossless for a  $N_t$ -MISO-MAC.

2) *Minimum Decoding Complexity:* Apart from having the information-losslessness property for large values of  $N_t$ , the proposed codes also have the single-symbol ML decodable property. From (47) and (48), the ML-decoding metrics for User-1 and User-2 are respectively given by

$$\hat{\mathbf{X}}_1 = \arg \min_{\mathcal{C}_1} \left\| \mathbf{Y}_I - \sqrt{\frac{\rho}{2N_t}} \mathbf{X}_1 \tilde{\mathbf{H}}^{(1)} \right\|^2 \quad \text{and}$$

$$\hat{\mathbf{X}}_2 = \arg \min_{\mathcal{C}_2} \left\| i\mathbf{Y}_Q - \sqrt{\frac{\rho}{2N_t}} \mathbf{X}_2 \tilde{\mathbf{H}}^{(2)} \right\|^2.$$

Since  $\mathbf{X}_1$  and  $\mathbf{X}_2$  are RODs, for each user, every symbol can be decoded independent of the rest of the symbols. For more details on decoding the class of STBCs from RODs, we refer the reader to [14], [15]. To the best of our knowledge, this is the first work that addresses the design of STBC pairs with single-symbol decodable property for two-user MISO-MAC.

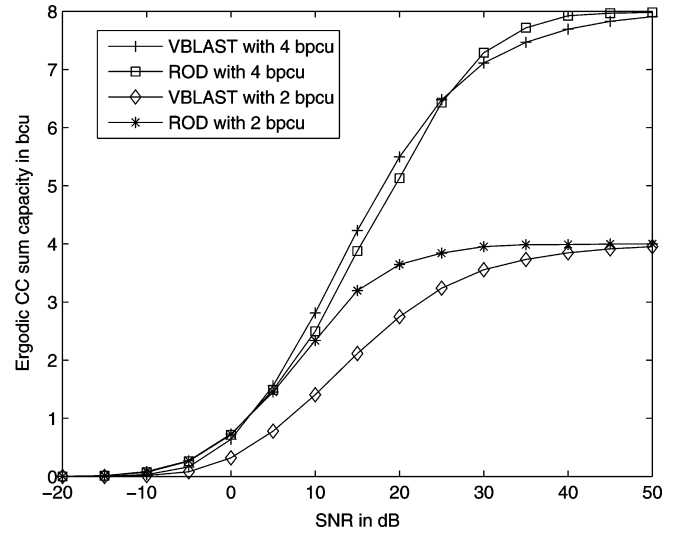


Fig. 25. CC ergodic sum-capacity of STBC pairs from ROD and VBLAST schemes for 2 bpcu and 4 bpcu.

3) *On the Diversity Order of STBCs From RODs in a  $N_t$ -MISO-MAC:* Since the columns of RODs are orthogonal, the channel equation in (47) can be written as  $\mathbf{Y}_I = \sqrt{\frac{\rho}{2N_t}} \hat{\mathbf{H}}^{(1)} \mathbf{x}_1 + \mathbf{N}_I$  where  $\mathbf{x}_1 \in \mathbb{R}^{T \times 1}$  consists of information symbols of User-1 and  $\hat{\mathbf{H}}^{(1)}$  is a scaled unitary matrix. Multiplying  $\hat{\mathbf{H}}^{(1)T}$  from the left, the above equation becomes  $\mathbf{Y}'_I = \sqrt{\frac{\rho}{2N_t}} \hat{\mathbf{H}}^{(1)T} \hat{\mathbf{H}}^{(1)} \mathbf{x}_1 + \mathbf{N}'_I$  (note that the matrix  $\hat{\mathbf{H}}^{(1)T} \hat{\mathbf{H}}^{(1)}$  is a diagonal matrix). As a result, the equivalent channel seen by each symbol of User-1 is Gamma distributed (with degrees of freedom  $2N_t$ ), and hence, STBC from RODs provide diversity order of  $N_t$  for User-1. Similarly, diversity order of  $N_t$  is obtained for User-2 as well.

4) *CC Ergodic Sum-Capacity of STBC Pairs From RODs in a  $N_t$ -MISO-MAC:* On the similar lines of the work in Section II, we present the CC ergodic sum-capacity of the STBCs from RODs. We also present the CC ergodic sum-capacity of the VBLAST scheme wherein independent uncoded symbols are transmitted from all the antennas simultaneously. For a fixed rate (in bits per channel use), CC ergodic sum-capacity of the STBCs from RODs is compared with that of VBLAST scheme in Fig. 25. From Fig. 25, it is clear that, in addition to the advantage of having minimum ML decoding complexity, the STBC pairs from RODs have comparable CC ergodic sum-capacity values with VBLAST schemes.

### C. Space-Time Block Codes With Low Sphere Decoding Complexity for Two-User MIMO-MAC

In the preceding section, STBC pairs were proposed with minimum ML decoding complexity for two-user MISO-MAC with the assumption of CSIT-P. However, when CSIT-P is not available, the proposed STBCs are not applicable. Hence, in this subsection, we propose STBC pairs for two-user MIMO fading MAC where (i) the two users have  $N_t$  antennas, (ii) the destination has  $N_r$  antennas, and (iii) the destination has the perfect knowledge of CSI [30]. In this setup, the two users do not have CSI (not even CSIT-P). In particular, the proposed STBC pairs  $(\mathcal{C}_1, \mathcal{C}_2)$  have reduced sphere decoding [20], [21] complexity.

The STBC pair  $(C_1, C_2)$  is specified by presenting a complex design pair  $(\mathbf{X}_1, \mathbf{X}_2)$  and a complex signal set pair  $(\mathcal{S}_1, \mathcal{S}_2)$  such that  $C_1$  and  $C_2$  are generated by making the complex variables of  $\mathbf{X}_1$  and  $\mathbf{X}_2$  take values from the signal sets  $\mathcal{S}_1$  and  $\mathcal{S}_2$  respectively. We only consider the class of linear designs for  $\mathbf{X}_1$  and  $\mathbf{X}_2$  [22]. Identical designs are employed for both the users and the complex variables of the design for User-1 and User-2 are denoted by  $\{x_{11}, x_{12}, \dots, x_{1k}\}$  and  $\{x_{21}, x_{22}, \dots, x_{2k}\}$  respectively where  $k$  denotes the number of complex variables in the design. Since the design is linear, it can be represented as

$$\mathbf{X}_i = [\mathbf{A}_1 \mathbf{x}_i + \mathbf{B}_1 \mathbf{x}_i^* \mathbf{A}_2 \mathbf{x}_i + \mathbf{B}_2 \mathbf{x}_i^* \dots \mathbf{A}_{N_t} \mathbf{x}_i + \mathbf{B}_{N_t} \mathbf{x}_i^*]$$

where

$$\{\mathbf{A}_i, \mathbf{B}_i \in \mathbb{C}^{T \times k} | i = 1 \text{ to } N_t\}$$

is the set of column vector representation matrices [15] of  $\mathbf{X}_1$  and  $\mathbf{X}_2$  and,  $\mathbf{x}_1^T = [x_{11}, x_{12}, \dots, x_{1k}]$ ,  $\mathbf{x}_2^T = [x_{21}, x_{22}, \dots, x_{2k}]$ . If STBCs from the above two designs are employed in two-user MIMO-MAC, the vector received at the  $j$ -th antenna of the destination is of the form

$$\mathbf{Y}_c(j) = \sqrt{\frac{\rho}{2N_t}} \mathbf{X}_1 \mathbf{H}_c^{(1)}(j) + \sqrt{\frac{\rho}{2N_t}} \mathbf{X}_2 \mathbf{H}_c^{(2)}(j) + \mathbf{N}_c(j).$$

Throughout the subsection, it is assumed that the destination performs sphere decoding for the symbols of User-1 and User-2 jointly. Therefore, the complex variables of the two designs need to take values from a lattice constellation, and hence, square  $M$ -QAM signal set is used as the underlying constellation. Also, the channel equation has to be rewritten in a particular form in the *real variables* which is amenable for sphere decoding. Towards that direction, using the column vector representations of  $\mathbf{X}_1$  and  $\mathbf{X}_2$ , for each  $j = 1$  to  $N_r$ ,  $\mathbf{Y}_c(j)$  can be written in terms of its real and imaginary components as

$$\tilde{\mathbf{Y}}_c(j) = \sqrt{\frac{\rho}{2N_t}} \tilde{\mathbf{H}}_c^{(1)}(j) \tilde{\mathbf{x}}_1 + \sqrt{\frac{\rho}{2N_t}} \tilde{\mathbf{H}}_c^{(2)}(j) \tilde{\mathbf{x}}_2 + \tilde{\mathbf{N}}_c(j) \quad (50)$$

where the matrices  $\tilde{\mathbf{H}}_c^{(1)}(j) \in \mathbb{R}^{2T \times 2k}$  and  $\tilde{\mathbf{H}}_c^{(2)}(j) \in \mathbb{R}^{2T \times 2k}$  are as given in (51) and (52), respectively, shown at the bottom of the page, with  $h_{i,j}^{(1)}$  denoting the channel from the  $i$ -th antenna of User-1 to the  $j$ -th antenna of the destination and,  $h_{i,j}^{(2)}$  denoting the channel from the  $i$ -th antenna of User-2 to the  $j$ -th antenna of the destination. Equation (50) can be written as

$$\tilde{\mathbf{Y}}_c(j) = \sqrt{\frac{\rho}{2N_t}} \left[ \tilde{\mathbf{H}}_c^{(1)}(j) \tilde{\mathbf{H}}_c^{(2)}(j) \right] \mathbf{z} + \tilde{\mathbf{N}}_c(j)$$

where  $\mathbf{z} = [(\tilde{\mathbf{x}}_1)^T (\tilde{\mathbf{x}}_2)^T]^T \in \mathbb{R}^{4k \times 1}$ . Juxtaposing  $\tilde{\mathbf{Y}}_c(j)$  for all  $j = 1$  to  $N_r$ , one below the other, the channel equation is given by

$$\mathbf{y} = \sqrt{\frac{\rho}{2N_t}} \mathbf{M} \mathbf{z} + \mathbf{n} \quad (53)$$

where

$$\mathbf{y} = \left[ (\tilde{\mathbf{Y}}_c(1))^T (\tilde{\mathbf{Y}}_c(2))^T \dots (\tilde{\mathbf{Y}}_c(N_r))^T \right]^T \in \mathbb{R}^{2TN_r \times 1}$$

$$\mathbf{n} = \left[ (\tilde{\mathbf{N}}_c(1))^T (\tilde{\mathbf{N}}_c(2))^T \dots (\tilde{\mathbf{N}}_c(N_r))^T \right]^T \in \mathbb{R}^{2TN_r \times 1}$$

and

$$\mathbf{M} = \begin{bmatrix} \tilde{\mathbf{H}}_c^{(1)}(1) & \tilde{\mathbf{H}}_c^{(2)}(1) \\ \tilde{\mathbf{H}}_c^{(1)}(2) & \tilde{\mathbf{H}}_c^{(2)}(2) \\ \vdots & \vdots \\ \tilde{\mathbf{H}}_c^{(1)}(N_r) & \tilde{\mathbf{H}}_c^{(2)}(N_r) \end{bmatrix} \in \mathbb{R}^{2TN_r \times 4k}. \quad (54)$$

The matrix  $\mathbf{M}$  can be used as the lattice generator for carrying out sphere decoding algorithm. Since the variables of the two designs take values from an identical square  $M$ -QAM constellation, each component of  $\mathbf{z}$  takes value from the corresponding  $\sqrt{M}$ -PAM signal set. For  $\mathbf{M}$  to have rank  $4k$ , the inequality  $2TN_r \geq 4k$  must hold. Hence, throughout this subsection, we assume  $N_r = \lceil \frac{2k}{T} \rceil$ . Viewing  $\mathbf{M}$  as a real linear design in the variables  $\text{Re}(h_{i,j}^{(1)})$ ,  $\text{Im}(h_{i,j}^{(1)})$ ,  $\text{Re}(h_{i,j}^{(2)})$  and  $\text{Im}(h_{i,j}^{(2)})$ , it can be written using the column vector representation as

$$\mathbf{M} = \left[ \mathbf{C}_1 \mathbf{h}^{(1)} \mathbf{C}_2 \mathbf{h}^{(1)} \dots \mathbf{C}_{2k} \mathbf{h}^{(1)} \mathbf{C}_1 \mathbf{h}^{(2)} \mathbf{C}_2 \mathbf{h}^{(2)} \dots \mathbf{C}_{2k} \mathbf{h}^{(2)} \right]$$

where

$$\mathbf{h}^{(1)} = \left[ \left( \tilde{\mathbf{H}}_c^{(1)}(1) \right)^T \left( \tilde{\mathbf{H}}_c^{(1)}(2) \right)^T \dots \left( \tilde{\mathbf{H}}_c^{(1)}(N_r) \right)^T \right]^T$$

$$\in \mathbb{R}^{2N_t N_r \times 1}$$

$$\mathbf{h}^{(2)} = \left[ \left( \tilde{\mathbf{H}}_c^{(2)}(1) \right)^T \left( \tilde{\mathbf{H}}_c^{(2)}(2) \right)^T \dots \left( \tilde{\mathbf{H}}_c^{(2)}(N_r) \right)^T \right]^T$$

$$\in \mathbb{R}^{2N_t N_r \times 1}$$

and  $\{\mathbf{C}_i \in \mathbb{R}^{2TN_r \times 2N_t N_r} | i = 1 \text{ to } 2k\}$  is the set of column vector representation matrices of  $\mathbf{M}$ . Since the design employed for both the users is the same, the set of column vector representation matrices for the first  $2k$  columns of  $\mathbf{M}$  and the last  $2k$  columns of  $\mathbf{M}$  are the same.

*Definition 7: (Column (Row) monomial matrix)* A matrix is said to be column (row) monomial, if there is at most one nonzero entry in every column (row) of it.

We design a special class of complex designs such that the resulting  $\mathbf{M}$  has the following properties:

- (p.1). The entries in the first  $2k$  columns of  $\mathbf{M}$  are of the form  $\pm \text{Re}(h_{i,j}^{(1)})$ ,  $\pm \text{Im}(h_{i,j}^{(1)}) \forall i, j$ .

$$\tilde{\mathbf{H}}_c^{(1)}(j) = \sum_{i=1}^{N_t} \begin{bmatrix} \text{Re}(h_{i,j}^{(1)} \mathbf{A}_i) + \text{Re}(h_{i,j}^{(1)} \mathbf{B}_i) & -\text{Im}(h_{i,j}^{(1)} \mathbf{A}_i) + \text{Im}(h_{i,j}^{(1)} \mathbf{B}_i) \\ \text{Im}(h_{i,j}^{(1)} \mathbf{A}_i) + \text{Im}(h_{i,j}^{(1)} \mathbf{B}_i) & \text{Re}(h_{i,j}^{(1)} \mathbf{A}_i) - \text{Re}(h_{i,j}^{(1)} \mathbf{B}_i) \end{bmatrix} \quad (51)$$

$$\tilde{\mathbf{H}}_c^{(2)}(j) = \sum_{i=1}^{N_t} \begin{bmatrix} \text{Re}(h_{i,j}^{(2)} \mathbf{A}_i) + \text{Re}(h_{i,j}^{(2)} \mathbf{B}_i) & -\text{Im}(h_{i,j}^{(2)} \mathbf{A}_i) + \text{Im}(h_{i,j}^{(2)} \mathbf{B}_i) \\ \text{Im}(h_{i,j}^{(2)} \mathbf{A}_i) + \text{Im}(h_{i,j}^{(2)} \mathbf{B}_i) & \text{Re}(h_{i,j}^{(2)} \mathbf{A}_i) - \text{Re}(h_{i,j}^{(2)} \mathbf{B}_i) \end{bmatrix} \quad (52)$$

- (p.2). The entries in the last  $2k$  columns of  $\mathbf{M}$  are of the form  $\pm \text{Re}(h_{i,j}^{(2)})$ ,  $\pm \text{Im}(h_{i,j}^{(2)}) \forall i, j$ .
- (p.3). Every column of  $\mathbf{M}$  has all the  $2N_t N_r$  variables appearing exactly once.

The above three properties imply that for each  $i = 1$  to  $2k$ ,  $\mathbf{C}_i$  is both row and column monomial. The class of lattice generators with the above set of conditions are referred to as row-column monomial lattice generators which are formally defined as follows:

*Definition 8: (Row-column monomial lattice generator)* A lattice generator  $\mathbf{M}$  is said to be row-column monomial (RC monomial) if the column vector representation matrices of  $\mathbf{M}$  are both row and column monomial.

Note that the property (p.3) implies that the norms of the first  $2k$  columns of  $\mathbf{M}$  are the same. Similarly, the norms of the last  $2k$  columns of  $\mathbf{M}$  are the same.

1) *Structure on  $\mathbf{M}$  for Reduction in the Decoding Complexity:* Applying Q-R decomposition on  $\mathbf{M}$  and multiplying  $\mathbf{Q}^T$  on both the sides of the channel equation in (53), we have

$$\tilde{\mathbf{y}} = \sqrt{\frac{\rho}{2N_t}} \mathbf{R} \mathbf{z} + \tilde{\mathbf{n}} \quad (55)$$

where  $\tilde{\mathbf{y}} = \mathbf{Q}^T \mathbf{y} \in \mathbb{R}^{2TN_r \times 1}$ ,  $\tilde{\mathbf{n}} = \mathbf{Q}^T \mathbf{n} \in \mathbb{R}^{2TN_r \times 1}$  and  $\mathbf{R} \in \mathbb{R}^{2TN_r \times 4k}$ . Since we have assumed  $N_r = \lceil \frac{2k}{T} \rceil$ , only the first  $4k$  rows of  $\mathbf{R}$  have nonzero entries, and hence,  $\tilde{\mathbf{y}}$  is essentially a  $4k \times 1$  vector and  $\mathbf{R}$  is essentially a square matrix (neglecting the last  $2TN_r - 4k$  rows) given by

$$\mathbf{R} = \begin{bmatrix} \mathbf{R}_{1,1} & \mathbf{R}_{1,2} \\ \mathbf{0} & \mathbf{R}_{2,2} \end{bmatrix}$$

with  $\mathbf{R}_{1,1}, \mathbf{R}_{1,2}, \mathbf{R}_{2,2} \in \mathbb{R}^{2k \times 2k}$  such that  $\mathbf{R}_{1,1}$  and  $\mathbf{R}_{2,2}$  are upper triangular matrices. The ML decoding metric is given by

$$\hat{\mathbf{z}} = \arg \min_{\mathbf{z}} \left\| \tilde{\mathbf{y}} - \sqrt{\frac{\alpha}{2N_t}} \mathbf{R} \mathbf{z} \right\|^2. \quad (56)$$

The following proposition shows that none of the entries in the sub-matrix  $\mathbf{R}_{1,2}$  can be zero when identical STBCs are employed in the two-user MIMO-MAC set-up.

*Proposition 4:* When identical STBCs are employed in two-user MIMO-MAC, it is not possible to have zero entries in the matrix  $\mathbf{R}_{1,2}$ .

*Proof:* The matrix  $\mathbf{R}$  arising out of the Q-R decomposition of  $\mathbf{M}$  is of the form

$$\mathbf{R} = \begin{bmatrix} \langle \mathbf{e}_1, \mathbf{c}_1 \rangle & \langle \mathbf{e}_1, \mathbf{c}_2 \rangle & \cdots & \langle \mathbf{e}_1, \mathbf{c}_{4k} \rangle \\ 0 & \langle \mathbf{e}_2, \mathbf{c}_2 \rangle & \cdots & \langle \mathbf{e}_2, \mathbf{c}_{4k} \rangle \\ 0 & 0 & \cdots & \langle \mathbf{e}_3, \mathbf{c}_{4k} \rangle \\ \vdots & \vdots & \ddots & \vdots \\ 0 & 0 & 0 & \langle \mathbf{e}_{4k}, \mathbf{c}_{4k} \rangle \end{bmatrix} \quad (57)$$

where  $\mathbf{c}_i$  denotes the  $i$ -th column of  $\mathbf{M}$ , the vector  $\mathbf{e}_i = \frac{\mathbf{u}_i}{\|\mathbf{u}_i\|}$  with

$$\mathbf{u}_i = \mathbf{c}_i - \sum_{j=1}^{i-1} \langle \mathbf{e}_j, \mathbf{c}_i \rangle \mathbf{e}_j \forall i = 1, 2, \dots, 4k. \quad (58)$$

Note that for  $1 \leq m \leq 2k$  and  $2k+1 \leq n \leq 4k$ ,  $[\mathbf{R}]_{m,n}$  is given by

$$[\mathbf{R}]_{m,n} = \langle \mathbf{e}_m, \mathbf{c}_n \rangle.$$

Also, note that the variables in the first  $2k$  columns of  $\mathbf{M}$  do not appear in the last  $2k$  columns of  $\mathbf{M}$ . In particular,  $\mathbf{e}_m$  is a vector in the variables  $\text{Re}(h_{i,j}^{(1)})$ ,  $\text{Im}(h_{i,j}^{(1)})$  whereas  $\mathbf{c}_m$  is a vector in the variables  $\text{Re}(h_{i,j}^{(2)})$ ,  $\text{Im}(h_{i,j}^{(2)})$ . Hence,  $\langle \mathbf{e}_m, \mathbf{c}_n \rangle \neq 0$ . Therefore, for any STBC employed in two-user MIMO-MAC, the matrix  $\mathbf{R}_{1,2}$  cannot have zero entries unless there exists at least one pair of columns (say  $\mathbf{c}_i$  and  $\mathbf{c}_j$ ) in the first  $2k$  columns of  $\mathbf{M}$  which are orthogonal. ■

From the above proposition, constructing STBCs which give rise to both  $\mathbf{R}_{1,1} \in \mathcal{D}$  and  $\mathbf{R}_{2,2} \in \mathcal{D}$  is the best thing that can be done towards constructing STBCs with reduced sphere decoding complexity (SDC). Hence, we study STBCs which results in  $\mathbf{M}$  (through (54)) such that the Q-R decomposition of  $\mathbf{M}$  gives rise to the  $\mathbf{R}$  matrix with (i)  $\mathbf{R}_{1,1} \in \mathcal{D}$ ,  $\mathbf{R}_{2,2} \in \mathcal{D}$  and (ii)  $\mathbf{R}_{1,1} \in \mathcal{D}$ ,  $\mathbf{R}_{2,2} \notin \mathcal{D}$  (such classes of STBCs are formally defined in the following definitions).

*Definition 9: (Average Sphere Decoding Complexity)* For two-user MIMO-MAC, an STBC is said to have reduced average SDC (ASDC), if the corresponding  $\mathbf{R}$  matrix is such that both  $\mathbf{R}_{1,1}, \mathbf{R}_{2,2} \in \mathcal{D}$ .

*Definition 10: (Worst-case Sphere Decoding Complexity)* For two-user MIMO-MAC, an STBC is said to have reduced worst-case SDC (WSDC), if the corresponding  $\mathbf{R}$  matrix is such that only  $\mathbf{R}_{1,1} \in \mathcal{D}$  (but  $\mathbf{R}_{2,2} \notin \mathcal{D}$ ).

In the next subsection, we quantify the reduction in the SDC when both  $\mathbf{R}_{1,1}$  and  $\mathbf{R}_{2,2}$  are diagonal matrices.

2) *Reduction in the Decoding Complexity When  $\mathbf{R}_{1,1}, \mathbf{R}_{2,2} \in \mathcal{D}$ :* For the decoder given by (56), we quantify the reduction in the SDC when  $\mathbf{R}_{1,1}, \mathbf{R}_{2,2} \in \mathcal{D}$ . Note that for point to point co-located MIMO channels, SDC has been reduced in [31], [32] and [33] by making certain entries of  $\mathbf{R}$  matrix take zero values. In our setup, since  $\mathbf{R}$  is upper triangular, the metric in (56) can be split as

$$\left\| \tilde{\mathbf{y}}_1 - \sqrt{\frac{\alpha}{2N_t}} (\mathbf{R}_{1,1} \tilde{\mathbf{x}}_1 + \mathbf{R}_{1,2} \tilde{\mathbf{x}}_2) \right\|^2 + \left\| \tilde{\mathbf{y}}_2 - \sqrt{\frac{\alpha}{2N_t}} \mathbf{R}_{2,2} \tilde{\mathbf{x}}_2 \right\|^2$$

where

$$\tilde{\mathbf{y}}_1 = [\tilde{\mathbf{y}}(1) \tilde{\mathbf{y}}(2) \cdots \tilde{\mathbf{y}}(2k)]^T$$

and

$$\tilde{\mathbf{y}}_2 = [\tilde{\mathbf{y}}(2k+1) \tilde{\mathbf{y}}(2k+2) \cdots \tilde{\mathbf{y}}(4k)]^T.$$

Note that each component of  $\tilde{\mathbf{x}}_2$  takes value from  $\sqrt{M}$ -PAM, and hence, the vector  $\tilde{\mathbf{x}}_2$  totally takes  $M^k$  distinct values. For a particular choice of  $\tilde{\mathbf{x}}_2$ , say  $\tilde{\mathbf{x}}_2 = \mathbf{a}$ , the metric for decoding  $\tilde{\mathbf{x}}_1$  is

$$\left\| \tilde{\mathbf{y}}_1^a - \sqrt{\frac{\alpha}{2N_t}} \mathbf{R}_{1,1} \tilde{\mathbf{x}}_1 \right\|^2 + \|\tilde{\mathbf{y}}_2^a\|^2 \quad (59)$$

where

$$\tilde{\mathbf{y}}_1^a = \tilde{\mathbf{y}}_1 - \sqrt{\frac{\alpha}{2N_t}} \mathbf{R}_{1,2} \mathbf{a} \quad \text{and} \quad \tilde{\mathbf{y}}_2^a = \tilde{\mathbf{y}}_2 - \sqrt{\frac{\alpha}{2N_t}} \mathbf{R}_{2,2} \mathbf{a}.$$

Since  $\mathbf{R}_{1,1} \in \mathcal{D}$ , for each  $i = 1$  to  $2k$ , the  $i$ -th real variable of  $\tilde{\mathbf{x}}_1$  can be decoded independent of the other real variables as

$$\hat{\tilde{\mathbf{x}}}_1(i) = \mathcal{Q} \left( \frac{\tilde{\mathbf{y}}_1^a(i)}{\sqrt{\frac{\alpha}{2N_i} [\mathbf{R}_{1,1}]_{i,i}}} \right)$$

where  $\mathcal{Q}(\cdot)$  denotes the nearest integer quantizer operation whose complexity is independent of the size of the constellation. Therefore, the worst-case decoding complexity is reduced from  $O(M^{2k})$  to  $O(M^k)$ . Note that, the worst-case complexity of the decoder remains to be  $O(M^k)$  irrespective of whether  $\mathbf{R}_{2,2} \in \mathcal{D}$  or otherwise. However, when  $\mathbf{R}_{2,2} \in \mathcal{D}$ , the ASDC is reduced as follows: When  $\mathbf{R}_{2,2} \in \mathcal{D}$ , in choosing a particular value for  $\tilde{\mathbf{x}}_2$ ,  $2k$  independent sorting operations are needed where each sorting operation involves sorting of  $\sqrt{M}$  integers based on a constraint function. However, in the worst-case, if  $\mathbf{R}_{2,2}$  is not diagonal (with all the upper diagonal entries of  $\mathbf{R}_{2,2}$  being nonzero), then there needs to be a single sorting operation of  $M^k$  vectors of length  $2k$  based on a constraint function. Thus, with  $\mathbf{R}_{2,2} \in \mathcal{D}$ , there is a reduction in the sorting complexity which is significant especially when  $M$  is large.

3) *Necessary and Sufficient Conditions on  $\mathbf{M}$  Such That  $\mathbf{R}_{1,1}, \mathbf{R}_{2,2} \in \mathcal{D}$ :* In this subsection, a set of necessary and sufficient conditions on the matrix set  $\{\mathbf{C}_1, \mathbf{C}_2, \dots, \mathbf{C}_{2k}\}$  is provided such that both  $\mathbf{R}_{1,1}$  and  $\mathbf{R}_{2,2}$  are diagonal matrices. The following definition is important towards proving the necessary and sufficient conditions.

*Definition 11: ( $k$ -group partition)* A  $k$ -group partition of the index set  $\mathcal{I}_{2k} = \{1, 2, \dots, 2k\}$  consists of  $k$  disjoint subsets,  $\mathcal{G}_1, \mathcal{G}_2, \dots, \mathcal{G}_k$  such that  $|\mathcal{G}_i| = 2\forall i = 1$  to  $k$ .

*Theorem 5:* The Q-R decomposition of  $\mathbf{M}$  results in a  $\mathbf{R}$  matrix with  $\mathbf{R}_{1,1}, \mathbf{R}_{2,2} \in \mathcal{D}$  if and only if the matrix set  $\{\mathbf{C}_1, \mathbf{C}_2, \dots, \mathbf{C}_{2k}\}$  satisfies the following conditions:

- 1) For  $i \neq j$ , the matrices in the set  $\{\mathbf{C}_1, \mathbf{C}_2, \dots, \mathbf{C}_{2k}\}$  must be Hurwitz-Radon orthogonal, i.e.,

$$\mathbf{C}_i^T \mathbf{C}_j + \mathbf{C}_j^T \mathbf{C}_i = \mathbf{0}_{2N_i N_r}.$$

- 2) For a fixed  $l, m \in \mathcal{I}_{2k}$  such that  $l \neq m$ , there exists a  $k$ -group partition of  $\mathcal{I}_{2k}$  given by  $\mathcal{P}^{l,m} = \{\mathcal{G}_1^{l,m}, \mathcal{G}_2^{l,m}, \dots, \mathcal{G}_k^{l,m}\}$  such that

$$\begin{aligned} \mathbf{C}_l^T \mathbf{C}_{\mathcal{G}_i^{l,m}(1)} &= \mathbf{C}_m^T \mathbf{C}_{\mathcal{G}_i^{l,m}(2)} \quad \text{and} \\ \mathbf{C}_m^T \mathbf{C}_{\mathcal{G}_i^{l,m}(1)} &= -\mathbf{C}_l^T \mathbf{C}_{\mathcal{G}_i^{l,m}(2)} \quad \forall i = 1 \text{ to } k. \end{aligned}$$

*Proof:* The ‘if’ part can be proved by substituting the conditions 1) and 2) (given in the statement of the theorem) in  $\mathbf{R}$  which is straightforward. Hence, we prove the ‘only if’ part of the theorem. Since  $\mathbf{R}_{1,1} \in \mathcal{D}$ , we have  $\langle \mathbf{e}_i, \mathbf{c}_j \rangle = 0$  for all  $i \neq j$  such that  $1 \leq i, j \leq 2k$ . This implies  $\langle \mathbf{c}_i, \mathbf{c}_j \rangle = 0$  for all  $i \neq j$  such that  $1 \leq i, j \leq 2k$ . Therefore, the first  $2k$  columns of  $\mathbf{M}$  are necessarily orthogonal to each other, and hence,

$$\mathbf{C}_i^T \mathbf{C}_j + \mathbf{C}_j^T \mathbf{C}_i = \mathbf{0}_{2N_i N_r} \quad \text{for all } i \neq j.$$

This proves the condition 1) of the theorem (this condition reduces the WSDC). In the rest of the proof, the condition in 2) is proved. The structure of the matrix  $\mathbf{R}_{2,2}$  is given in (60), shown at the bottom of the page. Since  $\mathbf{R}_{2,2} \in \mathcal{D}$ , we have  $\langle \mathbf{e}_l, \mathbf{c}_m \rangle = 0$  for  $l \neq m$  such that  $2k + 1 \leq l, m \leq 4k$ . This implies

$$\langle \mathbf{u}_l, \mathbf{c}_m \rangle = 0.$$

Using (58) in the above equation, we have

$$\langle \mathbf{u}_l, \mathbf{c}_m \rangle = \langle \mathbf{c}_l, \mathbf{c}_m \rangle - \sum_{j=1}^{l-1} \langle \mathbf{e}_j, \mathbf{c}_l \rangle \langle \mathbf{e}_j, \mathbf{c}_m \rangle = 0.$$

Since  $\mathbf{C}_i^T \mathbf{C}_j + \mathbf{C}_j^T \mathbf{C}_i = \mathbf{0}_{2N_i N_r}$  for all  $i \neq j$ , we have  $\langle \mathbf{c}_l, \mathbf{c}_m \rangle = 0$ , and hence

$$\sum_{j=1}^{l-1} \langle \mathbf{e}_j, \mathbf{c}_l \rangle \langle \mathbf{e}_j, \mathbf{c}_m \rangle = 0.$$

As  $l$  takes value from  $2k + 1$  to  $4k$ , the above summation can be split as

$$\sum_{j=1}^{2k} \langle \mathbf{e}_j, \mathbf{c}_l \rangle \langle \mathbf{e}_j, \mathbf{c}_m \rangle + \sum_{j=2k+1}^{l-1} \langle \mathbf{e}_j, \mathbf{c}_l \rangle \langle \mathbf{e}_j, \mathbf{c}_m \rangle = 0.$$

Since  $\mathbf{R}_{2,2} \in \mathcal{D}$ , each term in the second summand of the above equation is individually zero, and hence, we have

$$\sum_{j=1}^{2k} \langle \mathbf{e}_j, \mathbf{c}_l \rangle \langle \mathbf{e}_j, \mathbf{c}_m \rangle = 0.$$

As the first  $2k$  columns of  $\mathbf{M}$  are orthogonal to each other and have equal norms, we have

$$\sum_{j=1}^{2k} \langle \mathbf{c}_j, \mathbf{c}_l \rangle \langle \mathbf{c}_j, \mathbf{c}_m \rangle = 0.$$

---


$$\mathbf{R}_{2,2} = \begin{bmatrix} \langle \mathbf{e}_{2k+1}, \mathbf{c}_{2k+1} \rangle & \langle \mathbf{e}_{2k+1}, \mathbf{c}_{2k+2} \rangle & \cdots & \langle \mathbf{e}_{2k+1}, \mathbf{c}_{4k} \rangle \\ 0 & \langle \mathbf{e}_{2k+2}, \mathbf{c}_{2k+2} \rangle & \cdots & \langle \mathbf{e}_{2k+2}, \mathbf{c}_{4k} \rangle \\ 0 & 0 & \cdots & \langle \mathbf{e}_{2k+3}, \mathbf{c}_{4k} \rangle \\ \vdots & \vdots & \ddots & \vdots \\ 0 & 0 & 0 & \langle \mathbf{e}_{4k}, \mathbf{c}_{4k} \rangle \end{bmatrix} \quad (60)$$

As  $2k + 1 \leq l, m \leq 4k$ , we have  $\mathbf{c}_l = \mathbf{C}_l \mathbf{h}^{(2)}$ ,  $\mathbf{c}_m = \mathbf{C}_m \mathbf{h}^{(2)}$  and  $\mathbf{c}_j = \mathbf{C}_j \mathbf{h}^{(1)}$  where  $l' = l \bmod 2k$  and  $m' = m \bmod 2k$ , and hence

$$\sum_{j=1}^{2k} ((\mathbf{h}^{(2)})^T \mathbf{C}_l^T \mathbf{C}_j \mathbf{h}^{(1)}) ((\mathbf{h}^{(2)})^T \mathbf{C}_m^T \mathbf{C}_j \mathbf{h}^{(1)}) = 0.$$

Note that for a fixed  $m$ , the matrices  $\mathbf{C}_m^T \mathbf{C}_j$  and  $\mathbf{C}_m^T \mathbf{C}_i$  do not have nonzero entries at the same position for all  $i \neq j$ . Similarly, for a fixed  $l$ , the matrices  $\mathbf{C}_l^T \mathbf{C}_j$  and  $\mathbf{C}_l^T \mathbf{C}_i$  do not have nonzero entries at the same position for all  $i \neq j$ . Hence, for a given  $l, m$ , there exists a  $k$ -group partition  $\mathcal{P}^{l,m} = \{\mathcal{G}_1^{l,m}, \mathcal{G}_2^{l,m}, \dots, \mathcal{G}_k^{l,m}\}$  of the index set  $\mathcal{I}_{2k}$  such that

$$\begin{aligned} \mathbf{C}_l^T \mathbf{C}_{\mathcal{G}_i^{l,m}(1)} &= \mathbf{C}_m^T \mathbf{C}_{\mathcal{G}_i^{l,m}(2)} \quad \text{and} \\ \mathbf{C}_m^T \mathbf{C}_{\mathcal{G}_i^{l,m}(1)} &= -\mathbf{C}_l^T \mathbf{C}_{\mathcal{G}_i^{l,m}(2)} \quad \forall i = 1 \text{ to } k. \end{aligned}$$

This completes the proof.  $\blacksquare$

4) *Code Constructions*: In this subsection, we present explicit constructions of STBCs which have (i) reduced ASDC and (ii) reduced WSDC. Complex designs which results in the  $\mathbf{R}$  matrix with (i)  $\mathbf{R}_{1,1}, \mathbf{R}_{2,2} \in \mathcal{D}$  and (ii) only  $\mathbf{R}_{1,1} \in \mathcal{D}$  are presented. Henceforth, we denote a complex design for  $N_t$  antennas in  $k$  variables as  $\mathbf{X}(N_t, k)$ . First, we construct complex designs which results in  $\mathbf{R}_{1,1}, \mathbf{R}_{2,2} \in \mathcal{D}$ . Construction of these designs has been divided in to four cases depending on the values of  $N_t$  and  $k$ .

*Case 1*:  $N_t = 2a$  and  $k = 2b$  ( $a$  and  $b$  are positive integers): In this case, the design is constructed in the following 3 steps.

- Step (i): Let  $\Omega_m$  represent a  $2 \times 2$  Alamouti design in complex variables  $x_{2m+1}, x_{2m+2}$  for each  $m = 0, 1, \dots, b-1$ , given by

$$\Omega_m = \begin{bmatrix} x_{2m+1} & -x_{2m+2}^* \\ x_{2m+2} & x_{2m+1}^* \end{bmatrix}.$$

- Step (ii): Using  $\Omega_m$ , construct a  $2a \times 2a$  matrix  $\mathbf{X}_m$  given by

$$\mathbf{X}_m = \Omega_m \otimes \mathbf{I}_2^{\otimes(a-1)} \quad \text{for each } m = 0, 1, \dots, b-1.$$

- Step (iii): Using  $\Omega_m$ ,  $\mathbf{X}(N_t, k)$  is constructed as

$$\mathbf{X}(N_t, k) = [\mathbf{X}_0^T \mathbf{X}_1^T \dots \mathbf{X}_{b-1}^T]^T.$$

*Case 2*:  $N_t = 2a$  and  $k = 2b + 1$ : In this case,  $\mathbf{X}(N_t, k)$  is constructed in two steps as given below.

- Step (i): Construct  $\mathbf{X}(N_t, 2b)$  as given in Case 1.
- Step (ii):  $\mathbf{X}(N_t, k) = [\mathbf{X}(N_t, 2b)^T x_{2b+1} \mathbf{I}_{N_t}]^T$ .

*Case 3*:  $N_t = 2a + 1$  and  $k = 2b$ : In this case,  $\mathbf{X}(N_t, k)$  is constructed in the following 2 steps.

- Step (i): Construct  $\mathbf{X}(N_t + 2, k)$  as given in Case 1.
- Step (ii): Drop the last column of  $\mathbf{X}(N_t + 2, k)$ .

*Case 4*:  $N_t = 2a + 1$  and  $k = 2b + 1$ : In this case,  $\mathbf{X}(N_t, k)$  is constructed in the following 2 steps.

- Step (i): Construct  $\mathbf{X}(N_t + 2, k)$  as given in Case 2.

- Step (ii): Drop the last column of  $\mathbf{X}(N_t + 2, k)$ .

The rate (in complex symbols per channel use) of the above proposed designs is at most  $\frac{2}{N_t}$ . Therefore, whenever STBCs with minimum ASDC are desired (with both  $\mathbf{R}_{1,1} \in \mathcal{D}$  and  $\mathbf{R}_{2,2} \in \mathcal{D}$ ), there is a substantial loss in the rate of transmission especially when  $N_t > 2$ . However, if reduction of WSDC is targeted, then constructing complex designs which lead to only  $\mathbf{R}_{1,1} \in \mathcal{D}$  is sufficient. The following theorem states that the class of complex orthogonal designs [14], [15] (other than Alamouti design) results in the class of RC monomial lattice generators which in-turn lead to  $\mathbf{R}_{1,1} \in \mathcal{D}$  (but  $\mathbf{R}_{2,2} \notin \mathcal{D}$ ).

*Theorem 6*: For  $N_t > 2$ , STBCs from square complex orthogonal designs (CODs) reduce the WSDC for two-user MIMO-MAC.

*Proof*: We have to show that STBCs from the class of CODs (other than Alamouti design) results in a class of RC monomial lattice generators which in-turn lead to  $\mathbf{R}_{1,1} \in \mathcal{D}$  but  $\mathbf{R}_{2,2} \notin \mathcal{D}$ . It is straightforward to verify that the column vector representation matrices  $\{\mathbf{C}_i | i = 1 \text{ to } 2k\}$  of  $\mathbf{M}$  arising from CODs satisfy the sufficient condition 1) of Theorem 5. Hence, the corresponding class of  $\mathbf{R}$  matrices satisfy  $\mathbf{R}_{1,1} \in \mathcal{D}$ . In the rest of this paragraph, we only provide a sketch of the proof to show that the matrices  $\{\mathbf{C}_i | i = 1 \text{ to } 2k\}$  arising from CODs do not satisfy the sufficient conditions in 2) of Theorem 5 (this is to prove that  $\mathbf{R}_{2,2} \notin \mathcal{D}$ ). Recall that a COD in  $a + 1$  complex variables for  $N_t = 2^a$  antennas can be constructed in a recursive fashion from a COD in  $a$  variables for  $N_t = 2^{a-1}$  antennas for all  $a \geq 2$  (see Section III-D in [15]). We use the recursive construction technique of CODs to prove our result. First, it can be shown that the matrices  $\{\mathbf{C}_i | i = 1 \text{ to } 6\}$  arising from the COD for  $N_t = 4$  antennas do not satisfy the sufficient condition 2) of Theorem 5. Then, from the recursive construction technique of CODs, it can be proved that the matrices  $\{\mathbf{C}_i | i = 1 \text{ to } 2k\}$  arising CODs with larger number of antennas do not satisfy the sufficient conditions in 2) of Theorem 5 as well. This completes the proof.  $\blacksquare$

From the above theorem, it is clear that when only the WSDC is to be reduced, the rate of transmission can be increased from  $\frac{2}{N_t}$  to (i)  $\frac{a+1}{2^a}$  for the case of square designs where  $N_t = 2^a b$  for positive integers  $a$  and  $b$ .

5) *On the Diversity Order of the Proposed Codes With Reduced ASDC and WSDC*: Throughout the section, we have assumed that the destination performs sphere decoding of the symbols of User-1 and User-2 by decoding for a  $T \times 2N_t$  space-time codeword,  $\mathbf{Z} = [\mathbf{X}_1 \mathbf{X}_2]$  in a virtual  $2N_t \times N_r$  MIMO channel (where  $[\mathbf{X}_1 \mathbf{X}_2]$  denotes juxtaposing of the matrices  $\mathbf{X}_1$  and  $\mathbf{X}_2$ ). Therefore, applying the full diversity design criterion derived for space-time codes in point to point coherent MIMO channels [34] on the set of codewords of the form  $\mathbf{Z}$ , the diversity order for each user is  $N_t N_r$  provided each space-time block code  $\mathcal{C}_i$  is individually fully diverse for a point to point coherent co-located MIMO channel. Note that unlike the codes by [12], the proposed codes do not minimize the error event wherein the codewords of both the users are in error. However, considering average probability of error, the proposed codes provide diversity order of  $N_t N_r$ .

TABLE III  
DECODING COMPLEXITIES OF VARIOUS CODES IN TWO-USER MISO MAC WITH PHASE COMPENSATION FOR  $N_t = 2$

Code	ROD	Alamouti code	GB code	HV code
Decoding complexity	constant	$O(2M)$	$O(2M^2)$	$O(M^8)$

TABLE IV  
DECODING COMPLEXITIES OF VARIOUS CODES IN TWO-USER MISO MAC WITH OPTIONAL PHASE COMPENSATION FOR  $N_t = 2$

Code	ROD	Alamouti code	GB code	HV code
Decoding complexity	constant	$O(M^2)$	$O(M^4)$	$O(M^8)$

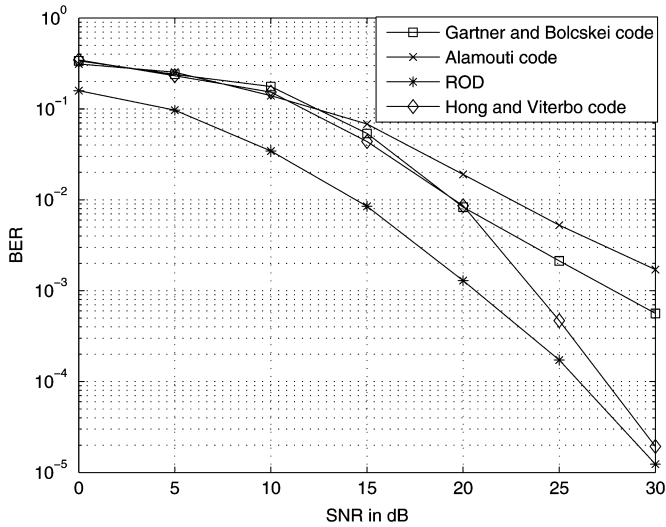


Fig. 26. BER comparison of STBC pairs from RODs with the STBC pairs in the literature with phase compensation.

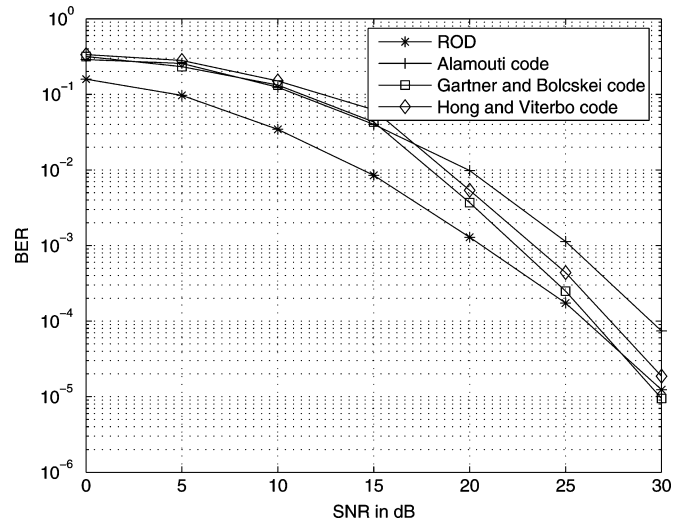


Fig. 27. BER comparison of STBC pairs from RODs (with CSITP) with the STBC pairs in the literature (without CSITP).

D. Simulation Results

In this subsection, we compare the performance of the proposed STBC pairs with those proposed in [12] and [13] for (i) two-user MISO-MAC with  $N_t = 2$ , and (ii) two-user MIMO-MAC with  $N_t = N_r = 2$ . The codes proposed in [12] and [13] are referred to as GB code and HV code respectively. For the error performance comparison, we present Bit Error Rate (BER) against the average receive SNR. For the decoding complexity comparison, we use the worst-case ML decoding complexity as the comparison metric.

1) Comparison for MISO-MAC With  $N_t = 2$ : For two-user MISO-MAC, we compare the BER and the decoding complexity of the STBC pair from the  $2 \times 2$  ROD with those of (i) the Alamouti code, (ii) the GB code and, (iii) the HV code pairs. For a fair comparison, transmission rate of 2 bits per channel use (bpcu) per user is maintained for all the four code pairs. To maintain 2 bpcu per user, for the class of STBC pairs from ROD, the variables of User-1 and User-2 take values from the 4-PAM signal sets,  $\sqrt{\frac{1}{5}}\{-3, -1, 1, 3\}$  and  $\sqrt{\frac{1}{5}}\{-3i, -1i, 1i, 3i\}$  respectively. However, the variables of Alamouti code, GB code and, HV code pairs take values from QPSK signal set. With phase compensation at the two-users, the BER comparison and the decoding complexity comparison are given in Fig. 26 and Table III respectively, which shows that STBC pairs from ROD

outperforms all other codes both in BER and decoding complexity. In Table III, the decoding complexity comparison is provided assuming that each user transmits  $\log_2(M)$  bits per channel use. From Fig. 26, note that both the Alamouti code pair and the GB code do not provide full diversity in Rayleigh fading channels.

The BER and the decoding complexities of the Alamouti code, HV code, and the GB code with no phase compensation at the two users are given in Fig. 27 and Table IV respectively. With no phase compensation, both the Alamouti code pair and the GB code provide full diversity, however, with increased decoding complexity.

2) Comparison for MIMO-MAC With  $N_t = N_r = 2$ : For two-user MIMO-MAC with  $N_t = N_r = 2$ , we compare the BER and the decoding complexity of the Alamouti code pair with those of (i) the GB code and (ii) the HV code pairs. Each user employs QPSK signal set to maintain a common transmission rate of 2 bpcu per user for all the three code pairs. The BER and the decoding complexity comparison are given in Fig. 28 and Table V respectively which shows that Alamouti code pair outperforms both GB and HV code pairs in decoding complexity (note that Alamouti has reduced ASDC). However, both the GB and HV code pairs marginally outperform Alamouti code pair in BER.

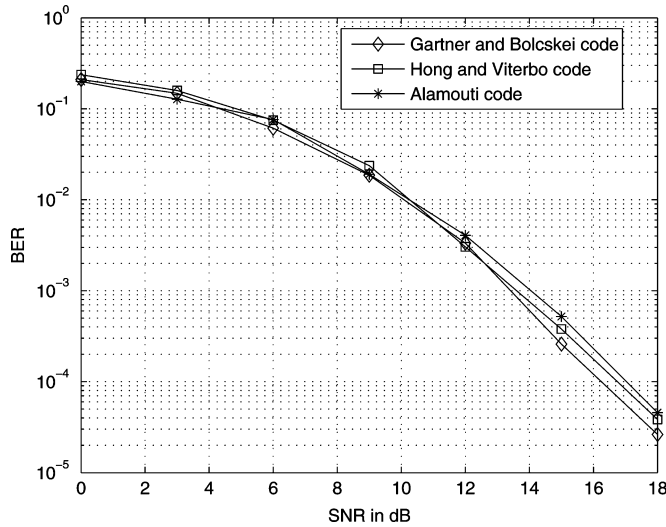


Fig. 28. BER comparison of STBC pairs from the Alamouti design with the STBC pairs in the literature for  $2 \times 2$  MIMO-MAC.

TABLE V  
DECODING COMPLEXITIES OF VARIOUS CODES IN TWO-USER MIMO MAC  
WITH  $N_t = N_r = 2$

Code	Alamouti code	GB code	HV code
Decoding complexity	$O(M^2)$	$O(M^4)$	$O(M^8)$

### VIII. DISCUSSION

We have computed the CC capacity regions of two-user GMAC and proposed TCM schemes with the class of  $M$ -PSK signal set pairs and  $M$ -PAM signal set pairs. We have also designed STBC pairs with low ML decoding complexity for two-user MISO-MAC and MIMO-MAC. Some possible directions for future work are as follows:

- As a generalization to this work, CC capacity/capacity regions for general multi terminal networks need to be computed since in practice, communication takes place only with finite input constellations. Also, design of coding schemes achieving rate tuples close to the CC capacity of general multi terminal networks is essential.
- The set partitioning result presented in this paper can be generalized to the class of  $M$ -QAM constellations.
- For the two-user GMAC, we assumed equal average power constraint for both the users. If unequal average power constraint is considered, optimal labeling rules on the individual trellis have to be designed depending on the ratio of the average power constraints of the two users.
- For two-user GMAC, trellis code pairs with  $M$ -PAM constellation pairs significantly reduce the ML decoding complexity at the destination compared to trellis code pairs with complex constellation pairs (Section V). For  $K$ -user GMAC with  $K > 2$ , designing coding schemes with low ML decoding complexity is an interesting direction of future-work.
- The rate (in complex symbols per channel use) of the proposed class of STBCs which reduces the ASDC is at most  $\frac{2}{N_t}$  for each user (in Section VII-C4). Using the necessary and sufficient conditions on the column vector representation matrices in Theorem 5, upper bounds on the

rate (in complex symbols per channel use) can be obtained and possibly STBCs with higher rates can be constructed.

- In Section VII-C, we have studied STBCs which result in a  $\mathbf{R}$  matrix such that  $\mathbf{R}_{1,1}$  and  $\mathbf{R}_{2,2}$  are diagonal matrices. Construction of STBCs which results in more number of nonzeros in the upper-diagonal entries of  $\mathbf{R}_{1,1}$  and  $\mathbf{R}_{2,2}$  is an interesting direction for future work. Such STBCs may have higher ASDC and/or higher WSDC but may lead to larger rates.

### ACKNOWLEDGMENT

The authors would like to thank G. R. Jithamithra, N. Shende, and G. Abhinav for their valuable inputs during discussions.

### REFERENCES

- [1] T. M. Cover and J. A. Thomas, *Elements of Information Theory*, 2nd ed. Hoboken, NJ: Wiley, 2006.
- [2] R. Gallager, "A perspective on multiaccess channels," *IEEE Trans. Inf. Theory*, vol. 31, no. 2, pp. 124–142, Mar. 1985.
- [3] E. Biglieri and L. Gyorf, *Multiple Access Channels: Theory and Practice*. Fairfax, VA: IOS, 2007, published in cooperation with NATO public Diplomacy Division.
- [4] R. Ahlswede, "Multi-way communication channels," in *Proc. IEEE Int. Symp. Information Theory (ISIT)* (in Armenian, S.S.R), 1971, pp. 23–52.
- [5] H. Liao, "A coding theorem for multiple access communications," presented at the IEEE Int. Symp. Information Theory (ISIT), Asilomar, CA, 1972.
- [6] F. N. Brannstrom, T. M. Aulin, and L. K. Rasmussen, "Constellation-constrained capacity for trellis code multiple access systems," in *Proc. IEEE GLOBECOM*, San Antonio, TX, Nov. 2001, vol. 02, pp. 11–15.
- [7] E. Biglieri, *Coding for Wireless Channels*. New York: Springer-Verlag, 2005.
- [8] T. Aulin and R. Espineira, "Trellis coded multiple access (TCMA)," in *Proc. IEEE International Conf. on Communications (ICC)*, Vancouver, BC, Canada, Jun. 1999, pp. 1177–1181.
- [9] F. N. Brannstrom, T. M. Aulin, and L. K. Rasmussen, "Iterative multi-user detection of trellis code multiple access using a posteriori probabilities," in *Proc. IEEE Int. Conf. Communications (ICC)*, Finland, Jun. 2001, pp. 11–15.
- [10] W. Zhang, C. D'Amours, and A. Yongacoglu, "Trellis coded modulation design form multi-user systems on AWGN channels," in *Proc. IEEE Vehicular Technology Conf.*, 2004, pp. 1722–1726.
- [11] G. Ungerboeck, "Channel coding with multilevel/phase signals," *IEEE Trans. Inf. Theory*, vol. 28, no. 1, pp. 55–67, Jan. 1982.
- [12] M. E. Gartner and H. Bolcskei, "Multiuser space-time/frequency code design," in *Proc. IEEE Int. Symp. Information Theory (ISIT)*, 2006, pp. 2819–2823.
- [13] Y. Hong and E. Viterbo, "Algebraic multiuser space-time block codes for  $2 \times 2$  MIMO," *IEEE Trans. Vehicular Technol.*, vol. 58, no. 6, pp. 3062–3066, Jul 2009.
- [14] V. Tarokh, H. Jafarkhani, and A. R. Calderbank, "Space-time block codes from orthogonal designs," *IEEE Trans. Inf. Theory*, vol. 45, no. 5, pp. 1456–1467, Sep. 1999.
- [15] X. Liang, "Orthogonal designs with maximal rates," *IEEE Trans. Inf. Theory*, vol. 49, no. 10, pp. 2468–2503, Oct. 2003.
- [16] Z. Khan and B. S. Rajan, "Single-symbol maximum likelihood decodable linear STBCs," *IEEE Trans. Inf. Theory*, vol. 52, no. 5, pp. 2062–2091, May 2006.
- [17] S. Karmakar and B. S. Rajan, "Minimum decoding complexity, maximum rate space-time block codes from Clifford algebras," in *Proc. of IEEE Int. Symp. Information Theory (ISIT)*, 2006, pp. 788–792.
- [18] J. Harshan and B. S. Rajan, "High-rate, single-symbol ML decodable precoded DSTBCs for cooperative networks," *IEEE Trans. Inf. Theory*, vol. 55, no. 5, pp. 2004–2015, May 2009.
- [19] W. He and C. N. Georghiadis, "Computing the capacity of MIMO fading channel under PSK signalling," *IEEE Trans. Inf. Theory*, vol. 51, no. 5, pp. 1794–1803, May 2005.
- [20] E. Viterbo and J. Boutros, "Universal lattice code decoder for fading channels," *IEEE Trans. Inf. Theory*, vol. 45, no. 5, pp. 1639–1642, Jul. 1999.
- [21] M. O. Damen, H. El Gamal, and G. Caire, "On maximum-likelihood detection and the search for the closest lattice point," *IEEE Trans. Inf. Theory*, vol. 49, no. 10, pp. 2389–2402, Oct. 2003.

- [22] B. Hassibi and B. M. Hochwald, "High-rate codes that are linear in space and time," *IEEE Trans. Inf. Theory*, vol. 48, no. 7, pp. 1804–18024, Jul. 2002.
- [23] J. Harshan and B. S. Rajan, "Finite signal-set capacity of two-user Gaussian multiple access channel," in *Proc. IEEE Int. Symp. Information Theory*, Toronto, ON, Canada, Jul. 06–11, 2008, pp. 1203–1207.
- [24] J. Harshan and B. S. Rajan, Trellis Coded Modulation for Unequal Rate Gaussian MAC, Aug. 2009, arXiv:0908.1163v1.
- [25] J. Harshan and B. S. Rajan, "Coding for two-user Gaussian MAC with PSK and PAM signal sets," in *Proc. IEEE Int. Symp. Information Theory*, Seoul, South Korea, Jun. 28–Jul. 3, 2009, pp. 1859–1863.
- [26] B. Rimoldi and R. Urbanke, "A rate-splitting approach to the Gaussian multiple-access channel," *IEEE Trans. Inf. Theory*, vol. 42, no. 2, pp. 364–375, Feb. 1996.
- [27] J. Harshan and B. S. Rajan, "Low complexity, information-lossless STBCs for two-user MISO-MAC with partial CSIT," presented at the IEEE National Conf. Communications (NCC), Chennai, India, Jan. 2010.
- [28] E. Telatar, "Capacity of multi-antenna Gaussian channels," *Eur. Trans. Telecommun.*, vol. 10, no. 6, pp. 585–595, 1999.
- [29] V. Shashidhar, B. S. Rajan, and B. A. Sethuraman, "Information-lossless space-time block codes from crossed-product algebras," *IEEE Trans. Inf. Theory*, vol. 52, no. 9, pp. 3913–3935, Sep. 2006.
- [30] J. Harshan and B. S. Rajan, "STBCs with minimum sphere decoding complexity for two-user MIMO MAC," in *Proc. IEEE GLOBECOM 2009*, Honolulu, HI, Nov. 30–Dec. 4, 2009.
- [31] E. Biglieri, Y. Hong, and E. Viterbo, "On fast-decodable space-time block codes," *IEEE Trans. Inf. Theory*, vol. 55, no. 2, pp. 524–530, Feb. 2009.
- [32] M. O. Sinnokrot and J. R. Barry, Fast Maximum-Likelihood Decoding of Golden Code Nov. 2008, arXiv:0811.2201[cs.IT].
- [33] K. P. Srinath and B. S. Rajan, Low ML-Decoding Complexity, Large Coding Gain, Full-Rate, Full-Diversity STBCs for 2 X 2 and 4 X 2 MIMO Systems Sept. 2008, arXiv:0809.0635[cs.IT].
- [34] V. Tarokh, N. Seshadri, and A. R. Calderbank, "Space-time codes for high data rate wireless communication: Performance criterion and code construction," *IEEE Trans. Inf. Theory*, vol. 44, no. 2, pp. 744–765, Feb. 1998.

**J. Harshan** received the B.E. degree in electronics and communication from the National Institute of Engineering, Mysore, India, and the Ph.D. degree in electrical communication engineering from the Indian Institute of Science, Bangalore, India, in 2004 and 2010, respectively.

From October 2004 to December 2005, he was with Robert Bosch (India) Limited, Bangalore. Since March 2010, he has been with Broadcom Communications, Bangalore. His primary research interests include wireless communications, space-time coding, coding for wireless relay networks, and coding for multiple access channels.

**B. Sundar Rajan** (S'84–M'91–SM'98) was born in Tamil Nadu, India. He received the B.Sc. degree in mathematics from Madras University, Madras, India, the B.Tech. degree in electronics from Madras Institute of Technology, Madras, and the M.Tech. and Ph.D. degrees in electrical engineering from the Indian Institute of Technology, Kanpur, India, in 1979, 1982, 1984, and 1989, respectively.

He was a faculty member with the Department of Electrical Engineering at the Indian Institute of Technology in Delhi, India, from 1990 to 1997. Since 1998, he has been a Professor in the Department of Electrical Communication Engineering at the Indian Institute of Science, Bangalore, India. His primary research interests include space-time coding for MIMO channels, distributed space-time coding and cooperative communication, coding for multiple-access, relay channels, and network coding with emphasis on algebraic techniques.

Dr. Rajan is an Associate Editor of the IEEE TRANSACTIONS ON INFORMATION THEORY, an Editor of the IEEE TRANSACTIONS ON WIRELESS COMMUNICATIONS, and an Editorial Board Member of the *International Journal of Information and Coding Theory*. He served as Technical Program Co-Chair of the IEEE Information Theory Workshop (ITW'02), held in Bangalore, in 2002. He is a Fellow of Indian National Academy of Engineering, a Fellow of the National Academy of Sciences, India, recipient of Prof. Rustom Choksi award by I.I.Sc for excellence in research in Engineering for the year 2009, and recipient of the IETE Pune Center's S.V.C Aiya Award for Telecom Education in 2004. He is also a Member of the American Mathematical Society.